MicroRNA in Diabetic and TGFbeta-Related Renal Glomerulopathy

by

Yi-Chun Lai

A dissertation submitted in partial fulfillment
of the requirements for the degree of
Doctor of Philosophy
(Cellular and Molecular Biology)
in The University of Michigan
2013

Doctoral Committee:

Assistant Professor Markus Bitzer, Chair
Professor Frank C. Brosius III
Professor Christin Carter-Su
Professor Ram K. Menon
Associate Professor Robert C. Thompson

Acknowledgments

First of all, I would like to show my greatest appreciation to my thesis advisor, Dr. Markus Bitzer, for his guidance and teaching. When I first met Markus in 2008, after a small discussion about his research, I immediately grew the enthusiasm to work with him and follow him. From clinical research to basic science, I enjoyed brainstorming with Markus, and under his leadership, I am capable of being intellectually independent. I am deeply grateful for Markus's patience to help me grow and I am also indebted to him for giving me this opportunity to pursue my PhD degree.

I am also thankful for the valuable feedback from my thesis committee members, Dr. Frank Brosius, Dr. Christin Carter-Su, Dr. Ram Menon, and Dr. Robert Thompson. With their insightful suggestion and assistance, I am able to advance my thesis work and make a good progress. I especially thank Dr. Frank Brosius and Dr. Robert Thompson for their support and help regarding fellowship application. In addition, I would like to thank Dr. Jessica Schwartz for recruiting me in the Cell and Molecular Biology program, and Cathy Mitchell for helping me with all kinds of presentation arrangement and financial support.

It has been a wonderful experience to work with my lab members, Jinghui Luo and Christopher O'Connor. I thank Jinghui for her technical support and experience sharing. I particularly give my deepest gratitude to Christopher O'Connor for all the experiments he has performed for me as well as the help to continue the research whenever I was not available.

Furthermore, I thank all the collaborators to our lab. Dr. David Turner and Huanqing Zhang have helped us with numerous microRNA experiments, and I thank for their generous sharing. I especially would like to acknowledge Dr. Matthias Kretzler's lab. I owe all my bioinformatics skills to them. I thank Celine Berthier, Felix Eichinger, Claudiu Komorowsky, Sebastian Martini, and Viji Nair for their system biology instruction. I also thank Ann Randolph to process the sample, and Courtenay Vining for any experiment support. Furthermore, I show my most gratefulness to Dr. Matthias Kretzler and Dr. Wenjun Ju for their insight, advice, and direction.

Other collaborators outside University of Michigan include Dr. Iddo Ben-Dov and Dr. Thomas Tuschl in The Rockefeller University. I am thankful for their assistance in terms of microRNA biology and bioinformatics. I also thank Robert G. Nelson in NIDDK, National Institutes of Health for his support in studying diabetic nephropathy of PIMA Indians. Finally, I would like to thank Dr. Stuart Orkin in Dana Farber Cancer Institute, Boston, for providing microRNA21 knockout mice.

Ultimately, I am deeply indebted to my parents for their unconditional love and endless care. 5 years ago, when I changed over my career path to United States, I totally appreciated their unselfishness and understanding. Moreover, I would like to recognize my two older brothers. Being medical professors and great physicians in National Taiwan University Hospital, they are always my heroes whom I look up to. I also would like to thank my previous mentor in National Taiwan University Children Hospital, Dr. Mei-Hwan Wu. Without her encouragement and endorsement, I would not have come to United States to fulfill my academic enthusiasm.

In the end, many thanks to my dearest husband for his heart to love me as the way I am, for his understanding to deal with my long working hour, for his gentleness to support any aspect I need, and for his patience to equip me with kindness and compassion.

TABLE OF CONTENTS

List of Figures

Figure

List of Tables

Table

ABSTRACT

MicroRNAs in Diabetic and TGF-beta-Related Renal Glomerular Injury

by

Jennifer Yi-Chun Lai

Chair: Markus Bitzer

Chronic kidney disease (CKD) decreases quality of life, increases mortality, and has limited treatment options. Glomerular injury is an early stage of diabetic nephropathy (DN), which is a leading cause of CKD, and is characterized by mesangial cell proliferation and hypertrophy, loss of podocytes, and increased extracellular matrix (ECM) deposition. Critical aspects of these cellular events are mediated by activation of the Transforming Growth Factor-beta (TGFβ) signaling cascade. MicroRNAs (miRNAs) regulate gene expression in a post-transcriptional level and have been implicated as important regulatory elements in the TGFβ signaling cascade. To determine the role of miRNAs in DN, we examined miRNA expression in micro-dissected glomeruli from kidney biopsies of patients with clinically early DN and correlated the expression levels with clinical manifestations.

We determined that miR-21 exhibits high expression in renal glomeruli and significant correlation with urine albumin-to-creatinine-ratio (ACR) of patients. miR-21 is a known regulator of TGFβ signaling and its level is positively associated with severity of renal phenotype in TGFβ transgenic mice. We further found that loss of miR-21 in TGFβ transgenic mice resulted in accelerated podocyte apoptosis and glomerulosclerosis. A similar phenotype was detected in streptozotocin-induced diabetic mice. In cultured glomerular cells, loss or inhibition of miR-21 led to increased apoptosis of podocytes and increased proliferation of primary mesangial cells. Further studies showed that miR-21 represses multiple pro-apoptotic pathways, including TGFβ/Smad7, P53, and PDCD4, cell cycle-related genes such as Cdk6 and Cdc25a, and ECM-related genes. These results suggest that miR-21 ameliorates glomerular injury through repression of multiple injury-mediating signaling pathways.

To further elucidate a miRNA-mediated network mediating DN progression, we examined mRNA expression in the same glomerular samples. We identified ACR-associated genes that are predicted targets of ACR-associated miRNAs and experimentally validated the sequence-dependent repression of candidate target genes of miR-200a. This led to the discovery of EXOC7 as a sequence-dependent target of

miR-200a.

In summary, correlating miRNA expression with specific clinical outcomes identified novel mechanisms regulating DN, including a protective role for miR-21 in glomerular injury. Furthermore, the approach, which links disease-associated miRNAs and mRNAs by target prediction, appears to facilitate identification of context-relevant miRNA-mRNA interactions.

Chapter I

Introduction

Chronic kidney disease (CKD) is the pathological change that develops after renal injury, such as high blood sugar (hyperglycemia), oxidative stress, or immune-mediated damage. CKD can lead to end-stage renal disease (ESRD) requiring dialysis support or kidney transplantation. It also results in high morbidity and mortality, partially due to an increased cardiovascular event rate, and thereby imposes a heavy burden on medical economics[1]. The increasing prevalence of CKD during the past 20 years highlights the public health importance of this disease[2]. According to the 2011 United States Renal Data System (USRDS), Taiwan, Japan, and United States are the three countries having the highest prevalence rate of ESRD worldwide[3]. In the United States, the incidence rate of ESRD in 2011 was about 1.3% among the Medicare population, but accounted for 8.1% of Medicare costs. Despite the high prevalence of ESRD and excessive costs, interventions to prevent or delay complications and progression of CKD remain limited. Furthermore, development of new treatment options is hampered by our limited understanding of the molecular

events associated with the progression from renal injury to ESRD. Facing such a medical difficulty, we felt there was an urgent need to advance the knowledge.

Among various renal injuries, diabetic nephropathy (DN), which is caused by diabetic mellitus (DM), is the leading cause of ESRD in the United States[3]. Therefore, it is essential to investigate the molecular mechanisms of DN in order to ameliorate the development of ESRD.

Kidney structure

The nephron is the functional unit of the kidney (Figure 1.1). It has two major compartments to maintain homeostasis. One is the renal glomerulus, a convolution of capillary loops that harbors mesangial, endothelial, and visceral glomerular epithelial cells (podocytes). Podocytes stand with extended pedicles on the urinary side of the glomerular basement membrane (GBM) of the capillary loops. The foot processes of podocytes are interdigiated and connected via a slit diaphragm. The endothelium, GBM, and the slit diaphragm and body of podocytes form the glomerular filtration barrier to generate primary urine. Mesangial cells are specialized smooth muscle cells that are located between the capillary loops, are not separated from endothelial cells by the GBM, and are thought to regulate renal blood

flow and pressure through glomerular capillaries. The other compartment is the tubulo-interstitium, which is composed of tubules that are lined by tubular epithelial cells which regulate urine composition through reabsorbing and excreting specific molecules from the primary urine. Injuries to the glomeruli (glomerulopathy) or tubule-interstitium can initiate a fibrotic response that leads to renal scaring and CKD. It has been proposed that glomerulopathy is an early event of DN, and initiates the damage in the tubulo-interstitial compartments of the kidney[4,5].

Diabetic Nephropathy

DN results from longstanding DM and is associated with the activation of the transforming growth factor-beta (TGFβ) signaling[6]. The earliest pathological finding of DN is glomerulopathy[7], characterized by mesangial expansion, podocyte depletion, nodular glomerulosclerosis. It clinically manifests as proteinuria followed by decreased glomerular filtration function[8]. The molecular events in glomeruli induced by hyperglycemia include increased TGFβ production in the glomerular cells leading to mesangial cell proliferation and hypertrophy, podocyte detachment from the basement and death, and increased extracellular matrix (ECM) deposition[9]. It has been proposed that podocyte depletion is the initiating event resulting in other pathological changes in glomerulopathy[10,11].

Transforming growth factor beta (TGFβ)

The TGFβ superfamily of ligands include Bone Morphogenetic Proteins (BMPs), Growth and Differentiation Factors (GDFs), Anti-müllerian Hormone (AMH), Activin, Nodal and TGFβs. Members of the TGFβ family are cytokines that bind to TGF beta type II receptor, a serine/threonine receptor kinase, which catalyzes the phosphorylation of the Type I receptor. Each class of ligands binds to specific type II receptors. In mammals, there are seven known type I receptors and five type II receptors. TGFβs promote cell proliferation, differentiation, regeneration, and apoptosis, but the effects of TGFβ are dependent on the context and organ system[12,13]. In general TGFβs maintain tissue homeostasis and regulate immunity, cancer, and fibrotic diseases[14].

Intracellular signaling is initiated by the binding of TGFβ to a type II receptor dimer, which recruits a type I receptor dimer to form a hetero-tetrameric complex with the ligand. This complex then phosphorylates intracellular signaling molecules. The receptor-phosphorylated Smad proteins (Smad2 and Smad3) are central downstream effectors to convey and carry out many important context-dependent TGFβ actions in the kidney, which are determined by the binding cofactors and the epigenetic status of the target gene[13] (Figure 1.2). Other than the canonical TGFβ-Smad signaling pathway, TGFβ receptor I and II can each individually phosphorylate and

activate other downstream kinases that regulate diverse biological functions[13].

The TGFβ-Smad signaling pathway has been found to be highly activated in DN. Among receptor-phosphorylated Smad proteins, Smad3 mediates important aspects in DN progression including podocyte loss due to apoptosis, mesangial cell proliferation/activation, and ECM deposition in glomerulus (Figure 1.3)[15,16]. In contrast, Smad2 has an opposing role to Smad3 in renal fibrosis[17]. In patients with DN, decreased podocyte number has been attributed to podocyte loss mediated by TGFβ/Smad3-induced apoptosis[18]. In addition to podocyte loss, mesangial cell proliferation and activation promoting ECM deposition is also an important factor in the development of glomerulopathy (Figure 1.3)[16,19-21].

Albumin-TGFβ_1 transgenic mice are characterized by overexpression of active TGFβ_1 in hepatocytes and high plasma levels of active TGFβ_1. Progressive glomerulosclerosis is the leading phenotype in TGFβ_1 transgenic mice and there are mild changes in other organ systems. Therefore, these mice are an established model to study the function and signaling of TGFβ in kidney injury[22,23]. The finding of podocyte apoptosis as an early event in TGFβ_1 transgenic mice supports the hypothesis that TGFβ-induced podocyte apoptosis leads to glomerulopathy[11].

However, despite the deleterious effects of increased TGFβ activity, TGFβ regulates essential homeostatic processes and inhibition of TGFβ ligands or inhibition of the ligand binding to its receptors causes pathologic changes[24,25]. Moreover, although Smad3 knockout (KO) mice, have attenuated fibrosis after renal injury[26,27], they develop mucosal abscesses and have a strongly reduced lifespan[28]. Therefore, it is critical to identify specific downstream signaling mediators in the TGFβ signaling cascade that can serve as potential therapeutic targets.

MicroRNAs (miRNAs)

MiRNAs are small non-coding RNAs that regulate gene expression at post-transcriptional level[29]. They were discovered in 1993 from *C. elegans* studies[30] and were found to be broadly conserved among different species[31]. MiRNAs are transcribed by RNA polymerase II to form approximately 70 nucleotide long pri-miRNAs with a hair-pin loop and stem structure[32,33] (Figure 1.4). Pri-miRNAs are cleaved by Drosha complex to form pre-miRNA[33] and then exported to cytoplasm to be further processed by Dicer to form 22 to 24 nucleotides double-strand miRNAs (ds-miRNAs)[34]. Integrating with RNA-induced silencing complex (RISC), the ds-miRNAs become mature single-strand miRNAs (ss-RNAs) and bind to complementary sequences in 3’ untranslated region (3’UTR) of the

target messenger RNAs (mRNAs) causing translational repression or mRNA degradation[35,36] (Figure 1.4).

Experimental results support functional redundancy between miRNAs and also between miRNAs and genes[37]. In addition to acting as classical binary off-switch regulators of genes, miRNAs may also act as neutral regulators to repress protein output without compromising biological function[35]. Some miRNAs are found to be critical in maintaining normal cell physiology and loss of the miRNA can result in lethality and/or severe functional defect in miRNA KO mice[38]. miRNAs are often integrated into positive and negative feedback loops in signaling pathways and have been implicated as modulators of stress responses in many physiologic and pathologic processes[39]. For instance, the transcription factor, P53, binds to the promoter region of miRNA34a (miR-34a) and promotes its gene expression. Subsequently, the upregulation of miR-34a promotes P53-mediated apoptosis and tumor suppression[40]. Being part of the feed-forward regulation loop, miR-34a targets SIRT1 to upregulate P53 activity and reinforces signaling functionality[41]. There are also miRNAs imposing a negative feedback mechanism on a signaling pathway in order to resolve the signaling activity[42] (Figure 1.5).

Relationship between TGFβ and miRNA

Recently, TGFβ/Smad proteins were found to participate in miRNA biogenesis and regulation[43,44]. Specifically, the TGFβ downstream effectors, Smad2/3 proteins, bind to the promoter region of miRNAs to increase miRNAs expression at a transcriptional level or bind to the stem region of pre-miRNAs to facilitate Drosha cleavage process to increase mature miRNA expression at a post-transcriptional level[45,46](Figure 1.6). Pre-miRNAs, such as miR-21 and miR-23a, have been found to have a consensus binding sequence in the stem region for Smad2/3 proteins and are regulated by TGFβ[45].

MiRNAs are potential oncogenes and also play an important role in heart disease[47,48]. Since TGFβ mediates DN and regulates biogenesis of miRNAs, miRNAs might be potential therapeutic targets in the treatment of DN. A few studies have explored the role of miRNAs in DN. To date, several miRNAs have been implicated in the development of DN[49,50]. For example, miR-192 is induced by TGFβ and targets the E-box promoter repressor, ZEB1/2, to increase E-box-related collagen production in mesangial cells[49]. miR-200 family members, regulated by E-box promoters, are also embedded in the ZEB1/2 regulatory network and might play a role in the pathogenesis of DN[51] (Figure 1.7). Furthermore, miR-377 expression is increased in

a high glucose environment in renal cell culture and in mouse model of DN, enhances fibronectin production and promotes ECM deposition[52]. However, those current studies focused on *in vitro* experiments or animal models. It remains unclear whether these findings are relevant for human DN.

Evidence is emerging that miRNAs modulate signaling cascades and thereby regulate physiologic processes as well as stress response. This raises tremendous interest in supplementing or blocking specific miRNA as a clinical intervention. Chemically modified oligonucleotide inhibitors have been shown to successfully deliver blockage of miRNA in specific tissue organs[53]. Inhibitors (antagomirs) of miR-122 which blocks Hepatitis C virus replication (HCV), can be successfully delivered into chimpanzees decreasing Hepatitis C viral load in serum[54,55]. miR-122 antagomir is currently in phase 2 clinical trials to target HCV.

Controversy among different studies of miRNAs

miR-21 is one of the first miRNAs to be linked to cancer biology[56]. miR-21 is associated with a variety of cancers and has an anti-apoptotic effect[57,58], and thereby is oncogenic[59]. In addition, miR-21 has also been associated with heart disease[48,60] and kidney disease[61,62]. In animal models, inhibition of miR-21 was found to

attenuate tubulo-interstitial fibrosis in unilateral ureteral obstruction (UUO)[61] and unilateral ischemia-reperfusion injury[62].

Because miR-21 is an anti-apoptotic factor, miR-21 might play a role in diabetic glomerulopathy, which is characterized by podocyte apoptosis. Furthermore, TGFβ signaling activity is known to induce podocyte apoptosis and regulates miR-21 biogenesis. However, previous studies about miR-21 focused on the tubulointerstitium of kidney[61,62].

As kidney is composed of different cell types and most miRNAs are multifaceted as well as cell-type-specific, results across different studies and strategies are often not consistent[49,50,63]. For example, Krupa et al. found that loss of miR-192 associates with increased fibrosis in kidney biopsies of human DN and loss of miR-192 promotes fibrogenesis in renal tubular cells[50]. However, Kato et al. proposed that miR-192 promotes fibrogenesis through enhancing TGFβ-induced collagen1a2 expression in mesangial cells[49]. Controversy still exists among different miRNA studies related to DN and therapeutic development is actively ongoing. For that reason, we were prompted to investigate whether miRNA plays a role specifically in diabetic glomerulopathy (DG).

MiRNA and mRNA interaction

MiRNAs repress gene expression by binding to mRNA transcripts thereby regulating their expression levels and the relationship between miRNA and mRNA expression has been broadly studied[64]. Several algorithms have been developed to predict the targeting between miRNAs and mRNA 3'UTR. One such algorithm is TargetScan, which is based on matching seed sequences and affinity and conservation across species of miRNA:mRNA binding sites[64-66]. MiRanda, calculates the thermodynamic energy of complimentary binding and dynamic alignment between miRNAs and mRNA[67,68]. However, the false prediction rate of those algorithms remains high and the number of experimentally verified targets is still low[69]. For example, human miR-21 has 164 predicted targets in Targetscan[64-66], but only has 42 validated target genes according to miRecord[70], a resource of experimentally verified miR-target interaction. The other 122 predicted targets were either not the sequence-dependent targets of miR-21 or have not been experimentally verified.

As a result, many studies have developed new approaches to explore miRNA-mRNA interaction that involves more than sequence binding prediction. For example, MAGIA integrates the correlation between miRNA and mRNA expression

data from the same subjects with pre-existing prediction algorithms[71]. Other tools apply new regression models[72,73] or Bayesian inference[74] to facilitate the search for target genes. However, it is still questionable whether these approaches improve the preciseness of identifying target genes or effectively determine the regulatory role of miRNA in disease progression.

Therefore, while studying the role of miRNA in human DG, we proposed a new approach to investigate miRNA-mRNA interaction based on the association between miRNA or mRNA levels and clinical manifestation of specific diseases.

Objectives and aims

American Indians of the Gila River Indian Community in Arizona are an ethnic group that exhibits high rates of type 2 diabetes mellitus and DN[75]. Previous studies have shown an association between inheritability and DN susceptibility in this cohort[76]. This research project, which aims at investigating whether miRNA plays a role specifically in DG, examined glomerular miRNA expression in those American Indian patients with early diabetic nephropathy in order to (1) determine the association between miRNA and human DG, and (2) identify miRNA that may modify disease progression. Using animal models including Albumin-TGFβ_1

transgenic mice, mice with streptozotocin (STZ)-induced beta cell dysfunction and DN, and miRNA KO mice[23,38], we further examined the role and the regulatory mechanisms of miR-21 in TGFβ-related renal glomerulopathy. At last, we proposed a new approach to effectively identify miRNA targets based on their association with clinical manifestations of specific diseases.

We address the aims and hypothesis in the following three chapters

Chapter II: MicroRNA-21 ameliorates transforming growth factor-beta-mediated glomerular injury

In this chapter, we determined the association between miRNAs and diabetic clinical manifestations, such as the urine albumin-to-creatinine ratio (ACR) and glomerular filtration rate (GFR). We profiled miRNA expression in renal glomeruli from kidney biopsies of American Indian diabetic patients by quantitative real-time PCR (qrt-PCR). We determined that several kidney-related miRNAs exhibited relatively high expression in renal glomeruli compared to other miRNAs and had a significant correlation with ACR. Among ACR-associated miRNAs, miR-21 had the highest expression in renal glomeruli.

In Albumin-TGFβ_1 transgenic mice levels of expression of miR-21 and TGFβ_1 are positively associated with severity of kidney damage based on histology scores[77].

Consistent with the previous studies[43,62], our data suggested that the higher level of TGFβ increases miR-21 in animals with greater renal damage. Apoptosis is a process in which cells are eliminated by a specific program[78]. Since TGFβ induces podocyte apoptosis[16] and miR-21 has been proposed as an anti-apoptotic factor in cancer and ovarian granulosa cells[57,58], we further hypothesize that miR-21 acts as a negative regulator to limit TGFβ-induced podocyte apoptosis.

We obtained ubiquitous miR-21 KO mice, which were generated by Cre-Lox recombination to remove the sequence of pri-miR21 from the genome[79]. In order to test the hypothesis that miR-21 protects against TGFβ-related glomerulopathy, we introduced progressive glomerulopathy into genetically mir21-deficient mice by crossing $TGF\beta_1$ transgenic (TG) mice with miR-21 KO mice to generate TG/miR-21 WT and TG/miR-21 KO offspring mice.

The renal phenotype of TG/miR-21 WT and TG/miR-21 KO littermates showed that loss of miR-21 resulted in increased podocyte apoptosis and loss, and progressive glomerulopathy. We further examined apoptosis in cultured mouse podocytes expressing miR-21 mimics or anti-miR-21 oligonucleotides (inhibitors). We found that depletion of miR-21 increased podocyte apoptosis.

TGFβ induces apoptosis through Smad7 and phosphorylation of Smad3[16]. In addition, P53 and programmed cell death 4 (PDCD4) are tumor suppressor proteins,

which induce apoptosis[80,81]. P53 is indirectly suppressed by miR-21[80] and PDCD4 is targeted by miR-21 in cancer cells[81]. Other important proteins involved in glomerulosclerosis are members of the metalloproteinase (MMP) family and the MMP inhibitor, tissue inhibitor of metalloproteinase (TIMP). TIMP inhibits MMP to breakdown ECM, and therefore TIMP promotes fibrosis in glomeruli[82,83].

In order to investigate miR-21 regulatory mechanisms in TGFβ-related glomerulopathy, we examined the expression levels of the apoptosis-related genes and ECM-related genes in TG/miR-21 WT and KO mice and mouse podocytes. We found that the mRNA levels of TGFβ receptor 2 (Tgfbr2), TGFβ induced (Tgfbi), Smad7, tissue inhibitor of metalloproteinase 3 (Timp3), collagen4a1 (Col4a1), and p53 (Tp53) were increased in glomeruli of TG/miR-21 KO mice, the protein levels of Pdcd4 as well as phosphorylation of Smad3 were increased in miR-21 inhibitors-transfected mouse podocytes. We further determined that Smad7 is a sequence-dependent target of miR-21.

Chapter III: Loss of miR-21 promotes mesangial cell proliferation and leads to increased mesangial expansion in diabetic mice

In order to test the protective role of miR-21 in glomerulopathy to a greater extent, we examined the role of miR-21 in STZ-induced diabetic mice[84]. We injected STZ

into miR-21 WT and KO mice to induce beta-cell dysfunction and thereby hyperglycemia and diabetic glomerulopathy. Our results indicated that loss of miR-21 in STZ-induced diabetic mice results in more proteinuria and mesangial expansion.

We further found that loss of miR-21 promotes baseline proliferation and cell cycle progression of mouse primary mesangial cells (PMC). Cell cycle represents a series of events leading from replication of the genetic material to cell division. It consisted of G0/G1, S, G2, and M phases and is facilitated by cyclin and cyclin-dependent kinases (CDK) complex, [85]. Cyclin-dependent kinase 6 (Cdk6) is a member of cyclin-dependent protein kinase family, which facilitates cell cycle progression[86]. Cell division cycle 25A (Cdc25a) is a member of phosphatase family that is required for cell cycle progression[87]. Both of them have been proposed as the sequence-dependent target of miR-21 in cancer cells[81,88]. For that reason, we performed qrt-PCR to demonstrate that the expression of Cdk6 and Cdc25a was increased in the glomeruli of STZ-treated miR-21 KO mice versus STZ-treated miR-21 WT mice. Therefore, we suggest that loss of miR-21 facilitates TGFβ-induced proliferation of mesangial cells by regulating cell cycle-related genes.

Chapter IV: Linking disease-associated miRNA and disease-associated mRNA identifies miRNA-mRNA interaction

In this chapter, miRNA and mRNA were profiled in the renal glomeruli from kidney biopsies of the patients with early DN. The levels of expression of both miRNA and mRNA were correlated with ACR of patients with early DN. Linking ACR-correlated miRNA and ACR-correlated mRNA by two prediction algorithms and data from Photoactivatable Ribonucleoside Enhanced Crosslinking and Immunoprecipitation (PAR-CLIP) RNA sequencing[89], we identified potential targets of miR-200a.

We further verified the potential targets of miR-200a experimentally. In human embryonic kidney (HEK) cells expressing miR-200a mimics, miR-200a repressed the expression of RALGPS2, SUPT6H, and EXOC7. We further confirmed that EXOC7 is a sequence-dependent target of miR200a by a luciferase assay. We concluded that miRNAs and their downstream regulatory genes are associated with diseases. Together with the previous findings about miR-21, we propose that some miRNAs increase with disease progression as an attempt to limit disease-associated gene upregulation and some miRNAs increase with disease progression to further repress gene downregulation in disease process. This new concept might provide an alternative approach to identify miR-mRNA interactions.

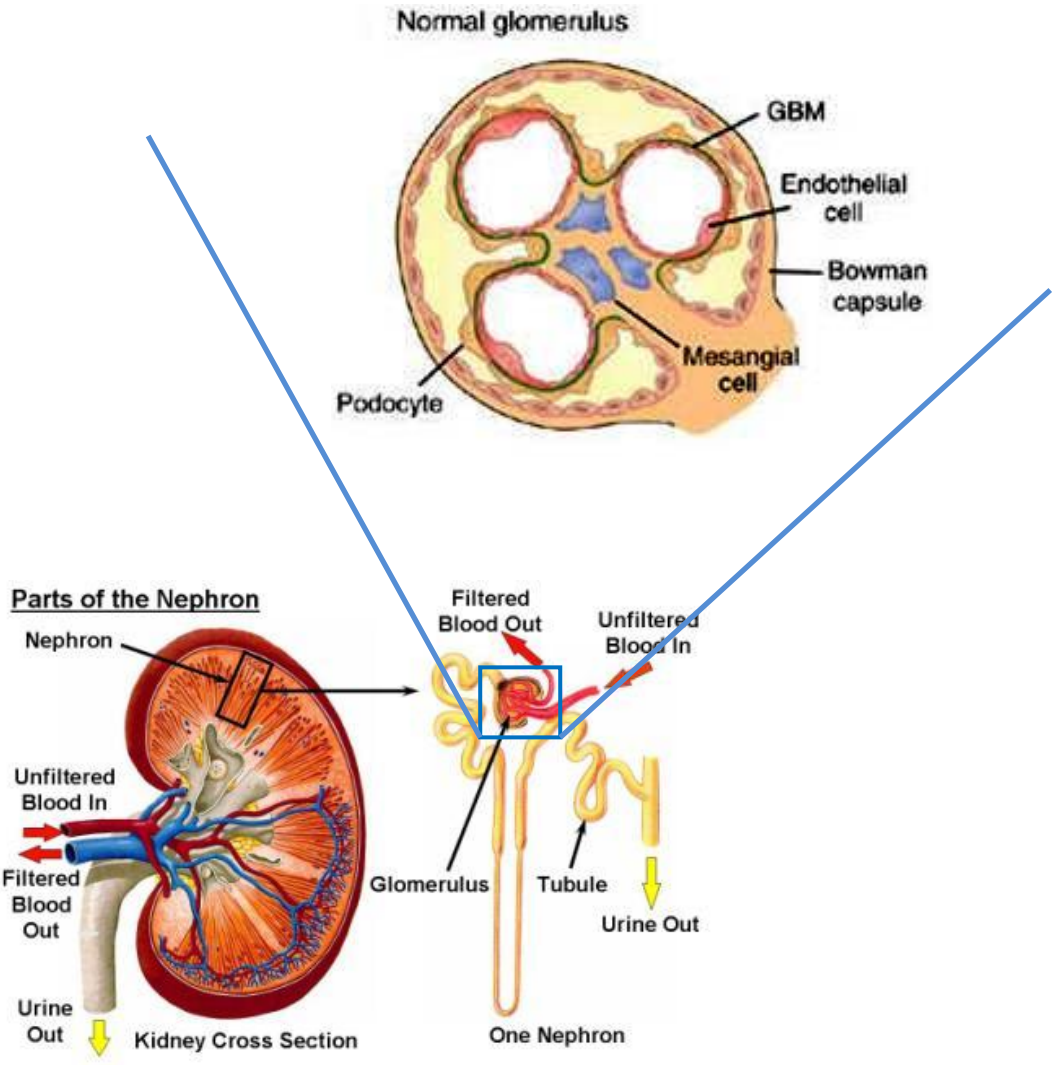

Figure 1.1. Overview of kidney, nephron and glomerulus structure. (Adapted from "Kidney health library" by UNC kidney center and "Proteinuria in diabetic kidney disease: A mechanistic viewpoint" by J.A. Jefferson et al, 2008, *KI*, *74*, P.25. Copyright 2001 by Nature Publishing Group. Used with permission).

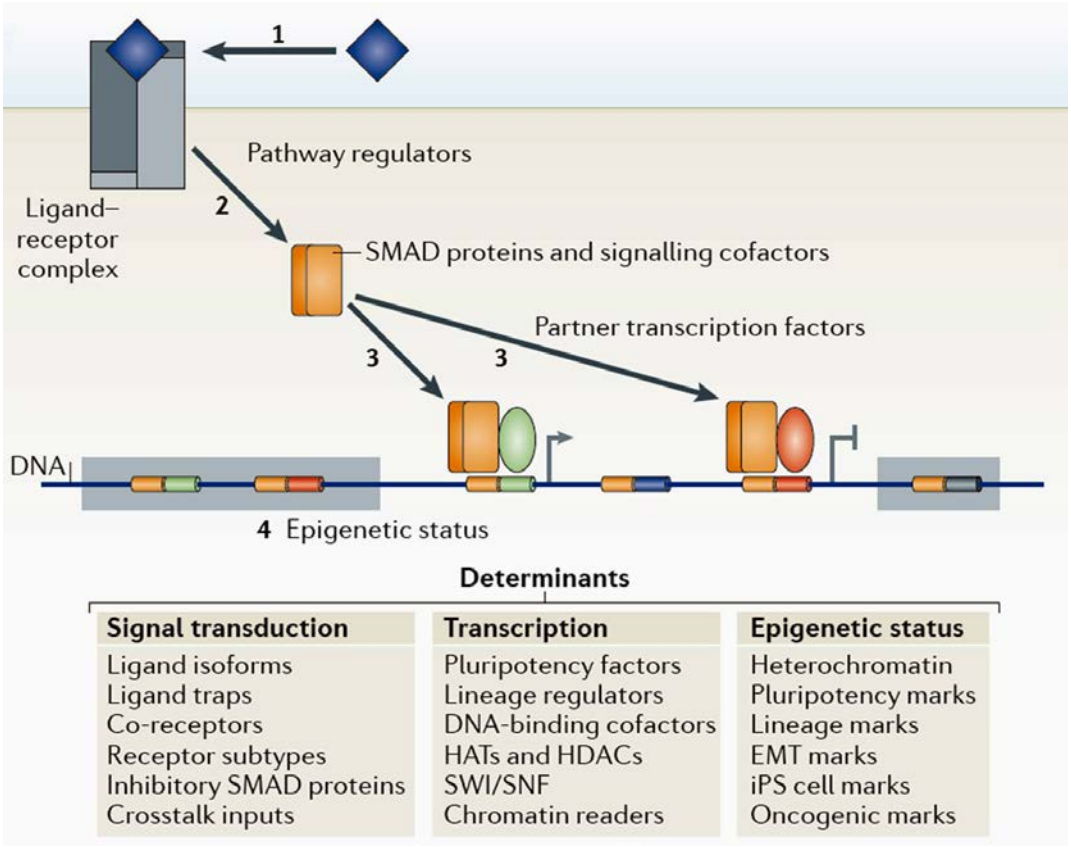

Figure 1.2. Contextual determinants of TGFβ action. (Adapted from "TGFβ signaling in context" by Joan Massagué, 2012, *Nature Reviews 13*, P.616. Copyright 2012 by Macmillan Publishers Limited. Used with permission).

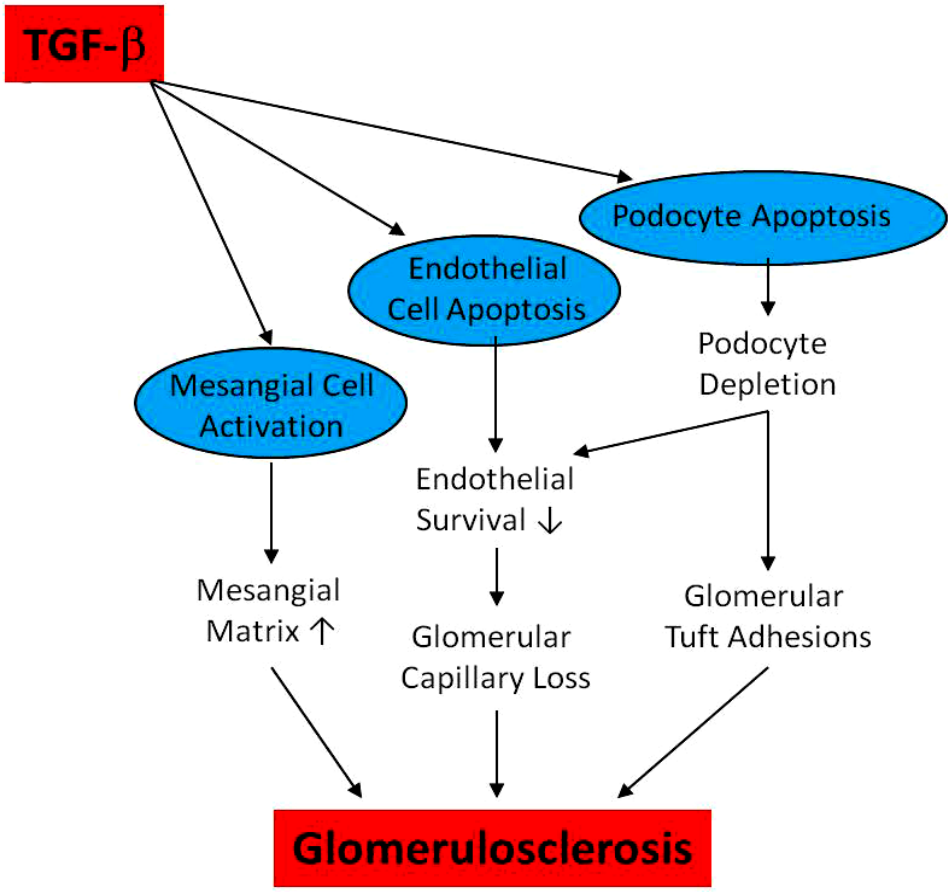

Figure 1.3. Cell-specific response to TGFβ and the mechanism leading to glomerulopathy. (Adapted from "TGF-beta signaling in renal disease" by E.P. Bottinger, and M. Bitzer, 2002, *J Am Soc Nephrol 13*, P.2604. Copyright 2002 by American Society of Nephrology. Used with permission).

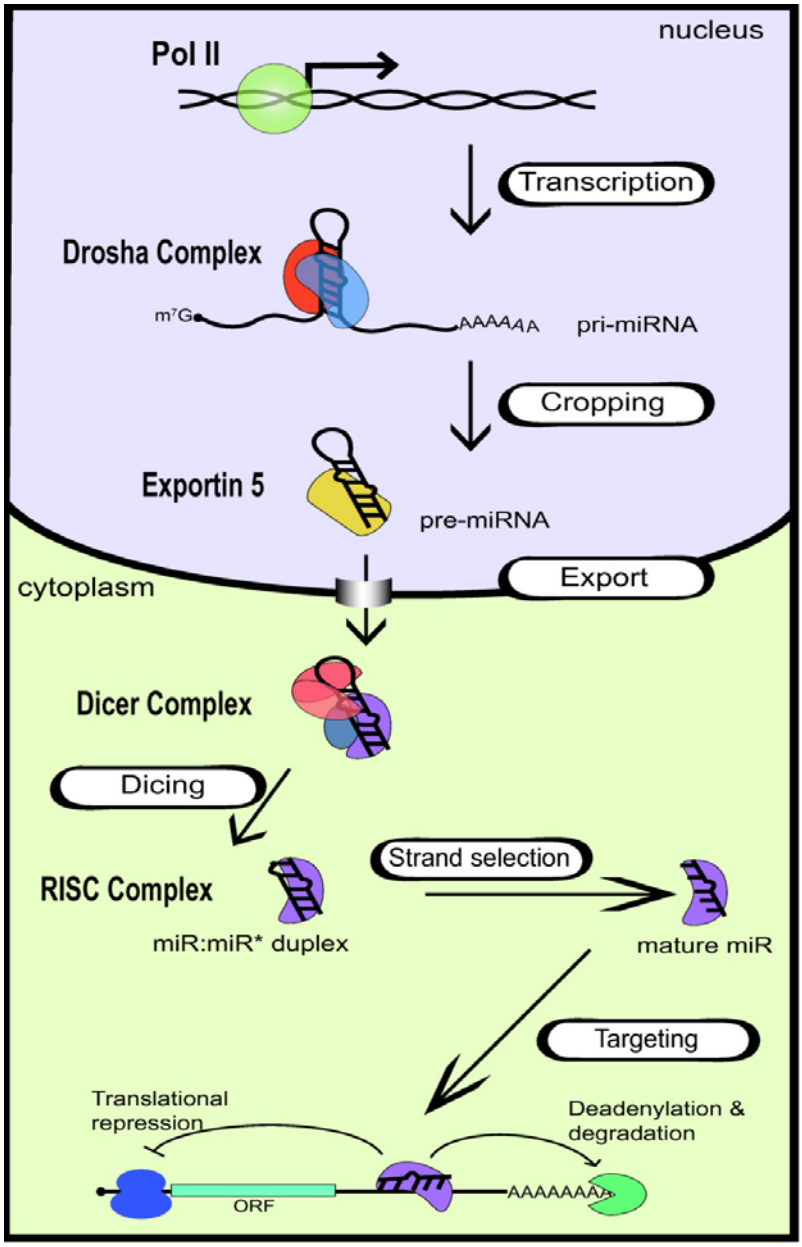

Figure 1.4. microRNA biogenesis and mRNA silencing mechanism. (Adapted from "Regulation of MicroRNA Biogenesis: A miRiad of mechanisms" by B.N. Davis, and A. Hata, 2009, *Cell Comm Signal 7*, P.18. Copyright 2009 by BioMed Central. Used with permission).

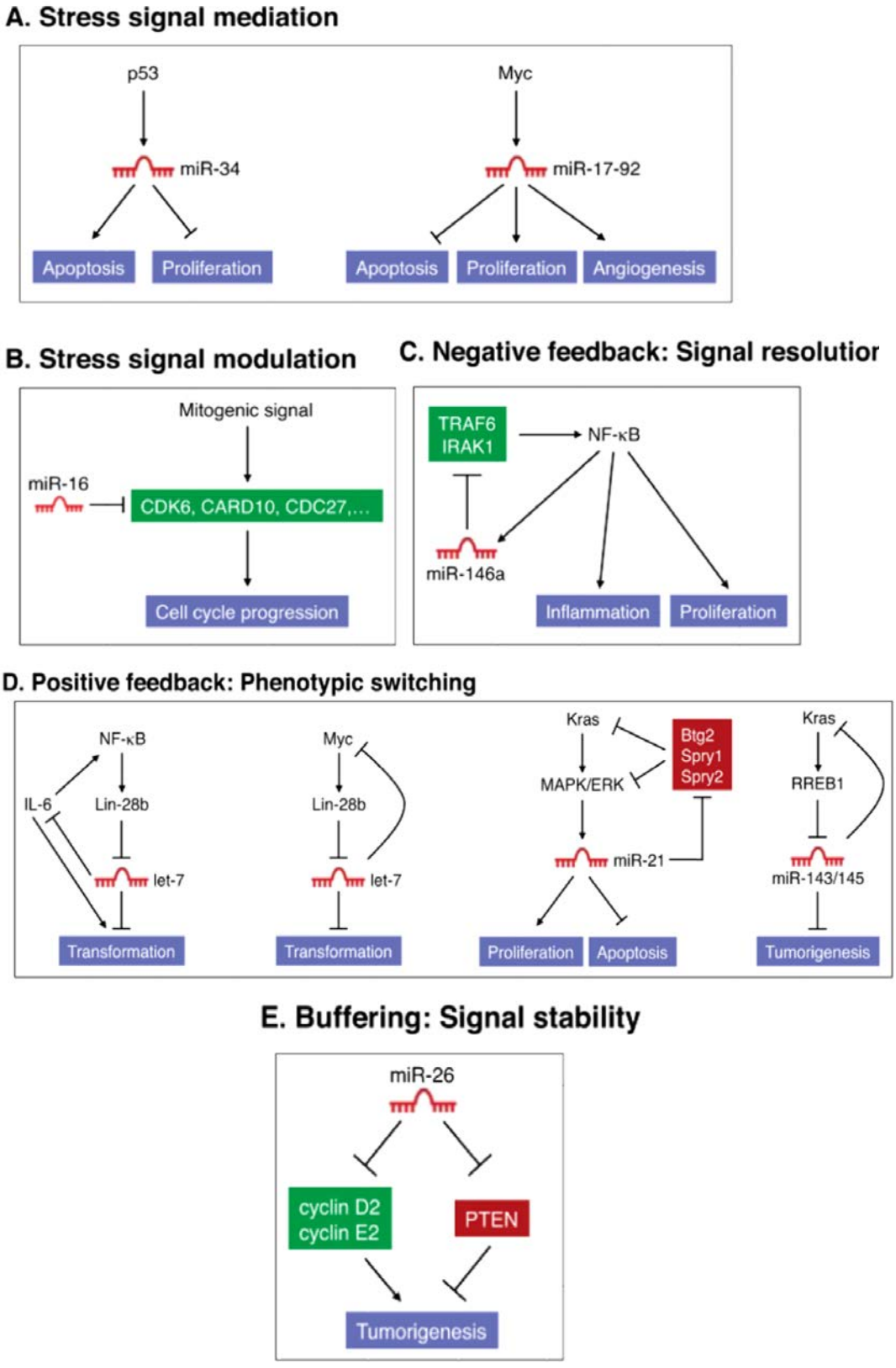

Figure 1.5. miRNA function in signaling mediation and modulation. (Adapted from "MicroRNAs in stress signaling and human disease" by J.T. Mendell, and E.N. Olson, 2012, *Cell 148*, P.1172. Copyright 2012 by Elsevier. Used with permission).

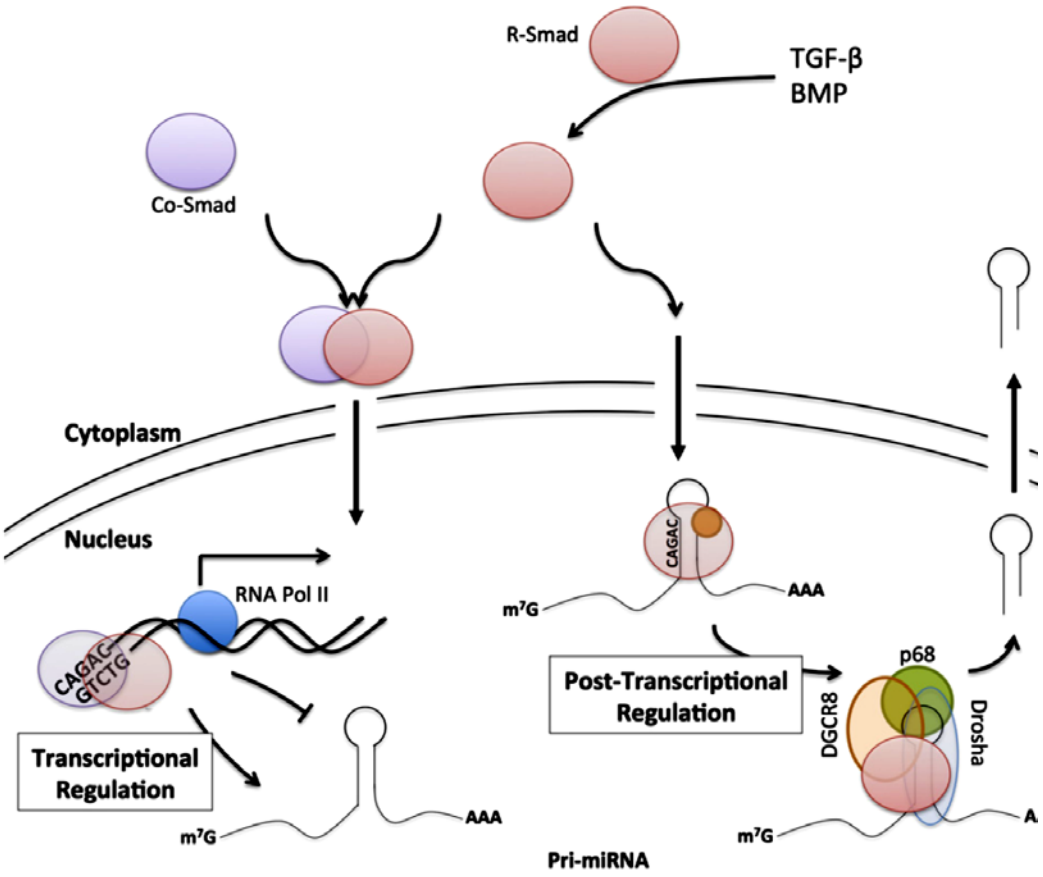

Figure 1.6. Regulation of miRNA transcription and maturation by TGFβ/Smad Signaling. (Adapted from "Smad-mediated regulation of microRNA biosynthesis" by M.T. Blahna, and A. Hata, 2012, *FEBS Letters 586*, P.1906. Copyright 2012 by Elsevier. Used with permission).

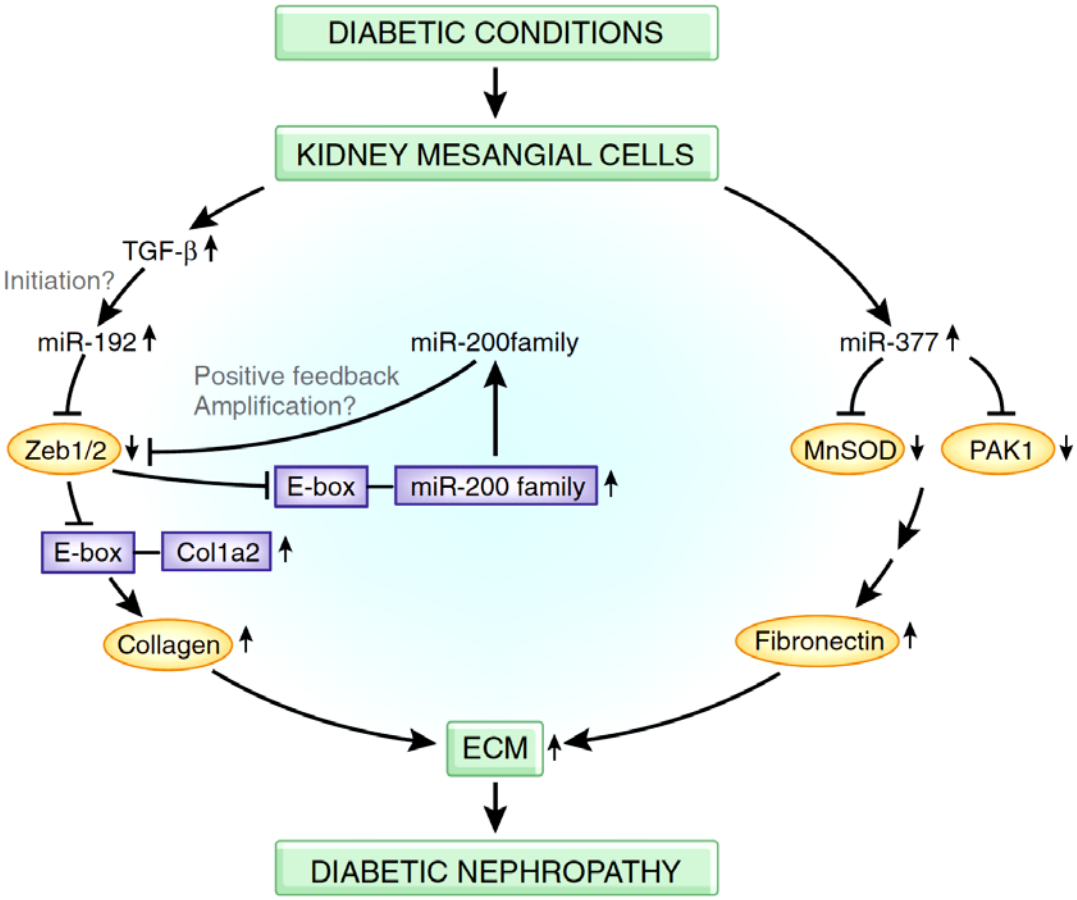

Figure 1.7. Regulatory mechanisms of miRNAs in diabetic nephropathy. (Adapted from "MicroRNAs and Their Role in Progressive Kidney Diseases" by M. Kato, L. Arce, and R. Natarajan, 2009, *Clin J Am Soc Nephrol 4* P.1255. Copyright 2009 by American Society of Nephrology. Used with permission).

References

1. Go, A.S., Chertow, G.M., Fan, D., McCulloch, C.E. & Hsu, C.Y. Chronic kidney disease and the risks of death, cardiovascular events, and hospitalization. *N Engl J Med* **351**, 1296-1305 (2004).
2. Coresh, J., *et al.* Prevalence of chronic kidney disease in the United States. *JAMA* **298**, 2038-2047 (2007).
3. US Renal Data System. USRDS 2011 Annual Data Report: Atlas of Chronic Kidney Disease and Eng Stage Renal Disease in the United States. (National Institutes of Health, National Institute of Diabetes and Digestive and Kidney Diseases, Bethesda, MD, 2011).
4. Wolf, G., Chen, S. & Ziyadeh, F.N. From the periphery of the glomerular capillary wall toward the center of disease: podocyte injury comes of age in diabetic nephropathy. *Diabetes* **54**, 1626-1634 (2005).
5. Reddy, G.R., Kotlyarevska, K., Ransom, R.F. & Menon, R.K. The podocyte and diabetes mellitus: is the podocyte the key to the origins of diabetic nephropathy? *Curr Opin Nephrol Hypertens* **17**, 32-36 (2008).
6. Goldfarb, S. & Ziyadeh, F.N. TGF-beta: a crucial component of the pathogenesis of diabetic nephropathy. *Transactions of the American Clinical and Climatological Association* **112**, 27-32; discussion 33 (2001).
7. Marshall, S.M. Recent advances in diabetic nephropathy. *Postgrad Med J* **80**, 624-633 (2004).
8. Jefferson, J.A., Shankland, S.J. & Pichler, R.H. Proteinuria in diabetic kidney disease: a mechanistic viewpoint. *Kidney Int* **74**, 22-36 (2008).
9. Fioretto, P. & Mauer, M. Histopathology of diabetic nephropathy. *Semin Nephrol* **27**, 195-207 (2007).
10. Kim, Y.H., *et al.* Podocyte depletion and glomerulosclerosis have a direct relationship in the PAN-treated rat. *Kidney Int* **60**, 957-968 (2001).
11. Schiffer, M., *et al.* Apoptosis in podocytes induced by TGF-beta and Smad7. *J Clin Invest* **108**, 807-816 (2001).
12. Massague, J. How cells read TGF-beta signals. *Nat Rev Mol Cell Biol* **1**, 169-178 (2000).
13. Massague, J. TGFbeta signalling in context. *Nat Rev Mol Cell Biol* **13**, 616-630 (2012).
14. Blobe, G.C., Schiemann, W.P. & Lodish, H.F. Role of transforming growth factor beta in human disease. *N Engl J Med* **342**, 1350-1358 (2000).
15. Lan, H.Y. Transforming growth factor-beta/Smad signalling in diabetic nephropathy. *Clinical and experimental pharmacology & physiology* **39**,

731-738 (2012).
16. Bottinger, E.P. & Bitzer, M. TGF-beta signaling in renal disease. *J Am Soc Nephrol* **13**, 2600-2610 (2002).
17. Meng, X.M., *et al.* Smad2 protects against TGF-beta/Smad3-mediated renal fibrosis. *J Am Soc Nephrol* **21**, 1477-1487 (2010).
18. Steffes, M.W., Schmidt, D., McCrery, R., Basgen, J.M. & International Diabetic Nephropathy Study, G. Glomerular cell number in normal subjects and in type 1 diabetic patients. *Kidney Int* **59**, 2104-2113 (2001).
19. Wharram, B.L., *et al.* Podocyte depletion causes glomerulosclerosis: diphtheria toxin-induced podocyte depletion in rats expressing human diphtheria toxin receptor transgene. *J Am Soc Nephrol* **16**, 2941-2952 (2005).
20. Shankland, S.J. The podocyte's response to injury: role in proteinuria and glomerulosclerosis. *Kidney Int* **69**, 2131-2147 (2006).
21. Qian, Y., Feldman, E., Pennathur, S., Kretzler, M. & Brosius, F.C., 3rd. From fibrosis to sclerosis: mechanisms of glomerulosclerosis in diabetic nephropathy. *Diabetes* **57**, 1439-1445 (2008).
22. Sanderson, N., *et al.* Hepatic expression of mature transforming growth factor beta 1 in transgenic mice results in multiple tissue lesions. *Proc Natl Acad Sci U S A* **92**, 2572-2576 (1995).
23. Kopp, J.B., *et al.* Transgenic mice with increased plasma levels of TGF-beta 1 develop progressive renal disease. *Lab Invest* **74**, 991-1003 (1996).
24. Yang, L. TGFbeta, a potent regulator of tumor microenvironment and host immune response, implication for therapy. *Curr Mol Med* **10**, 374-380 (2010).
25. Gordon, K.J. & Blobe, G.C. Role of transforming growth factor-beta superfamily signaling pathways in human disease. *Biochim Biophys Acta* **1782**, 197-228 (2008).
26. Wang, A., *et al.* Interference with TGF-beta signaling by Smad3-knockout in mice limits diabetic glomerulosclerosis without affecting albuminuria. *Am J Physiol Renal Physiol* **293**, F1657-1665 (2007).
27. Inazaki, K., *et al.* Smad3 deficiency attenuates renal fibrosis, inflammation,and apoptosis after unilateral ureteral obstruction. *Kidney Int* **66**, 597-604 (2004).
28. Zanninelli, G., *et al.* Smad3 knock-out mice as a useful model to study intestinal fibrogenesis. *World journal of gastroenterology : WJG* **12**, 1211-1218 (2006).
29. Bartel, D.P. MicroRNAs: genomics, biogenesis, mechanism, and function. *Cell* **116**, 281-297 (2004).

30. Lee, R.C., Feinbaum, R.L. & Ambros, V. The C. elegans heterochronic gene lin-4 encodes small RNAs with antisense complementarity to lin-14. *Cell* **75**, 843-854 (1993).
31. Pasquinelli, A.E., *et al.* Conservation of the sequence and temporal expression of let-7 heterochronic regulatory RNA. *Nature* **408**, 86-89 (2000).
32. Lee, Y., *et al.* MicroRNA genes are transcribed by RNA polymerase II. *EMBO J* **23**, 4051-4060 (2004).
33. Gregory, R.I., Chendrimada, T.P. & Shiekhattar, R. MicroRNA biogenesis: isolation and characterization of the microprocessor complex. *Methods Mol Biol* **342**, 33-47 (2006).
34. Lund, E. & Dahlberg, J.E. Substrate selectivity of exportin 5 and Dicer in the biogenesis of microRNAs. *Cold Spring Harb Symp Quant Biol* **71**, 59-66 (2006).
35. Bartel, D.P. MicroRNAs: target recognition and regulatory functions. *Cell* **136**, 215-233 (2009).
36. Kusenda, B., Mraz, M., Mayer, J. & Pospisilova, S. MicroRNA biogenesis, functionality and cancer relevance. *Biomed Pap Med Fac Univ Palacky Olomouc Czech Repub* **150**, 205-215 (2006).
37. Brenner, J.L., Jasiewicz, K.L., Fahley, A.F., Kemp, B.J. & Abbott, A.L. Loss of individual microRNAs causes mutant phenotypes in sensitized genetic backgrounds in C. elegans. *Current biology : CB* **20**, 1321-1325 (2010).
38. Park, C.Y., Choi, Y.S. & McManus, M.T. Analysis of microRNA knockouts in mice. *Human molecular genetics* **19**, R169-175 (2010).
39. Mendell, J.T. & Olson, E.N. MicroRNAs in stress signaling and human disease. *Cell* **148**, 1172-1187 (2012).
40. Chang, T.C., *et al.* Transactivation of miR-34a by p53 broadly influences gene expression and promotes apoptosis. *Mol Cell* **26**, 745-752 (2007).
41. Feng, Z., Zhang, C., Wu, R. & Hu, W. Tumor suppressor p53 meets microRNAs. *Journal of molecular cell biology* **3**, 44-50 (2011).
42. Leung, A.K. & Sharp, P.A. MicroRNA functions in stress responses. *Mol Cell* **40**, 205-215 (2010).
43. Davis, B.N., Hilyard, A.C., Lagna, G. & Hata, A. SMAD proteins control DROSHA-mediated microRNA maturation. *Nature* **454**, 56-61 (2008).
44. Kong, W., *et al.* MicroRNA-155 is regulated by the transforming growth factor beta/Smad pathway and contributes to epithelial cell plasticity by targeting RhoA. *Mol Cell Biol* **28**, 6773-6784 (2008).
45. Davis, B.N., Hilyard, A.C., Nguyen, P.H., Lagna, G. & Hata, A. Smad proteins bind a conserved RNA sequence to promote microRNA maturation

by Drosha. *Mol Cell* **39**, 373-384 (2010).
46. Blahna, M.T. & Hata, A. Smad-mediated regulation of microRNA biosynthesis. *FEBS Lett* **586**, 1906-1912 (2012).
47. He, L., *et al.* A microRNA polycistron as a potential human oncogene. *Nature* **435**, 828-833 (2005).
48. Thum, T., *et al.* MicroRNAs in the human heart: a clue to fetal gene reprogramming in heart failure. *Circulation* **116**, 258-267 (2007).
49. Kato, M., *et al.* MicroRNA-192 in diabetic kidney glomeruli and its function in TGF-beta-induced collagen expression via inhibition of E-box repressors. *Proc Natl Acad Sci U S A* **104**, 3432-3437 (2007).
50. Krupa, A., *et al.* Loss of MicroRNA-192 promotes fibrogenesis in diabetic nephropathy. *J Am Soc Nephrol* **21**, 438-447 (2010).
51. Kato, M., Arce, L. & Natarajan, R. MicroRNAs and their role in progressive kidney diseases. *Clinical journal of the American Society of Nephrology : CJASN* **4**, 1255-1266 (2009).
52. Wang, Q., *et al.* MicroRNA-377 is up-regulated and can lead to increased fibronectin production in diabetic nephropathy. *FASEB journal : official publication of the Federation of American Societies for Experimental Biology* **22**, 4126-4135 (2008).
53. Krutzfeldt, J., *et al.* Silencing of microRNAs in vivo with 'antagomirs'. *Nature* **438**, 685-689 (2005).
54. Lanford, R.E., *et al.* Therapeutic silencing of microRNA-122 in primates with chronic hepatitis C virus infection. *Science* **327**, 198-201 (2010).
55. Jopling, C.L., Yi, M., Lancaster, A.M., Lemon, S.M. & Sarnow, P. Modulation of hepatitis C virus RNA abundance by a liver-specific MicroRNA. *Science* **309**, 1577-1581 (2005).
56. Cho, W.C. OncomiRs: the discovery and progress of microRNAs in cancers. *Molecular cancer* **6**, 60 (2007).
57. Chan, J.A., Krichevsky, A.M. & Kosik, K.S. MicroRNA-21 is an antiapoptotic factor in human glioblastoma cells. *Cancer Res* **65**, 6029-6033 (2005).
58. Carletti, M.Z., Fiedler, S.D. & Christenson, L.K. MicroRNA 21 blocks apoptosis in mouse periovulatory granulosa cells. *Biol Reprod* **83**, 286-295 (2010).
59. Medina, P.P., Nolde, M. & Slack, F.J. OncomiR addiction in an in vivo model of microRNA-21-induced pre-B-cell lymphoma. *Nature* **467**, 86-90 (2010).
60. Thum, T., *et al.* MicroRNA-21 contributes to myocardial disease by

stimulating MAP kinase signalling in fibroblasts. *Nature* **456**, 980-984 (2008).

61. Zhong, X., Chung, A.C., Chen, H.Y., Meng, X.M. & Lan, H.Y. Smad3-mediated upregulation of miR-21 promotes renal fibrosis. *J Am Soc Nephrol* **22**, 1668-1681 (2011).
62. Chau, B.N., *et al.* MicroRNA-21 promotes fibrosis of the kidney by silencing metabolic pathways. *Sci Transl Med* **4**, 121ra118 (2012).
63. Eddy, A.A. The TGF-beta route to renal fibrosis is not linear: the miR-21 viaduct. *J Am Soc Nephrol* **22**, 1573-1575 (2011).
64. Lewis, B.P., Burge, C.B. & Bartel, D.P. Conserved seed pairing, often flanked by adenosines, indicates that thousands of human genes are microRNA targets. *Cell* **120**, 15-20 (2005).
65. Grimson, A., *et al.* MicroRNA targeting specificity in mammals: determinants beyond seed pairing. *Mol Cell* **27**, 91-105 (2007).
66. Friedman, R.C., Farh, K.K., Burge, C.B. & Bartel, D.P. Most mammalian mRNAs are conserved targets of microRNAs. *Genome Res* **19**, 92-105 (2009).
67. Enright, A.J., *et al.* MicroRNA targets in Drosophila. *Genome Biol* **5**, R1 (2003).
68. Betel, D., Wilson, M., Gabow, A., Marks, D.S. & Sander, C. The microRNA.org resource: targets and expression. *Nucleic Acids Res* **36**, D149-153 (2008).
69. Yue, D., Liu, H. & Huang, Y. Survey of Computational Algorithms for MicroRNA Target Prediction. *Curr Genomics* **10**, 478-492 (2009).
70. Xiao, F., *et al.* miRecords: an integrated resource for microRNA-target interactions. *Nucleic Acids Res* **37**, D105-110 (2009).
71. Sales, G., *et al.* MAGIA, a web-based tool for miRNA and Genes Integrated Analysis. *Nucleic Acids Res* **38**, W352-359 (2010).
72. Li, X., Gill, R., Cooper, N.G., Yoo, J.K. & Datta, S. Modeling microRNA-mRNA interactions using PLS regression in human colon cancer. *BMC Med Genomics* **4**, 44 (2011).
73. Muniategui, A., *et al.* Quantification of miRNA-mRNA interactions. *PLoS One* **7**, e30766 (2012).
74. Huang, J.C., Morris, Q.D. & Frey, B.J. Bayesian inference of MicroRNA targets from sequence and expression data. *J Comput Biol* **14**, 550-563 (2007).
75. Nelson, R.G., *et al.* Incidence of end-stage renal disease in type 2 (non-insulin-dependent) diabetes mellitus in Pima Indians. *Diabetologia* **31**,

730-736 (1988).
76. Imperatore, G., Knowler, W.C., Nelson, R.G. & Hanson, R.L. Genetics of diabetic nephropathy in the Pima Indians. *Curr Diab Rep* **1**, 275-281 (2001).
77. Ju, W., *et al.* Renal gene and protein expression signatures for prediction of kidney disease progression. *Am J Pathol* **174**, 2073-2085 (2009).
78. Kerr, J.F., Wyllie, A.H. & Currie, A.R. Apoptosis: a basic biological phenomenon with wide-ranging implications in tissue kinetics. *Br J Cancer* **26**, 239-257 (1972).
79. Orban, P.C., Chui, D. & Marth, J.D. Tissue- and site-specific DNA recombination in transgenic mice. *Proc Natl Acad Sci U S A* **89**, 6861-6865 (1992).
80. Papagiannakopoulos, T., Shapiro, A. & Kosik, K.S. MicroRNA-21 targets a network of key tumor-suppressive pathways in glioblastoma cells. *Cancer Res* **68**, 8164-8172 (2008).
81. Frankel, L.B., *et al.* Programmed cell death 4 (PDCD4) is an important functional target of the microRNA miR-21 in breast cancer cells. *J Biol Chem* **283**, 1026-1033 (2008).
82. Keeling, J. & Herrera, G.A. Human matrix metalloproteinases: characteristics and pathologic role in altering mesangial homeostasis. *Microsc Res Tech* **71**, 371-379 (2008).
83. Thrailkill, K.M., Clay Bunn, R. & Fowlkes, J.L. Matrix metalloproteinases: their potential role in the pathogenesis of diabetic nephropathy. *Endocrine* **35**, 1-10 (2009).
84. Like, A.A. & Rossini, A.A. Streptozotocin-induced pancreatic insulitis: new model of diabetes mellitus. *Science* **193**, 415-417 (1976).
85. Nigg, E.A. Cyclin-dependent protein kinases: key regulators of the eukaryotic cell cycle. *Bioessays* **17**, 471-480 (1995).
86. Ekholm, S.V. & Reed, S.I. Regulation of G(1) cyclin-dependent kinases in the mammalian cell cycle. *Current opinion in cell biology* **12**, 676-684 (2000).
87. Boutros, R., Lobjois, V. & Ducommun, B. CDC25 phosphatases in cancer cells: key players? Good targets? *Nature reviews. Cancer* **7**, 495-507 (2007).
88. Wang, P., *et al.* microRNA-21 negatively regulates Cdc25A and cell cycle progression in colon cancer cells. *Cancer Res* **69**, 8157-8165 (2009).
89. Hafner, M., *et al.* Transcriptome-wide identification of RNA-binding protein and microRNA target sites by PAR-CLIP. *Cell* **141**, 129-141 (2010).

Chapter II

MicroRNA-21 Ameliorates TGF-beta Mediated Glomerular Injury

Abstract

Glomerulopathy is a hallmark of diabetic nephropathy (DN), the leading cause of end-stage renal disease (ESRD) in the US. Glomerulopathy is associated with imbalance of signaling cascades regulated by transforming growth factor-beta (TGFβ), contributing to loss of podocytes and albuminuria. MicroRNAs (miRNAs) regulate cellular functions through modulation of signaling cascades via feed-forward loops.

To identify miRNAs that regulate initiation and development of human DN, we associated miRNA expression with albuminuria in micro-dissected glomeruli of 26 American Indian patients exhibiting clinically early stages of DN. Twenty out of 377 miRNAs exhibited significant correlation with urine albumin-to-creatinine ratio (ACR) ($R>0.6$; $P<0.0001$); of those, miR-21 was highly abundant and also exhibited significant correlation with ACR in a second cohort (n=22). miR-21 is regulated by $TGF\beta_1$, which is increased in glomeruli of patients with DN. miR-21-deficient $TGF\beta_1$ transgenic mice exhibit increased proteinuria and glomerular extracellular matrix

(ECM) deposition, and decreased number of podocytes. MiR-21-deficiency was accompanied by increased TGFβ/Smad-signaling activity and expression of p53, Smad7, Pdcd4 and Timp3.

We conclude that miR-21 functions as a feed-forward loop ameliorating glomerular injury through inhibition of TGFβ-induced podocyte loss and ECM deposition, consistent with its role in cancer.

Introduction

DN is a common and devastating microvascular complication in patients with diabetes and the leading cause of renal failure in patients requiring dialysis[1]. Although understanding of the underlying mechanisms has progressed significantly and interventions have been implemented, diabetic patients with kidney disease continue to have a much higher risk of death than diabetic patients with normal renal function[2], suggesting the need for new drug targets.

MiRNAs are ~22 nucleotide RNAs that guide RISC to 3'UTR of target mRNAs and thereby repress expression of protein-coding genes. miRNAs can regulate large numbers of target genes and are often integrated in positive and negative feedback loops and have been implicated as modulators of stress responses in many physiologic and pathologic processes[3].

In animal models, several miRNAs have been identified that mediate initiation and development of DN by altering the expression of TGFβ signaling components[4]. TGFβ is a key factor in the initiation and progression of DN by promoting extracellular matrix deposition and loss of podocytes[5]. TGFβ also regulates expression of miRNAs on a transcriptional and post-transcritpional level[6]. Significantly less is known about the role of miRNAs in human DN, but available data support that the current knowledge about miRNAs in murine models of DN is

also relevant in patients with DN[7].

Here we report our findings from the analysis of miRNA expression in micro-dissected glomeruli of kidney biopsies from patients with DN and its associations with proteinuria, a clinically relevant parameter of kidney damage and prognostic marker of DN progression. Furthermore, we provide experimental evidence that miR-21 protects against TGFβ-mediated renal injury by preventing podocyte apoptosis via inhibition of pro-apoptotic members of the TGFβ signaling cascade. This finding is contrary to the reported pro-fibrotic role of miR-21 in models of tubulo-interstitial kidney injury, but it is in line with its well-established oncogenic and anti-apoptotic capacity in cancer.

Results

General characteristics of study cohorts

Study subjects were divided into two cohorts for testing and validation. Both cohorts included more female subjects. Urine was collected over 24 hours and urine albumin to creatinine ratio (ACR) was measured. Participants in our cohorts exhibited a broad range of ACR (μg/mg), while the mean glomerular filtration rate (GFR, iothalamate clearance) was above 90 ml/min/1.73m^2 for both cohorts (Table 2.1). There was no statistical difference in age, gender distribution, ACR, or GFR at time of biopsy between the cohorts.

MiRNA expression profiles generated by RNA sequencing and quantitative reanl time PCR (qrt-PCR) exhibit a high correlation

The amount of total RNA isolated from micro-dissected glomeruli is limited (usually ranging from 20 to 200ng per sample). The Taqman-based miRNA array (Applied Biosystems) is suitable for these small amounts of total RNA when using pre-amplification. We did not detect significant differences in miRNA expression with or without pre-amplification using human kidney biopsy tissues. As different miRNA profiling methods have been shown to exhibit variable correlations[8,9], we compared the Taqman-qrt-PCR-based array method with RNA sequencing using the

same RNA pool from whole kidneys of a 3 month- old C57BI/6J mouse. We found that miRNA sequence reads from RNA sequencing correlated with miRNA cycle time generated from qrt-PCR-based miR array (R=0.7, Figure 2.1). For example, miR-21 showed very high expression using both RNA sequencing and qrt-PCR array. In view of the low RNA content in renal glomeruli and good correlation of miRNA profiling between RNA sequencing and qrt-PCR array, we proceeded to apply qrt-PCR-based miRNA array with amplification to profile miRNA in the renal glomeruli of our cohorts as described[10].

Correlation of miRNA expression with ACR

To identify miRNA relevant for glomerular injury, we associated miRNA expression levels with clinical-relevant phenotypes, such as ACR or GFR in our American Indian cohorts. Highly significant correlations with ACR were detected for 20 miRNAs. Among those, miR-21 has the lowest CT value (highest relative abundance in the glomeruli) and a statistically very high correlation with ACR in cohort 1 (testing cohort) (R=0.8, Table 2.2A). Because validation in the same sample was not feasible due to a limited amount of RNA, we further validated these findings in cohort 2 (validating cohort). miR-21 maintained the high expression in renal glomeruli as well as the significant correlation with ACR (R=0.51, Table 2.2B).

However, there was no significant correlation between miRNA and GFR (P-value > 0.05 for all miRNA). Patients with normo- versus micro-albuminuria did not have differences in miR-21 levels, whereas patients with macro-albuminuria exhibited significantly increased miR-21 in glomeruli (Figure 2.2).

Increased TGFβ gene expression in human DN

Glomerular mRNA expression profiles of living donors and the American Indian subjects with DN have been recently reported[11]. In this data set, $TGF\beta_1$ mRNA expression (TGFB1) was higher in glomeruli of subjects with DN compared with living donor (fold change=1.22, FDR<0.0001), consistent with previous findings in other cohorts[12].

miR-21 and TGFβ levels correlate with kidney damage severity in $TGF\beta_1$ transgenic mice

As miR-21 has been shown to be regulated by $TGF\beta_1$, transgenic overexpression of $TGF\beta_1$ causes proteinuria and progressive glomerulosclerosis[13,14], and miR-21 levels are highly correlated with proteinuria in humans, we examined miR-21 expression in $TGF\beta_1$ transgenic mice. We found that miR-21 expression in kidneys of $TGF\beta_1$ transgenic mice increased progressively with the severity of kidney

damage based on histological scores as described[15] (Figure 2.3A). Furthermore, TGFβ_1 mRNA levels also positively correlated with the severity of kidney damage (Figure 2.3B). Therefore, we chose TGFβ_1 transgenic mice to further examine the function of miR-21 in glomerular injury.

TGFβ_1 transgenic/miR-21 KO mice develop increased proteinuria, extracellular matrix deposition, and diffuse glomerulosclerosis

In order to investigate the function of miR-21 in TGFβ-related glomerular injury, we obtained miR-21 KO mice. These mice showed no evidence of structural abnormalities in the kidney compared to miR-21 WT mice (Figure 2.4). We crossed miR-21 KO with TGFβ_1 transgenic mice to generate TGFβ_1 transgenic (TG)/miR-21 WT and TG/miR-21 KO littermates in the C57BI/6J background and examined the kidney function and structure of those littermates at 4 weeks of age. Qualitative and quantitative analysis of urine samples showed increased proteinuria in TG/miR-21 WT mice as expected, but nearly 50% of TG/miR-21 KO mice developed strongly increased albuminuria compared to TG/miR-21 WT mice (Figure 2.5). Plasma TGFβ_1 concentration (Figure 2.6A) and glomerular TGFβ_1 mRNA levels (Figure 2.6B) were not different between of TG/miR-21 WT and KO mice.

Histologically, glomeruli of TG/miR-21 KO mice exhibited increased deposition of

Periodic Acid-Schiff (PAS)-positive material (Figure 2.7A) as well as picrosirius red staining intensity (Figure 2.7A&B). Consistent with these results, in glomeruli, collagen III protein (Figure 2.7A), and collagen III, IV and VI mRNA expression were increased (Figure 2.7C). The pattern of ECM deposition in glomeruli of TG/miR-21 KO was nodular (Figure 2.7A). No differences were detected in the tubulointerstitium between TG/miR-21 WT and TG/miR-21 KO mice. The findings are consistent with accelerated glomerulosclerosis induced by TGFβ in the absence of miR-21.

Loss of miR-21 is associated with decreased podocyte density in TGFβ$_1$ transgenic mice

Loss of podocytes causes glomerulosclerosis[16] and has been detected in TGFβ$_1$ transgenic mice[17]. To examine whether accelerated glomerulosclerosis in TG/miR-21 KO mice is associated with decreased podocyte density, we determined podocyte number per glomerular tuft in TG/miR-21 WT and KO mice.

We applied podocyte-specific nuclear protein, WT1, to identify podocytes in glomeruli. Using DAPI nucleic acid and WT1 immunofluorescent staining, we found that TG/miR-21 KO mice have a similar number of total cells and WT1-positive cells per glomerular tuft compared to their TG/miR-21 WT littermates

at 2 weeks of age (Figure 2.8A). At 4 weeks of age, we detected a decreased number of total cells and WT1-positive nuclei per glomerular tuft in TG/miR-21-KO mice compared to the WT littermates (Figure 2.8B). The data suggested that the decreased number of total cells and WT1-positive cells in TG/miR-21 KO mice is due to loss of podocytes from 2 weeks old to 4 weeks old.

Loss of miR-21 promotes glomerular cell apoptosis

miR-21 is an anti-apoptotic factor in cancer and other cells[18,19]. Podocyte apoptosis has been demonstrated to be the initiating event leading to glomerulosclerosis[20]. Therefore, we examined apoptotic events prior to depletion of podocytes in glomeruli of 2 weeks old TG/miR-21 WT and KO mice by determining activation and cleavage of caspase 3[21,22]. As predicted we detected cleaved caspase 3 by immunohistochemistry in both TG/miR-21 WT and KO mice. Furthermore, significantly more positive cells were seen in glomeruli of TG/miR-21 KO mice (Figure 2.9A).

To determine specifically whether miR-21 regulates podocyte death, we examined podocyte apoptosis in cultured murine podocytes after transfection with antisense miR-21 or scramble oligonucleotides. Apoptosis was identified by annexin V-FITC and propidium iodide (PI) double-labeling using flow cytometry after serum

withdrawal. We found that podocytes transfected with antisense miR-21 oligonucleotides have significantly more apoptotic cells than podocytes transfected with scramble oligonucleotides (Figure 2.9B). Furthermore, when apoptosis was assessed by measuring loss of mitochondrial membrane potential, at 24 hours after $TGF\beta_1$ treatment, podocytes transfected with miR-21 mimic or antisense oligonucleotides exhibited decreased and increased apoptosis, respectively, compared to cells transfected with scramble oligonucleotides (Figure 2.9C). These findings suggested that increased podocyte apoptosis underlies the accelerated glomerulosclerosis in $TGF\beta_1$ transgenic mice deficient for miR-21.

Loss of miR-21 leads to increased expression of pro-apoptotic proteins

TGFβ is known to induce apoptosis through Smad7 and phosphorylation of Smad3[23]. P53 (Trp53) and programmed cell death 4 (Pdcd4) are tumor suppressor proteins, which induce apoptosis[24,25]. Trp53 was indirectly suppressed by miR-21[24] and Pdcd4 was targeted by miR-21 in cancer cells[25]. Cross referencing proteins in pro-apoptotic pathways with miR-21 predicted targets using TargetScan prediction algorithm 6.1[26], we found that TGFβ receptor 2 (Tgfbr2), TGFβ induced (Tgfbi), Smad7, which are members of the TGFβ-signaling cascade and mediators of TGFβ-induced apoptosis[26], and Pdcd4 are predicted targets of miR-21 (Figure 2.10A).

To determine whether miR-21 regulates TGFβ-signaling activity in podocytes, we first examined Smad signaling activity in murine podocytes exposed to TGFβ and transfected with antisense miR-21 oligonucleotides. Smad3 phosphorylation was increased 4 and 24 hours after exposure to TGFβ_1 and the phosphorylation of Smad3 was even higher when miR-21 was suppressed (Figure 2.10B). Levels of Pdcd4 was downregulated by TGFβ_1 (Figure 2.10C). However, levels of Pdcd4 were increased in cells when miR-21 was suppressed. *In vivo*, Tgfbr2, Tgfbi, Smad7, and Trp53 mRNAs expression were increased in glomeruli of TG/miR-21 KO mice compared to TG/miR-21 WT mice (Figure 2.10D). miR-21 has been reported to target the 3'UTRs of Pdcd4[25] and Tgfbr2[27].

In podocytes, Smad7 is shown to be induced by TGFβ and induces apoptosis[28]. While inhibition of miR-21 had no effect on Smad7 levels in unchallenged podocytes, inhibition of miR-21 led to increased mRNA levels of Smad7 after 24 hours exposure to TGFβ_1 (Figure 2.10E). In a luciferase assay, we co-transfected Smad7 3'UTR luciferase construct and miR-21 mimic or antisense miR-21 oligonucleotides into 293T human embryonic kidney cells. We found the luciferase activity of Smad7 3'UTR decreased by miR-21 overexpression and increased by miR-21 inhibition in cells (Figure 2.10F). We confirmed that Smad7 is a direct target of miR-21 as previously reported[29]. These results suggest that the anti-apoptotic

capacity of miR-21 is at least in part mediated by inhibition of multiple pro-apoptotic signals, including Smad7, Trp53, Pdcd4, and TGFβ/Smad3 signaling via Tgfbr2.

miR-21 regulates glomerular ECM deposition

Increased ECM deposition is another hallmark of TGFβ-related glomerulopathy and contributes to development and progression of glomerulosclerosis. ECM deposition is enhanced by increased collagen production or decreased breakdown of extracellular collagen by metalloproteinases (MMPs). Tissue inhibitors of metalloproteinase (TIMP) diminish the degradative capacity of extracellular MMPs. We found collagen4a1 (Col4a1) as well as Timp3 mRNA was increased in glomeruli of TG/miR-21 KO mice versus TG/miR-21 WT mice (Figure 2.7C & 2.10D). Both mRNAs are predicted targets of miR-21 (Figure 2.10A). To demonstrate the specificity of the increased mRNA levels of the listed miR-21 predicted targets in our mice, we showed that Ras homolog gene family member B (RhoB), another predicted target genes of miR-21, which have also been implicated in TGFβ signaling[30], remained unchanged in TG/miR-21 KO mice versus TG/miR-21 WT mice (Figure 2.10D). Furthermore, we also found that Timp3 mRNA levels were increased in cultured mouse podocytes transfected with antisense miR-21

oligonucleotides (Figure 2.10E), and Timp3 mRNA has been experimentally confirmed as a miR-21 target in glioma cells[31].

Discussion

In this study, we determined the expression of glomerular miR-21 and miR-221 exhibiting significant correlation with ACR in a total of 48 patients with early to intermediate histopathologic alterations of DN secondary to type 2 diabetes mellitus[11]. Few studies have explored miRNA expression in patients with DN. Krupa et al. have identified miRNAs that differentially expressed in kidney tissues of 22 patients with progressive and non-progressive DN as well as with different disease stages[7]. Because of the different designs from our study including pooled formalin-fixed material from whole kidney biopsies, which constitutes mainly tubulo-interstitium, significant lower eGFR, and using miR-16 as the reference miRNA for normalization, the results from Krupa et al. and ours are not comparable. Another study has shown that urinary miR-21 levels were higher in adolescent Hong Kong Chinese with albuminuria than that without albuminuria[32]. We also detected increased miR-21 levels in adolescent patients with FSGS compared to controls or minimal change disease (personal communication Robert P. Woroniecki and Markus Bitzer, unpublished results; ASN 2008, abstract [TH-P0349]). miR-21 is important also because it has been identified as a widely expressed and consistently elevated miRNA in human cancer and it is a candidate target for intervention because inhibition of miR-21 limits tumor growth[33]. In animal models of kidney injury,

miR-21 expression is consistently increased. However, its function remains controversial as it has been shown to promote or protect from tubulo-interstitial[34,35] as well as glomerular[36,37] damage in different model systems.

miR-21 is of special interest because in murine models of tubulo-interstitial kidney[35] and lung disease[38], miR-21 promotes fibrosis through multiple mechanisms including regulation of TGFβ signaling. But the function of miR-21 is complex. In the heart, miR-21 has been reported to contribute to myocardial disease[39], ameliorates development of heart failure after cardiac ischemia[40], but is not essential for cardiac remodeling[41]. We have recently shown that inhibition of miR-21 in a murine model of myelodysplastic syndrome leads to stimulation of hematopoiesis and improvement of phenotype[29]. Furthermore, miR-21 exhibits oncogenic activity through inhibition of apoptosis in most solid cancers and is explored as a therapeutic target[33]. Podocytopenia is an important cause of glomerulosclerosis[16] and is a robust predictor of disease progression in DN[5]. Podocyte apoptosis has been detected in various animal models of glomerular injury including DN[42] and TGFβ$_1$ transgenic mice[17], and can be induced by TGFβ in cultured podocytes[17]. Our finding that loss of miR-21 results in increased podocyte loss is consistent with anti-apoptotic function of miR-21 in cancer, thereby promoting cancer progression[24]. Albuminuria is strongly associated with podocyte damage and miR-21 is strongly correlated with

ACR. Therefore, promoting podocyte survival is an important and possibly the most prominent function of miR-21 in glomerular injury.

We determined that miR-21 represses multiple signals that have been shown to promote apoptosis in podocytes, including TGFβ/Smad3 signaling[17], Smad7[28] and Trp53[43]. Furthermore, Pdcd4 has been shown to be a pro-apoptotic molecule involved in $TGF\beta_1$-induced apoptosis in human hepatocellular carcinoma cells. Increased Smad3 phosphorylation is likely mediated by de-repression of Tgfbr2, a previously reported target of miR-21[27]. While miR-21 binds the 3'UTR thereby repressing expression of Smad7[38] and Pdcd4[24], miR-21 inhibits Trp53 expression indirectly via targeting Trp53-binding proteins[24]. Tgfbi induces apoptosis in cancer cells[44] and it is a predicted target of miR-21, however, it has not been studied in podocytes. The increased detection of pro-apoptotic signals in TGmiR-21 KO mice is not mediated through $TGF\beta_1$ *per se*, because plasma and intra-renal $TGF\beta_1$ levels were not different between genotypes (Figure 2.6). Thus, miR-21 mediates its function through a large set of target genes.

The diverse function of miR-21 depends on organ systems and injuries and it is also likely to be secondary to the differential expression of target genes. TGFβ activates multiple signaling cascades, exhibits cell-type and context-specific functions, and is integrated in a complex regulatory network with feed-forward and feedback loops[23].

Furthermore, maintaining a tight homeostasis of TGFβ-signaling is essential for proper function of cells and organ system, underscored by the fact that abundant TGFβ1 leads to organ fibrosis[45] whereas TGFβ1-deficiency leads to excessive inflammatory responses[46]. Similar to miR-21, miR-192 and miR-200a have been implicated in feedback regulation of TGF-beta signaling in DN[4].

The high abundance of miR-21 in human glomeruli and mouse kidneys (Figure 2.1 & Table 2.2) suggests its high biological activity, because miRNAs are in stoichiometric competition with other miRNAs on RISC-loading and they target equivalent amounts of mRNA[47]. Therefore, it is somewhat surprising that miR-21-deficient mice do not exhibit developmental or anatomic abnormalities and are fertile[48] (Figure 2.4). This is consistent with the concept that few target genes are repressed by miR-21 under normal cellular conditions but the repression is enhanced under cellular stress[49].

In addition to its anti-apoptotic effect, miR-21 regulates ECM deposition. Collagen 4a1 is a direct target of miR-21[50] and was increased in glomeruli of TG.miR-21 KO mice. TIMPs inhibit the capacity of MMPs to degrade extracellular collagens and thus promote ECM accumulation. We had shown inverse correlation of Timp3 and miR-21 expression in human tissues[51] and others confirmed repression of Timp3 expression by miR-21 via direct targeting of the Timp3 3'UTR[31]. In our study, we

showed increased ECM deposition and Timp3 expression in glomeruli of TG/miR-21 KO mice. These findings suggest that inhibition of ECM deposition by miR-21 contributes to protection against glomerulopathy.

In summary, our findings support a feed-forward loop in the TGFβ/Smad signaling cascade, in which miR-21 represses multiple TGFβ target genes thereby preventing TGFβ-induced podocyte apoptosis and ECM deposition in glomeruli (Figure 2.11). Our findings further support a context-dependent function and interaction between TGFβ-signaling and miR-21.

Methods and Materials

Study subjects. Kidney biopsy samples were collected from 111 Southwestern American Indians enrolled in a randomized, placebo-controlled, clinical trial to test the renoprotective efficacy of losartan in early type 2 diabetic kidney disease (ClinicalTrials.gov No. NCT00340678) as described[52]. In brief, subjects were treated with either losartan or placebo for a median of 5.9 years and a percutaneous kidney biopsy was obtained at the end of the treatment period. Kidney biopsy specimens were placed into RNA*later*® and stored in -20ºC until glomeruli were micro-dissected from biopsy cores as described[53]. Tissue specimens from 48 subjects were included in this study.

Urinary albumin and creatinine as well as iothalamate concentrations for GFR determination were measured as described[52] and values of the examination closest to the kidney biopsy were used in the present analyses. This study was approved by the Review Board of the National Institute of Diabetes and Digestive and Kidney Diseases. Each participant gave informed consent.

miRNA expression analysis. miRNA profiling was obtained using TaqMan miRNA assays (Applied Biosystems) as described[54]. In brief, small RNA fraction (<200 nt) was isolated from micro-dissected glomeruli using RNeasy® and MinElute®

Cleanup kits (Qiagen) and reverse transcribed using TaqMan Megaplex RT primers (Applied Biosystems). Human glomerular small RNA was amplified by Megaplex PreAmp primers (Applied Biosystems). TaqMan array human and rodent miRNA 'A' cards (Applied Biosystems) were used to obtain miRNA profiles according to the manufacturer's protocol. miRNA expression values, threshold cycle (CT), were normalized by U6 small nuclear RNA (snRNA), and RNU44 and RNU48 small nucleolar RNA (snoRNA). Delta cycle time (ΔCT) was calculated by subtracting miRNAs' CT from geometric mean of snRNA's and snoRNA's CT. Expression level in arbitrary units were calculated from 2 to the power of delta cycle time ($2^{\Delta\Delta CT}$). The same protocol was used to determine miRNA expression in kidneys of C57Bl/6j mice for comparison with RNA-sequencing method as described below.

RNA sequencing. Total RNA was isolated from kidneys of 3 months old, male C57Bl/6j wildtype mice (Jackson lab) using TRIzol® (Invitrogen) as described[55] and 1 µg of total RNA was used for isolation of the small RNA fraction ranging from 18 to 40nt size by denaturing polyacrylamide gel electrophoresis. Library preparation and sequencing was performed in the Genomics Core Facility of Albert Einstein College of Medicine using Illumina's Genome Analyzer III. The protocol was described as (http://wasp.einstein.yu.edu/index.php/Protocol:RNA_seq).

Sequence reads (approximately $8x10^6$ per sample) were aligned to the Genome Reference Consortium Mouse and miRNAs were annotated using a published automated bioinformatics pipeline[56].

Qrt-PCR. For expression analysis of specific transcripts, mRNA and miRNA-specific stem-loop primers and TaqMan probe sets (Applied Biosystem) were used according to manufacturer's protocols, on an ABI 7900HT real-time PCR system as described[54].

Mouse models. miR-21 knockout mice (miR-21-KO) were generated from disruption of the miR-21 sequence as described[48], and crossed with albumin-TGFβ_1 transgenic mice (TGFb-TG)[45]. Experiments were conducted in male littermates in C57Bl/6j background. These procedures were in accordance with the policies of the University of Michigan Institutional Animal Care and Use Committee.

Tissue staining. Periodic acid Schiff and picrosirius red staining was performed on formalin-fixed paraffin-embedded mouse kidney sections as described[28]. For picrosirius red staining, percent glomerular area exceeding a minimum HSI (hue, saturation, intensity) threshold were determined from images of at least 50 glomeruli

per sample at 20x magnification using MetaMorph® image analysis software. WT1 staining was performed as described[28].

Glomerular podocyte density. Podocyte density was determined for at least 30 glomeruli of each sample using nuclear (DAPI-staining) and podocyte (WT1-staining) counts normalized to glomerular volume calculated using glomerular tuft area measurements and the Weibel equation as described[57].

Urine protein and creatinine measurement. Spot urine samples were collected non-invasively from mice. Urine creatinine concentrations were determined by QuantiChrom™ Creatinine Assay Kit (BioAssay Systems). Urine protein was qualitatively assessed by Coomassie blue staining of SDS-PAGE gel loaded with equal amounts of urine and quantitatively by Bio-Rad protein assay (Bio-Rad).

Isolation of mouse glomeruli. Isolation of glomeruli from TG/miR-21 WT and KO mice using beads and sieving method was performed as described achieving >90% purity[58] .

Cell culture. Conditionally immortalized murine podocytes were cultured as

described[28].

miRNA transfection. miR-21 oligonucleotide mimic (Ambion) or inhibitor (Exiqon) were applied with Lipofectamine® RNAiMAX Reagent (Invitrogen) to transfect podocytes at least 10 days after thermoshift. Using fluorescence-labeled scrambled oligo's we detected about 40 to 50% of cells with positive fluorescence signals.

Immunoblot assay. Total and phosphorylated proteins were detected by Western blotting using the following primary antibodies: phospho-smad3 (Rockland, 600-401-919), total smad2/3 (cell signaling, #3102) and GAPDH (Sigma, G8795). IRDye® secondary antibodies and Odyssey infrared imaging system (LI-COR Biosciences) were used for quantification.

Apoptosis assays. *In vivo* apoptosis was detected by immunohistochemistry with cleaved-caspase-3 antibody (Cell Signaling, Asp175) on FFPE tissue sections and manual counting of positive cells. For quantification of apoptosis of cultured cells, annexin-V/propidium iodide positive cells (determined by flow cytometry, Invitrogen assay kit) and cells negative for mitochondrial membrane potential (DePsipher assay, R&D system; fluorescent plate reader) were assayed as

described[17].

Luciferase reporter assays. The Smad7 3'UTR was amplified by PCR using genomic DNA from mouse embryonic fibroblasts; sequence of the sense primer AATAACTAGTTCGGTCGTGTGGTGGGGAGAAGA; antisense primer GATAAGCTTGCGCAAAGTGCATCTTTTCTTTATTCT. The amplified PCR product was cloned into pMIR-REPORT™ miRNA Expression Reporter Vector (Ambion/Invitrogen) between SpeI and HindIII sites downstream of the luciferase coding sequence. The 3'UTR construct, renilla luciferase plasmid, and miR-21 mimic or anti-sense oligonucleotides were co-transfected into 293T human kidney embryonic cells using lipofectamine LTX and plus reagents (Invitrogen). Luciferase activity was measured 48 hours after transfection in luciferase assay plate reader.

Statistical analysis. Participants in the kidney biopsy protocol were placed at random into either cohort one (training cohort) or two (validation cohort). General characteristics, including age and GFR, were compared between cohorts using t-tests, while two-group proportion test was used for gender distribution. Wilcoxon rank sum test was used for comparison of the non-normally distributed ACR values between Pima cohorts. Correlation analysis and significance was determined by

Pearson correlation using an R script. T-tests were used to compare sirius red intensity, cell numbers, mRNA and protein levels between miR-21-WT and -KO mice.

Table 2.1. Characteristics of American Indian testing and validating cohort

	Testing cohort	Validating cohort	P-value
No. of subject	26	22	
Age: Mean (SD)	43(9.1)	46(11.3)	0.3974
Gender: % of female	81%	82%	0.9292
ACR: Mean (SD)	498(1492)	194(518)	0.2466
GFR: Mean (SD)	159(58)	137(38)	0.1436

ACR: urine albumin-to-creatinine ratio (μg/mg). GFR: glomerular filtration rate (ml/min/1.73m^2)

SD: standard deviation.

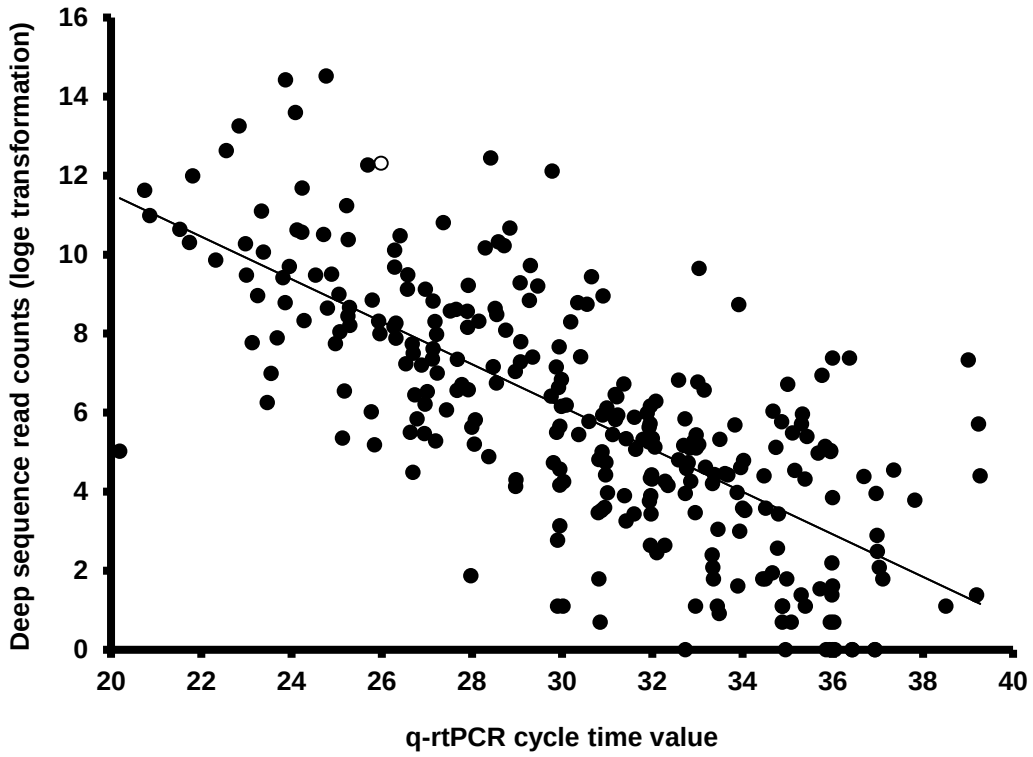

Figure 2.1. miRNA expression profiling in the mouse kidney using RNA sequencing and qrt-PCR. Expression levels of miRNAs determined by RNA sequencing and qrt-PCR were significantly correlated (R=0.7, P < 0.0001, No. of miRNAs included: 287; miRNA with 0 counts in RNA sequencing or undetermined cycle time (CT) in qrt-PCR were excluded). RNA sequencing read counts were transformed to natural logarithmic value. miR-21 (white circle) was highly expressed according to both assays.

Table 2.2A. Correlation between miRNA and ACR in testing cohort

miRNA	P value	Correlation with ACR	Expression level
hsa-miR-21	<0.00001	0.80	high
hsa-miR-150	<0.00001	0.74	high
hsa-miR-192	<0.00001	0.70	high
hsa-miR-221	<0.00001	0.67	high
hsa-miR-532-3p	<0.00001	0.64	high
hsa-miR-135a	<0.00001	0.81	medium
hsa-miR-429	<0.00001	0.79	medium
hsa-miR-660	<0.00001	0.77	medium
hsa-miR-142-3p	<0.00001	0.77	medium
hsa-miR-200a	<0.00001	0.76	medium
hsa-miR-218	<0.00001	0.74	medium
hsa-miR-455-5p	<0.00001	0.71	medium
hsa-miR-450a	<0.00001	0.66	medium
hsa-miR-181a	<0.00001	0.65	medium
hsa-miR-642	<0.00001	0.89	low
hsa-miR-32	<0.00001	0.85	low
hsa-miR-511	<0.00001	0.77	low
hsa-miR-187	<0.00001	0.74	low
hsa-miR-452	<0.00001	0.69	low
hsa-miR-501-5p	<0.00001	0.65	low

Table 2.2B. Correlation between miRNA and ACR in validating cohort

miRNA	P value	Correlation with ACR	Expression level
hsa-miR-132	<0.00001	0.64	high
hsa-miR-454	<0.00001	0.59	high
hsa-miR-337-5p	<0.00001	0.58	high
hsa-miR-21	0.01	0.51	high
hsa-miR-191	0.03	0.47	high
hsa-miR-221	0.03	0.46	high
hsa-miR-186	0.03	0.46	high
hsa-miR-140-5p	0.03	0.46	high
hsa-miR-125a-5p	0.03	0.46	high
hsa-miR-212	<0.00001	0.96	medium
hsa-miR-224	<0.00001	0.94	medium
hsa-miR-133b	<0.00001	0.58	medium
hsa-miR-18a	0.02	0.51	medium
hsa-miR-140-3p	0.03	0.46	medium
hsa-miR-148b	0.03	0.46	medium
hsa-miR-133a	0.04	0.43	medium
hsa-miR-299-5p	<0.00001	0.83	low
hsa-miR-34c	0.02	0.48	low

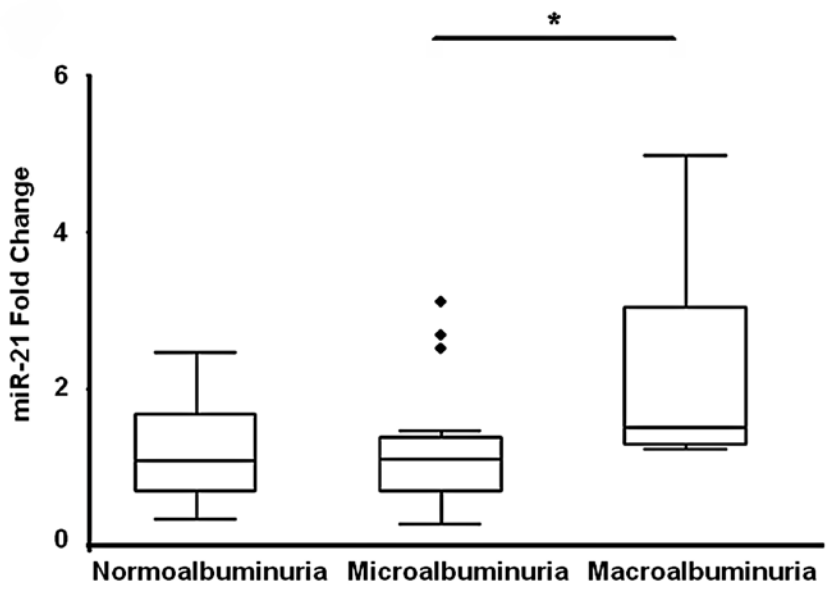

Figure 2.2. Glomerular miR-21 levels in American Indian patients with normo-albuminuria, micro-albuminuria and macro-albuminuria. miR-21 levels determined by qrt-PCR were similar in patients with normo- (N=19) and micro-albuminuria (N=22) (P=0.8). However, miR-21 levels increased significantly in patients with macro-albuminuria (N=7) (*P = 0.01 versus micro-albuminuria).

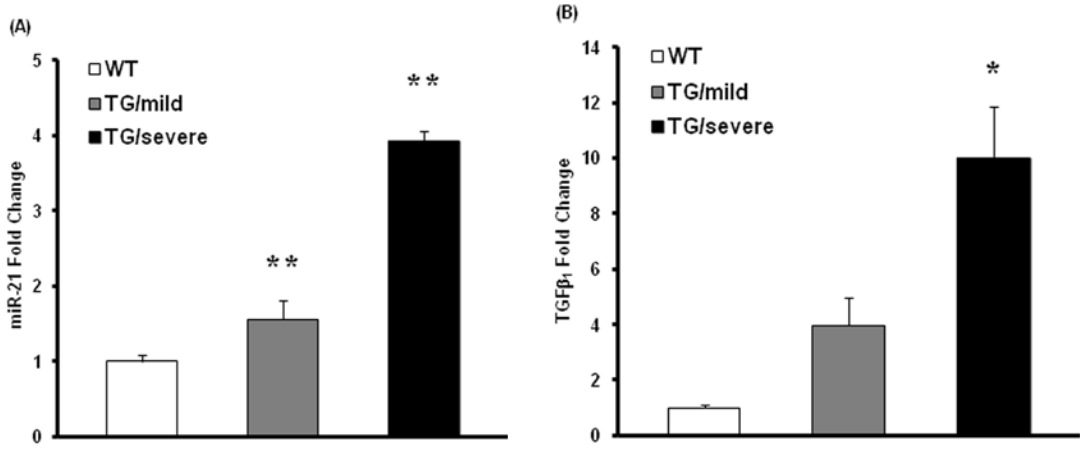

Figure 2.3. miR-21 and TGFβ1 expression levels in kidneys of $TGF\beta_1$ transgenic mice. Qrt-PCR showed (A) miR-21 levels increased with kidney damage severity inferred from histology score. Levels were significantly higher in TG severe phenotype (TG/severe) (N=8) and mild phenotype (TG/mild) (N=6) compared to wild type (WT) (N=5) ($P < 0.001$ in $^{\#}$TG/severe versus TG/mild and *TG/mild versus WT). (B) $TGF\beta_1$ levels also increased with kidney damage severity. Levels were significantly higher in TG/severe (N=3) compared to WT (N=3) (*P = 0.01).

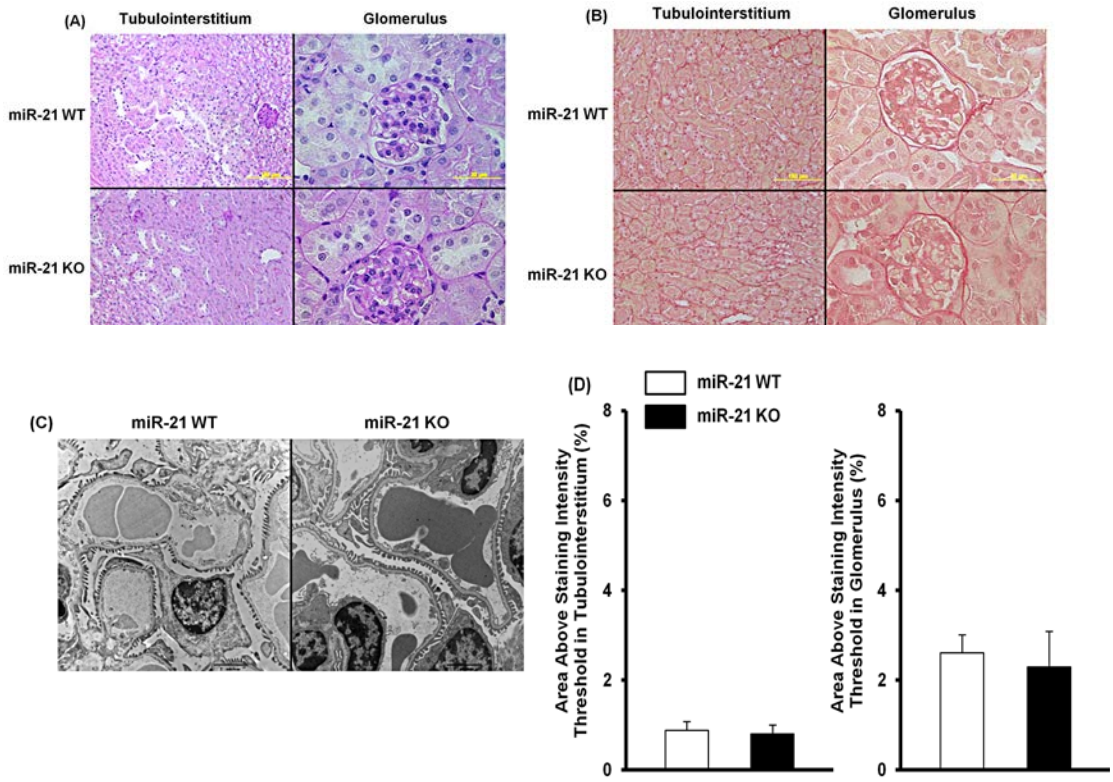

Figure 2.4. Kidney histology and structure in miR-21 WT and KO C57BI/6J mouse at 12 weeks old. (A) Periodic acid Schiff (PAS) staining of tubulointerstitium or glomerulus showed normal kidney structure in miR-21 WT and KO littermates. (B) Sirius red staining of tubulointerstitium or glomerulus showed no staining difference between miR-21 WT and KO littermates. (C) Transmission electron microscopy (TEM) showed normal podocyte morphology and slit diaphragm in miR-21 WT and KO littermates. (D) Histogram and statistical analysis of sirius red staining intensity showed no difference in tubulointerstitium or glomerulus between miR-21 WT (N=4) and KO (N=5) littermates (P = 0.8 in tubulointerstitium; P = 0.68 in glomerulus).

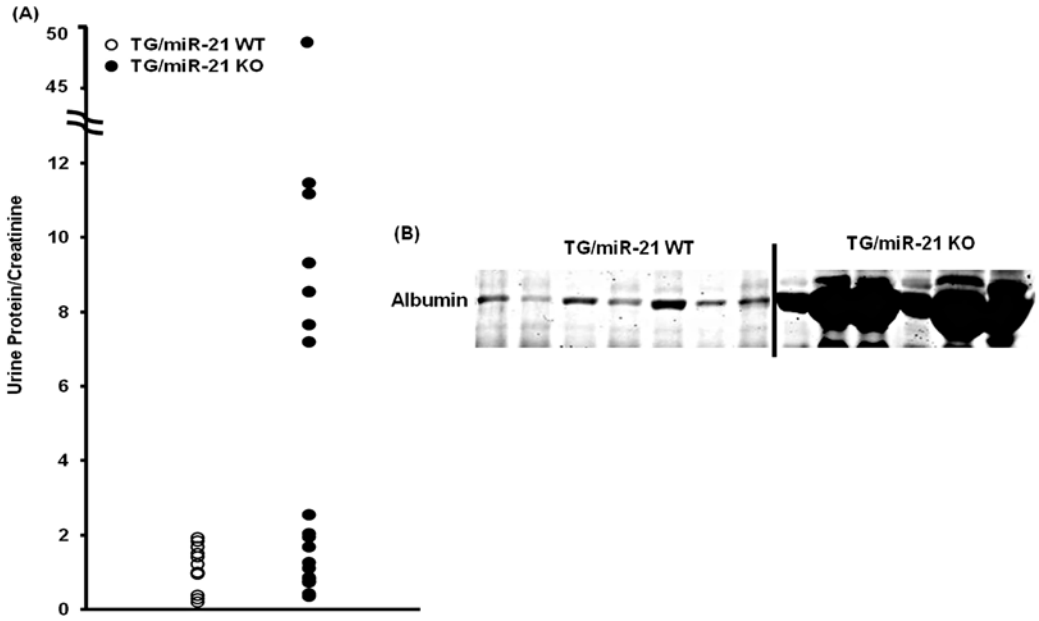

Figure 2.5. Examination of proteinuria in TG/miR-21 WT and KO mice. (A) Urine protein to creatinine ratio showed that TG/miR-21 KO mice (N=19) had increased proteinuria with more variability than TG/miR-21 WT mice (N=12) at 4 weeks of age. (B) Coomassie blue stain of urine showed that TG/miR-21 KO mice (N=6) had more severe proteinuria than TG/miR-21 WT mice (N=7; normalized by loading 2μg creatinine equivalents of urine for each sample).

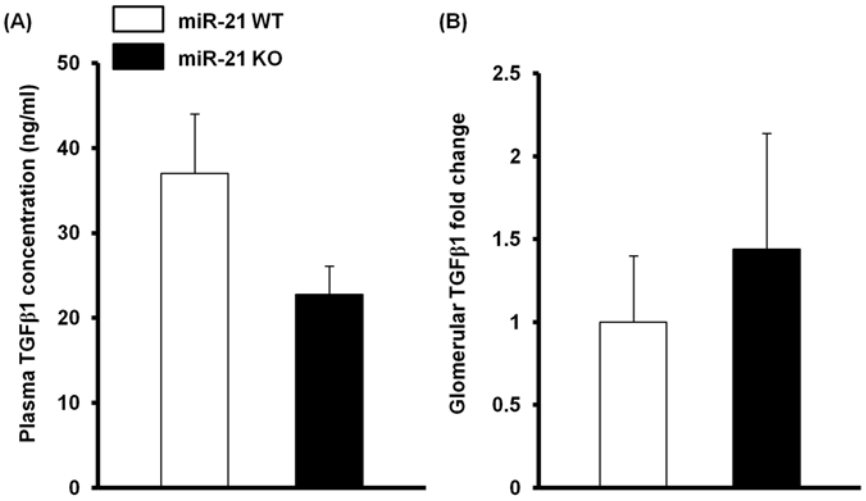

Figure 2.6. TGFβ_1 levels in TG/miR-21 WT and KO mice. (A) Plasma TGFβ_1 levels were not different between TG/miR-21 WT (N=11) and KO (N=17) mice (P = 0.053). (B) Qrt-PCR showed that glomerular TGFβ_1 mRNA levels were not different between TG/miR-21 WT (N=11) and KO (N=17) mice (P = 0.6).

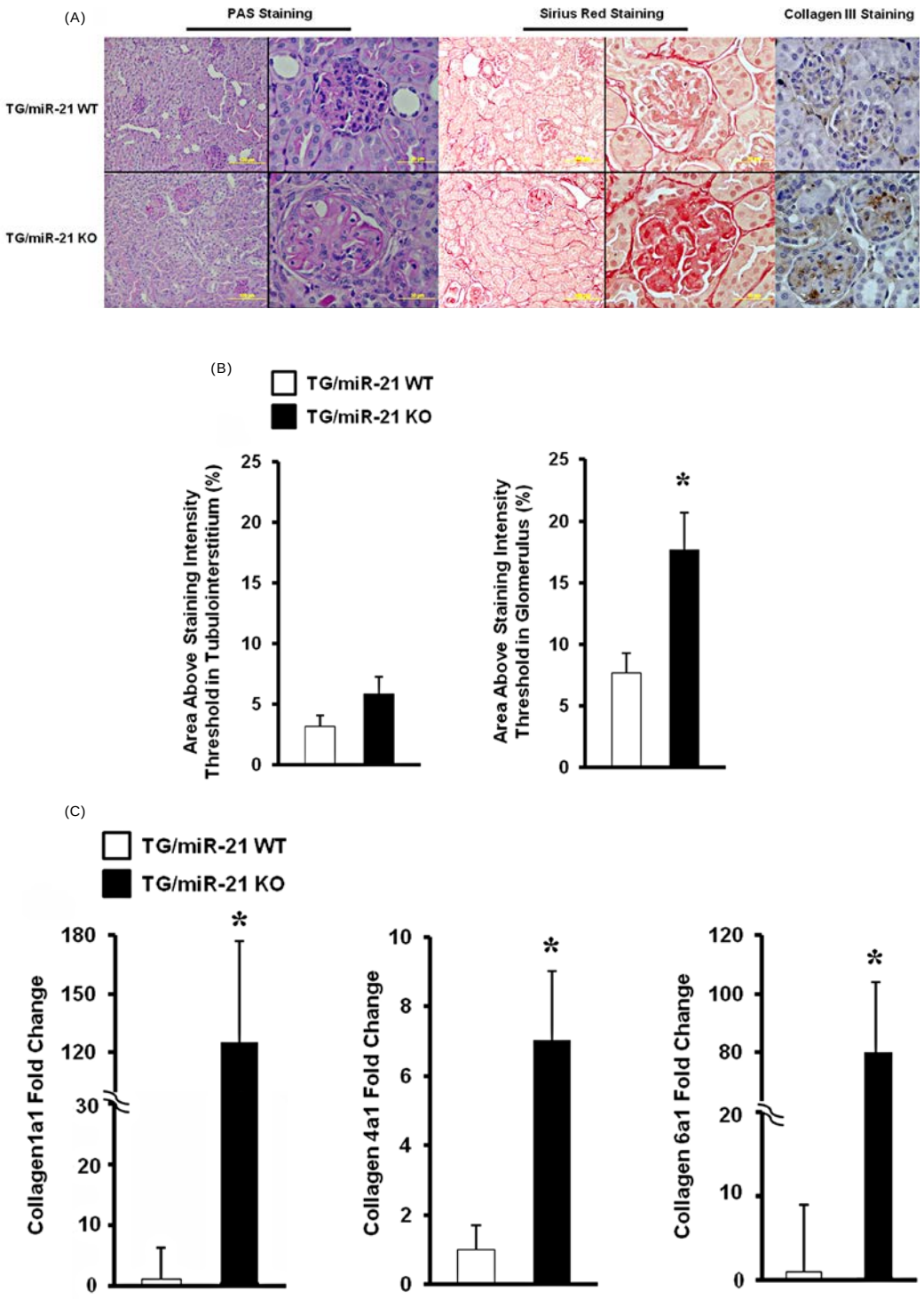

Figure 2.7. Examination of kidney histology in TG/miR-21 WT and KO mice. (A) PAS staining showed increased deposition of PAS material and decreased cellularity in glomeruli of TG/miR-21 KO compared to TG/miR-21 WT mice, but no difference in the tubulointerstitial area. Picrosirius red staining of glomerulus showed increased signal intensity and development of nodular pattern in glomeruli of TG/miR-21 KO compared to TG/miR-21 WT mice, again with no difference in

the tubulointerstitial area. Consistent with increased ECM deposition detected by picrosirius red staining, immunohistochemistry staining showed increased collagen III deposition in the glomerulus of TG/miR-21 KO. (B) Histogram and statistical analysis of picrosirius red staining intensity showed significantly higher staining intensity in glomeruli of TG/miR-21 KO (N=7) versus WT mice (N=9) (*$P < 0.01$). In the tubulointerstitium, staining intensity between TG/miR-21 WT and KO mice was not significantly difference ($P = 0.08$). (C) Qrt-PCR showed higher expression of collagen1a1, collagen4a1, collagen6a1 mRNA levels in glomeruli of TG/miR-21 KO mice (N=3) compared to WT mice (N=4) (*$P < 0.05$).

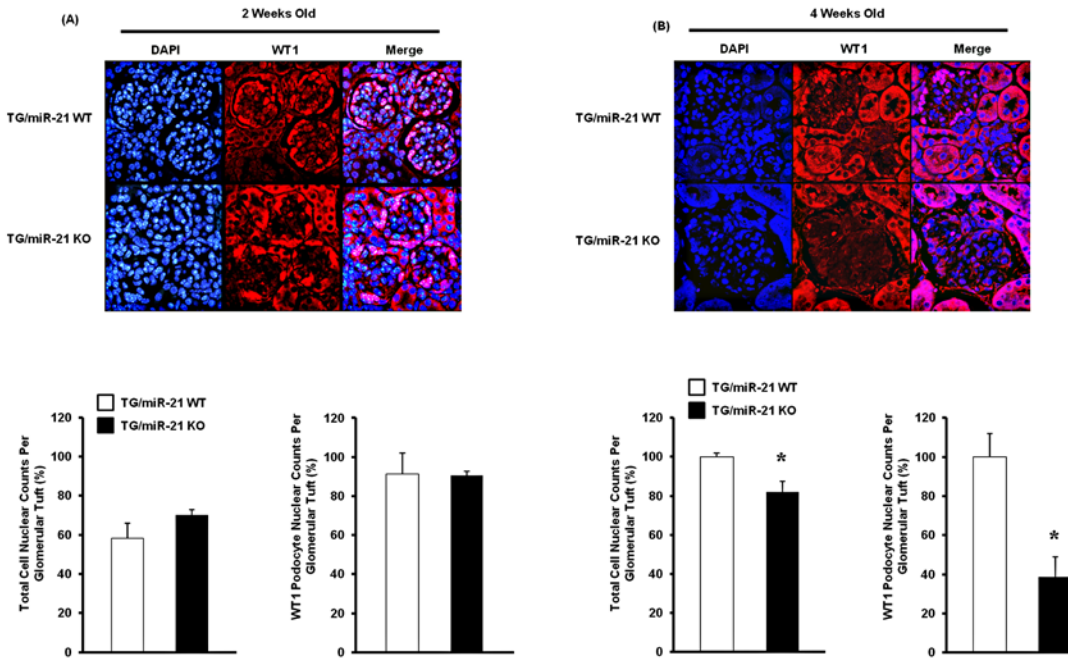

Figure 2.8. Podocyte number in glomeruli of TG/miR-21 WT and KO mice. (A) The immunofluorescent staining did not reveal difference in the number of cells (DAPI-positive) and podocytes (DAPI- and WT1-positive) per glomerular tuft in TG/miR-21 WT (N=3) versus KO mice (N=5) at 2 weeks of age. (B) The number of total cells (*P < 0.05) and podocytes (*P < 0.01) per glomerular tuft were significantly decreased in TG/miR-21-KO mice (N=4) versus TG/miR-21-WT mice (N=5) at 4 weeks of age. DAPI (blue), WT1 (red), podocytes (pink in merge). The number of cells per glomerular tuft was normalized by the number of DAPI-positive cells in TG/miR-21 WT mice at 4 weeks old.

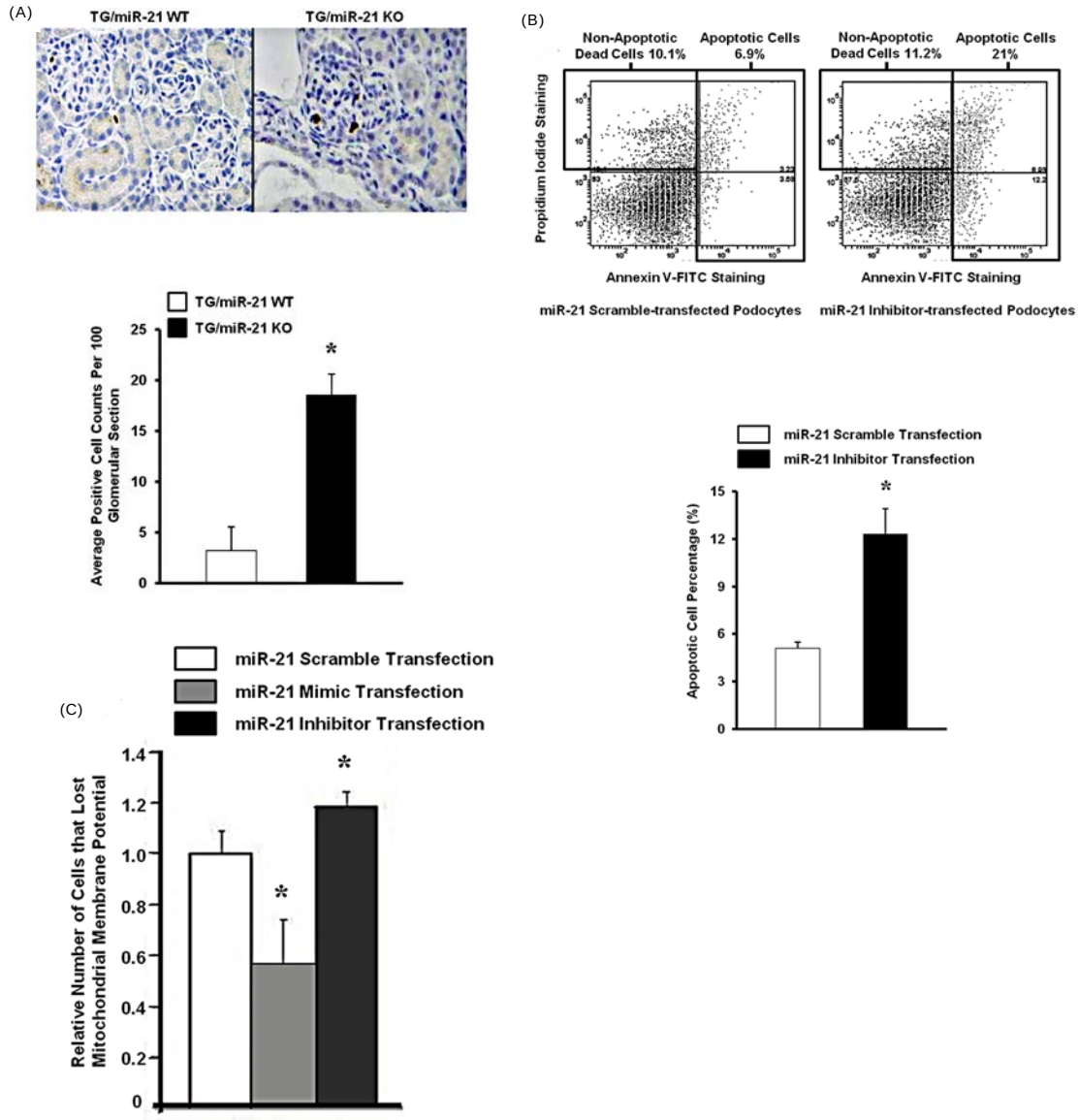

Figure 2.9. Apoptotic events in glomeruli of TG/miR-21 WT and KO mice and in miR-21 mimic or antisense oligonucleotide-transfected immortalized mouse podocytes. (A) Cleaved caspase-3 staining showed a higher number of positively stained cells per 100 glomerular section of TG/miR-21 KO mice (N=7) compared to the WT mice (N=3) at 2 weeks old. (B) Annexin V-FITC and propidium iodide (PI) double labeling in flow cytometry showed that mouse podocytes transfected with antisense miR-21 oligonucleotide (miR-21 inhibitor) exhibited increased number of apoptotic cells than the scramble transfection (21% v.s. 6.9%) (C) Staining of mitochondrial membrane potential in mouse podocytes transfected with miR-21 mimic or inhibitor and treated with TGFß$_1$ (10 ng/ml) for 24 hours indicated that inhibition of miR-21 results in loss of mitochondrial membrane potential consistent with increased apoptosis, whereas overexpression of miR-21 results in decreased apoptosis compared to the scramble transfection. *In vitro* experiments were performed as triplicates (*P < 0.05).

(A)

Position 206-212 of **TGFBR2** 3' UTR	5'	..UGACAUUGUCAUAGG-*AUAAGCU*G...
hsa/mmu-miR-21	3'	GUUGUAGUCAGAC*UAUUCGA*U
Position 425-432 of **TGFBI** 3' UTR	5'	...AGAAAUGGCAUCAUU---*AUAAGCU*A...
hsa/mmu-miR-21	3'	AGUUGUAGUCAGAC*UAUUCGA*U
Position 1122-1129 of **SMAD7** 3' UTR	5'	...UGUUUAGACUUUAAC*AUAAGCU*A...
hsa/mmu-miR-21	3'	AGUUGUAGUCAGAC*UAUUCGA*U
Position 242-249 of **PDCD4** 3' UTR	5'	..AAGUGGAAUAUUCUA*AUAAGCU*A...
hsa/mmu-miR-21	3'	AGUUGUAGUCAGAC*UAUUCGA*U
Position 1032-1039 of **TIMP3** 3' UTR	5'	..UACCCACAUGGGGAC*AUAAGCU*A...
hsa/mmu-miR-21	3'	AGUUGUAGUCAGAC*UAUUCGA*U
Position 194-200 of **COL4A1** 3' UTR	5'	..GAGAAAAAGACAGCG--*AUAAGCU*U...
hsa/mmu-miR-21	3'	AGUUGUAGUCAGAC*UAUUCGA*U

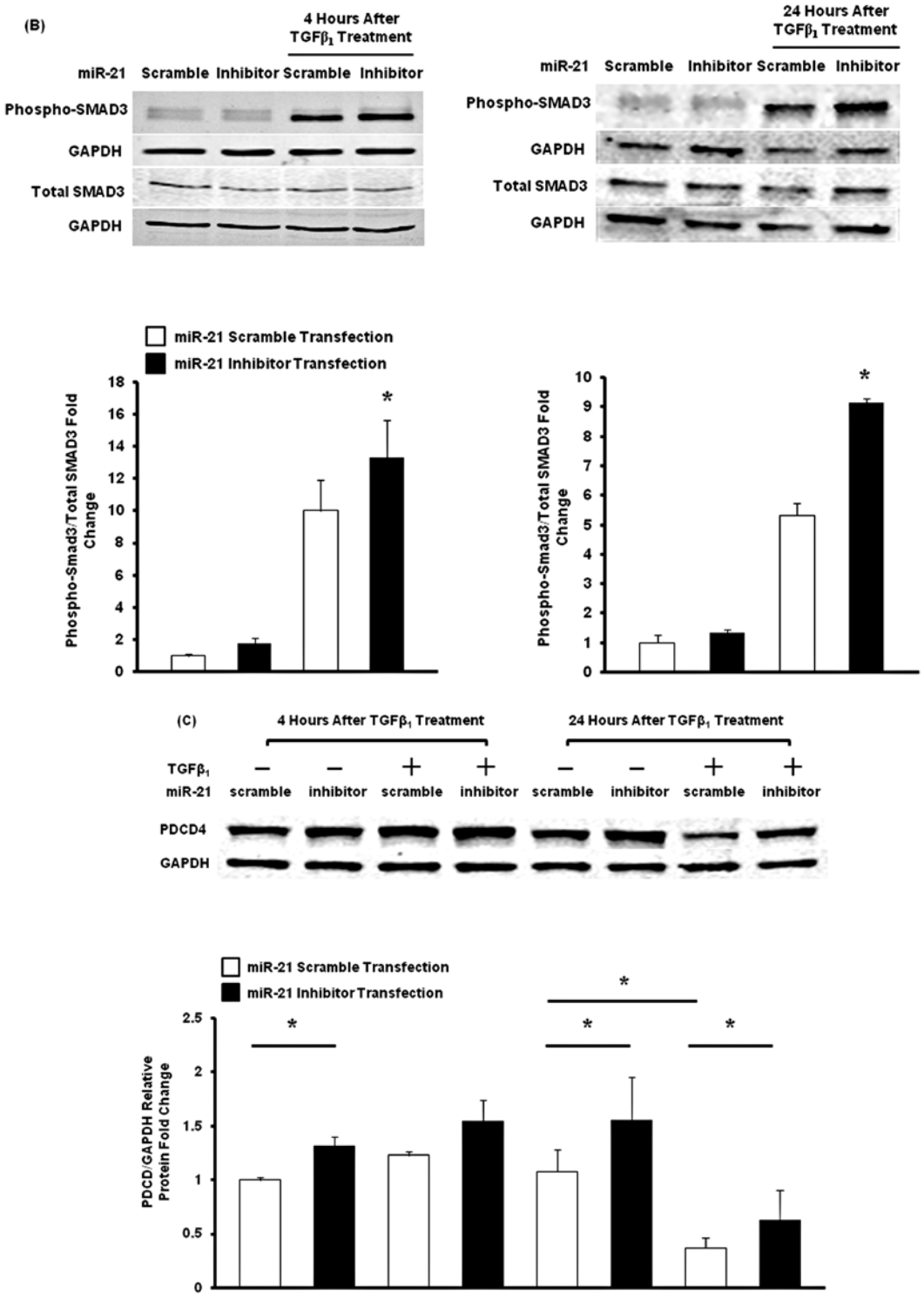

Figure 2.10. Examination of candidate miR-21 target gene expression in mouse podocytes and glomeruli of TG/miR-21 WT and KO mice. (A) Predicted target sites of miR-21 in 3'UTRs of Tgfbr2, Tgfbi, Smad7, Pdcd4, Timp3, and Col4a1 (www.targetscan.org). (B) Protein measurement showed increased level of phospho-Smad3 in miR-21 inhibitor transfected podocytes compared to the scramble transfection at 4 and 24 hours after TGFß$_1$ (10ng/ml) treatment (*P < 0.05; N=3,). (C) PDCD4 protein level was decreased in podocytes at 24 hours after TGFß$_1$ treatment compared to no treatment (*P < 0.05; N=4). PDCD4 was increased in miR-21 inhibitor transfected podocytes compared to scramble transfection with or without TGFß$_1$ treatment (*P < 0.05; N=3 to 4).

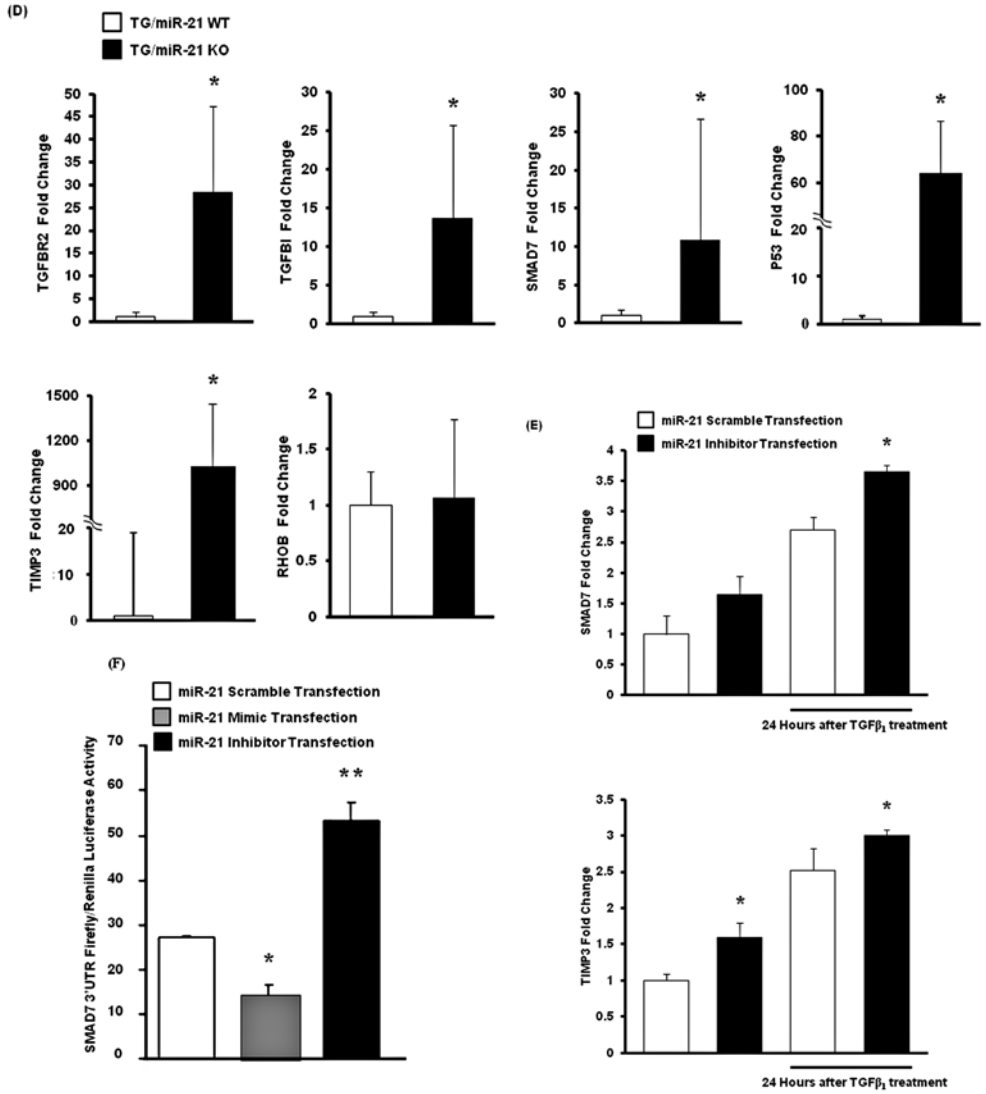

Figure 2.10. Examination of candidate miR-21 target gene expression in mouse podocytes and glomeruli of TG/miR-21 WT and KO mice. (D) TG/miR-21-KO mice (N=3) exhibit higher glomerular mRNA expression of Tgfbr2, Tgfbi, Smad7, Tp53, and Timp3 compared to TG/miR-21-WT mice (N=4) assayed by qrt-PCR (*P < 0.05). The level of RhoB, also a predicted target of miR-21, did not differ between TG/miR-21-WT and KO mice (P = 0.9). (E) At 24 hours of TGFß$_1$ treatment, Smad7 and Timp3 were increased in miR-21 inhibitor-transfected podocytes. Timp3 was also increased in miR-21 inhibitor-transfected podocytes without TGFß$_1$ treatment (*P < 0.05, N=6). (F) Luciferase assay of 293T human embryonic kidney cells co-transfected with Smad7 3'UTR luciferase construct and miR-21 mimic or inhibitor showed decreased luciferase activity after miR-21 overexpression (*P < 0.01, N=3) and increased luciferase activity after miR-21 inhibition (**P < 0.001, N=3).

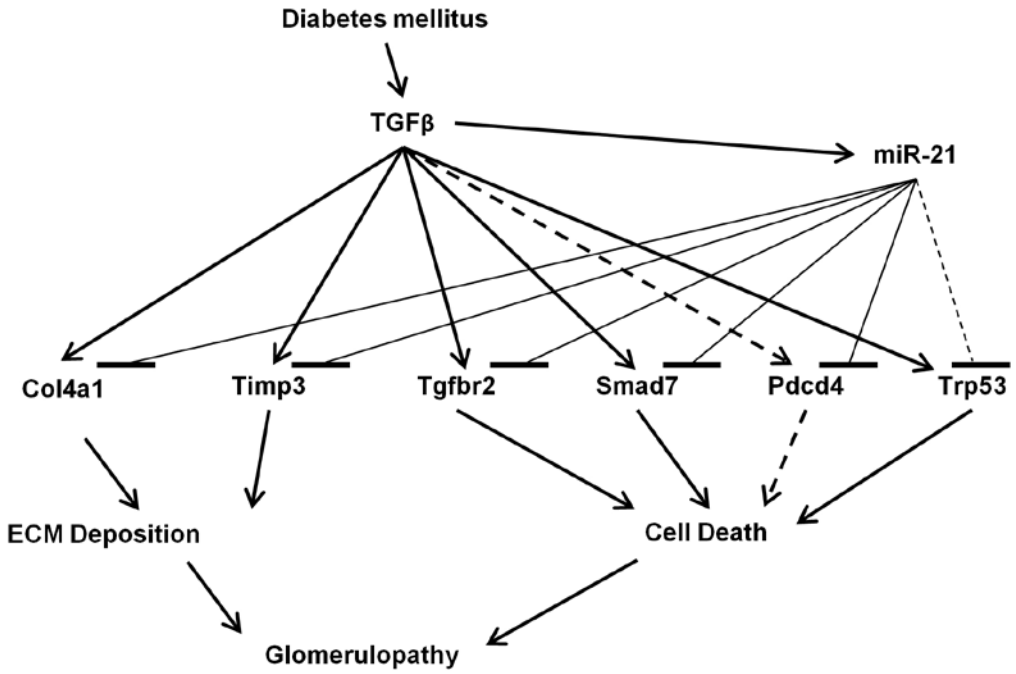

Figure 2.11. Proposed function of miR-21 as a feed-forward loop in TGFβ signaling in glomerular injury. The role of Pdcd4 (dashed line) in TGFβ-induced renal cell survival and death has not been explored yet. Trp53 is indirectly regulated by miR-21 (dot line).

Reference

1. US Renal Data System. USRDS 2012 Annual Data Report. in *Atlas of Chronic Kidney Disease and End-Stage Renal Disease in the United States*, Vol. 1 (National Institutes of Health, National Institute of Diabetes and Digestive and Kidney Diseases, Bethesda, MD, 2012).
2. Afkarian, M., *et al.* Kidney disease and increased mortality risk in type 2 diabetes. *J Am Soc Nephrol* **24**, 302-308 (2013).
3. Mendell, J.T. & Olson, E.N. MicroRNAs in stress signaling and human disease. *Cell* **148**, 1172-1187 (2012).
4. Kato, M. & Natarajan, R. MicroRNA circuits in transforming growth factor-beta actions and diabetic nephropathy. *Semin Nephrol* **32**, 253-260 (2012).
5. Pagtalunan, M.E., *et al.* Podocyte loss and progressive glomerular injury in type II diabetes. *J Clin Invest* **99**, 342-348 (1997).
6. Davis, B.N., Hilyard, A.C., Lagna, G. & Hata, A. SMAD proteins control DROSHA-mediated microRNA maturation. *Nature* **454**, 56-61 (2008).
7. Krupa, A., *et al.* Loss of MicroRNA-192 promotes fibrogenesis in diabetic nephropathy. *J Am Soc Nephrol* **21**, 438-447 (2010).
8. Git, A., *et al.* Systematic comparison of microarray profiling, real-time PCR, and next-generation sequencing technologies for measuring differential microRNA expression. *RNA* **16**, 991-1006 (2010).
9. Willenbrock, H., *et al.* Quantitative miRNA expression analysis: comparing microarrays with next-generation sequencing. *RNA* **15**, 2028-2034 (2009).
10. Bitzer, M., Ju, W., Jing, X. & Zavadil, J. Quantitative analysis of miRNA expression in epithelial cells and tissues. *Methods Mol. Biol.* **820**, 55-70 (2012).
11. Hodgin, J.B., *et al.* Identification of Cross-Species Shared Transcriptional Networks of Diabetic Nephropathy in Human and Mouse Glomeruli. *Diabetes* (2012).
12. Border, W.A. & Noble, N.A. TGF-beta in kidney fibrosis: a target for gene therapy. *Kidney Int* **51**, 1388-1396 (1997).
13. Kopp, J.B., *et al.* Transgenic mice with increased plasma levels of TGF-beta 1 develop progressive renal disease. *Laboratory Investigation* **74**, 991-1003 (1996).
14. Sanderson, N., *et al.* Hepatic expression of mature transforming growth factor beta 1 in transgenic mice results in multiple tissue lesions. *Proceedings of the National Academy of Sciences of the United States of*

America **92**, 2572-2576 (1995).
15. Ju, W., *et al.* Renal gene and protein expression signatures for prediction of kidney disease progression. *American Journal of Pathology* **174**, 2073-2085 (2009).
16. Wharram, B.L., *et al.* Podocyte depletion causes glomerulosclerosis: diphtheria toxin-induced podocyte depletion in rats expressing human diphtheria toxin receptor transgene. *J Am Soc Nephrol* **16**, 2941-2952 (2005).
17. Wu, D.T., Bitzer, M., Ju, W., Mundel, P. & Bottinger, E.P. TGF-beta concentration specifies differential signaling profiles of growth arrest/differentiation and apoptosis in podocytes. *J Am Soc Nephrol* **16**, 3211-3221 (2005).
18. Chan, J.A., Krichevsky, A.M. & Kosik, K.S. MicroRNA-21 is an antiapoptotic factor in human glioblastoma cells. *Cancer Research* **65**, 6029-6033 (2005).
19. Carletti, M.Z., Fiedler, S.D. & Christenson, L.K. MicroRNA 21 blocks apoptosis in mouse periovulatory granulosa cells. *Biology of Reproduction* **83**, 286-295 (2010).
20. Kim, Y.H., *et al.* Podocyte depletion and glomerulosclerosis have a direct relationship in the PAN-treated rat. *Kidney International* **60**, 957-968 (2001).
21. Erhardt, P. & Cooper, G.M. Activation of the CPP32 apoptotic protease by distinct signaling pathways with differential sensitivity to Bcl-xL. *Journal of Biological Chemistry* **271**, 17601-17604 (1996).
22. Nicholson, D.W., *et al.* Identification and inhibition of the ICE/CED-3 protease necessary for mammalian apoptosis. *Nature* **376**, 37-43 (1995).
23. Bottinger, E.P. & Bitzer, M. TGF-beta signaling in renal disease. *J Am Soc Nephrol* **13**, 2600-2610 (2002).
24. Papagiannakopoulos, T., Shapiro, A. & Kosik, K.S. MicroRNA-21 targets a network of key tumor-suppressive pathways in glioblastoma cells. *Cancer Res* **68**, 8164-8172 (2008).
25. Frankel, L.B., *et al.* Programmed cell death 4 (PDCD4) is an important functional target of the microRNA miR-21 in breast cancer cells. *J Biol Chem* **283**, 1026-1033 (2008).
26. Lewis, B.P., Burge, C.B. & Bartel, D.P. Conserved seed pairing, often flanked by adenosines, indicates that thousands of human genes are microRNA targets. *Cell* **120**, 15-20 (2005).
27. Yu, Y., *et al.* MicroRNA-21 induces stemness by downregulating transforming growth factor beta receptor 2 (TGFbetaR2) in colon cancer cells. *Carcinogenesis* **33**, 68-76 (2012).

28. Schiffer, M., *et al.* Apoptosis in podocytes induced by TGF-beta and Smad7. *J Clin Invest* **108**, 807-816 (2001).
29. Bhagat, T.D., *et al.* miR-21 mediates hematopoietic suppression in MDS by activating TGF-beta signaling. *Blood* (2013).
30. Engel, M.E., Datta, P.K. & Moses, H.L. RhoB is stabilized by transforming growth factor beta and antagonizes transcriptional activation. *J Biol Chem* **273**, 9921-9926 (1998).
31. Gabriely, G., *et al.* MicroRNA 21 promotes glioma invasion by targeting matrix metalloproteinase regulators. *Molecular and Cellular Biology* **28**, 5369-5380 (2008).
32. Kong, A.P., *et al.* Associations between microRNA (miR-21, 126, 155 and 221), albuminuria and heavy metals in Hong Kong Chinese adolescents. *Clinica Chimica Acta* **413**, 1053-1057 (2012).
33. Pan, X., Wang, Z.X. & Wang, R. MicroRNA-21: a novel therapeutic target in human cancer. *Cancer Biol Ther* **10**, 1224-1232 (2010).
34. Xu, X., *et al.* Delayed ischemic preconditioning contributes to renal protection by upregulation of miR-21. *Kidney Int* **82**, 1167-1175 (2012).
35. Chau, B.N., *et al.* MicroRNA-21 promotes fibrosis of the kidney by silencing metabolic pathways. *Sci Transl Med* **4**, 121ra118 (2012).
36. Dey, N., *et al.* MicroRNA-21 orchestrates high glucose-induced signals to TOR complex 1, resulting in renal cell pathology in diabetes. *J Biol Chem* **286**, 25586-25603 (2011).
37. Zhang, Z., *et al.* MicroRNA-21 protects from mesangial cell proliferation induced by diabetic nephropathy in db/db mice. *FEBS Lett* **583**, 2009-2014 (2009).
38. Liu, G., *et al.* miR-21 mediates fibrogenic activation of pulmonary fibroblasts and lung fibrosis. *J Exp Med* **207**, 1589-1597 (2010).
39. Thum, T., *et al.* MicroRNA-21 contributes to myocardial disease by stimulating MAP kinase signalling in fibroblasts. *Nature* **456**, 980-984 (2008).
40. Sayed, D., *et al.* MicroRNA-21 is a downstream effector of AKT that mediates its antiapoptotic effects via suppression of Fas ligand. *J Biol Chem* **285**, 20281-20290 (2010).
41. Patrick, D.M., *et al.* Stress-dependent cardiac remodeling occurs in the absence of microRNA-21 in mice. *J Clin Invest* **120**, 3912-3916 (2010).
42. Susztak, K., Raff, A.C., Schiffer, M. & Bottinger, E.P. Glucose-induced reactive oxygen species cause apoptosis of podocytes and podocyte depletion at the onset of diabetic nephropathy. *Diabetes* **55**, 225-233 (2006).

43. Niranjan, T., *et al.* The Notch pathway in podocytes plays a role in the development of glomerular disease. *Nature medicine* **14**, 290-298 (2008).
44. Zamilpa, R., *et al.* C-terminal fragment of transforming growth factor beta-induced protein (TGFBIp) is required for apoptosis in human osteosarcoma cells. *Matrix Biol* **28**, 347-353 (2009).
45. Sanderson, N., *et al.* Hepatic expression of mature transforming growth factor beta 1 in transgenic mice results in multiple tissue lesions. *Proc Natl Acad Sci U S A* **92**, 2572-2576 (1995).
46. Kulkarni, A.B., *et al.* Transforming growth factor beta 1 null mutation in mice causes excessive inflammatory response and early death. *Proceedings of the National Academy of Sciences of the United States of America* **90**, 770-774 (1993).
47. Mukherji, S., *et al.* MicroRNAs can generate thresholds in target gene expression. *Nature Genetics* **43**, 854-859 (2011).
48. Lu, T.X., *et al.* MicroRNA-21 limits in vivo immune response-mediated activation of the IL-12/IFN-gamma pathway, Th1 polarization, and the severity of delayed-type hypersensitivity. *J Immunol* **187**, 3362-3373 (2011).
49. Androsavich, J.R., Chau, B.N., Bhat, B., Linsley, P.S. & Walter, N.G. Disease-linked microRNA-21 exhibits drastically reduced mRNA binding and silencing activity in healthy mouse liver. *RNA* **18**, 1510-1526 (2012).
50. Mase, Y., *et al.* MiR-21 is Enriched in the RNA-Induced Silencing Complex and Targets COL4A1 in Human Granulosa Cell Lines. *Reprod Sci* **19**, 1030-1040 (2012).
51. Zavadil, J. & Bitzer, M. MicroRNAs in epithelial cell plasticity and carcinogenesis. in *Human Epithelial Tumor Cell Plasticity:Implications for Cancer Progression and Metastasis* (ed. Higgins, P.J.) (2008).
52. Weil EJ, *et al.* Effect of losartan on prevention and progression of early diabetic nephropathy in American Indians with type 2 diabetes. *Diabetes* **in press**(2013).
53. Cohen, C.D., Frach, K., Schlondorff, D. & Kretzler, M. Quantitative gene expression analysis in renal biopsies: a novel protocol for a high-throughput multicenter application. *Kidney International* **61**, 133-140 (2002).
54. Bitzer, M., Ju, W., Jing, X. & Zavadil, J. Quantitative analysis of miRNA expression in epithelial cells and tissues. *Methods Mol Biol* **820**, 55-70 (2012).
55. Bitzer, M., *et al.* A mechanism of suppression of TGF-beta/SMAD signaling by NF-kappa B/RelA. *Genes & development* **14**, 187-197 (2000).
56. Farazi, T.A., *et al.* Bioinformatic analysis of barcoded cDNA libraries for

small RNA profiling by next-generation sequencing. *Methods* **58**, 171-187 (2012).

57. Fukuda, A., *et al.* Angiotensin II-dependent persistent podocyte loss from destabilized glomeruli causes progression of end stage kidney disease. *Kidney International* **81**, 40-55 (2012).
58. Takemoto, M., *et al.* A new method for large scale isolation of kidney glomeruli from mice. *Am J Pathol* **161**, 799-805 (2002).

Chapter III

Loss of miR-21 promotes mesangial cell proliferation and leads to increased mesangial expansion in diabetic mice

Abstract

DN is the leading cause of ESRD and imposes heavy burden on the medical economy. Mesangial expansion is an early finding in DN, and is associated with mesangial cell proliferation as well as hypertrophy. We have previously identified miR-21 to be increased in micro-dissected glomeruli of patients with early to intermediate pathologic changes of DN. In addition, we had shown that loss of miR-21 is associated with acceleration of glomerulopathy in Albumin-TGFß transgenic mcie. To test the hypothesis that miR-21 inhibits the development of mesangial expansion and DN, we examined glomerular pathology in streptozotocin (STZ)-induced hyperglycemic, miR-21 KO mice.

STZ (50mg/kg) was injected intraperitoneally (IP) into 10 weeks old miR-21 wildtype (WT), heterozygous (HET), and knockout (KO) mice in pure DBA background for 5 days. Proteinuria was assessed every 4 weeks for 20 weeks after STZ treatment.

Kidney histology and mRNA expression were examined at 20 weeks after STZ treatment. For in vitro studies, primary mesangial cells (PMC) were isolated from miR-21 WT and KO mice. Cell proliferation and cell cycle distribution were studied in miR-21WT and KO PMCs.

STZ-treated miR-21 KO mice developed more albuminuria and glomerular mesangial expansion compared to the WT or HET littermates. miR-21 KO PMC showed faster proliferation and more cells accumulating at the synthesis (S) phase of the cell cycle than miR-21 WT PMC. The mRNA expression of cell cycle regulators, cyclin-dependent kinase 6 (Cdk6) and cell division cycle 25A (Cdc25a), were increased in the renal glomeruli of STZ-treated miR-21 KO mice versus STZ-treated miR-21 WT mice.

Our results suggested that miR-21 targets Cdk6 and Cdc25a to protect against mesangial expansion in DN. Therefore, we propose that miR-21 limits DN by inhibiting cell cycle progression in mesangial cells.

Introduction

DN is the renal injury caused by hyperglycemia. Clinically, it manifests as proteinuria and loss of kidney function. Histologically, it is characterized by mesangial expansion, glomerulosclerosis and tubulointerstitial fibrosis[1]. DN is the leading cause of ESRD in the United States and increases cardiovascular events as well as mortality[2]. Therefore, several different diabetic murine models have been developed to mimic human DN to explore mechanisms for DN and develop new therapies[3]. Nevertheless, to date, none of these diabetic murine models recapitulate all the microvascular and macrovascular injury observed in human DN[3]. STZ-induced DN in mice is a well-established diabetic murine model. It is characterized by mesangial expansion, nodular sclerosis, and arteriolar hyalinosis[3]. However, different susceptibilities to DN were noted in different inbred mouse strains. For instance, C57BL/6 mice are relatively resistant to diabetic kidney injury, while DBA mice develop mesangial expansion and mesangial sclerosis, which represent early human DN[3,4].

In previous chapters, we determined the role and regulatory mechanisms of miR-21 in progressive glomerulopathy in TGFβ transgenic mice. We noticed that miR-21 inhibits apoptosis in podocytes exposed to TGFβ. However, because miR-21 has been linked to fibroblast activation in heart disease[5] and epithelial mesenchymal

transition (EMT) in rat tubular cells[6], the latter findings suggest that the interaction of miR-21 with TGFβ signaling may be context-dependent and/or cell-specific. Therefore, the function of miR-21 in DN needs to be further validated.

Therefore, we used STZ-induced glomerulopathy in DBA mice to test our hypothesis that miR-21 has a protective role in mesangial expansion and DN. We also determined the function of miR-21 in primary mesangial cells from miR-21 WT and KO mice to study the impact of loss of miR-21 *in vitro*.

Result

STZ-treated miR-21 WT and KO DBA mice developed hyperglycemia

In order to investigate the function of miR-21 in DN, we injected STZ into miR-21 WT, HET and KO DBA mice to selectively induce pancreatice beta-cell dysfunction and associated hyperglycemia. All miR-21 WT, HET and KO mice developed hyperglycemia with blood glucose levels up to 400 mg/dl at 2 weeks and 600 mg/dl at 20 weeks after STZ treatment (Figure 3.1). No difference in blood glucose levels was detected between genotypes.

STZ-treated miR-21 KO mice developed more proteinuria

Before treatment with STZ, miR-21 KO mice showed no evidence of structural abnormalities in the kidney compared to miR-21-WT mice (Figure 2.4). Since proteinuria is an indicator of glomerular damage, we measured urine albumin-to-creatinine ratio (ACR) in STZ-treated miR-21 WT and KO mice. After 4 weeks of STZ treatment, miR-21 WT, HET and KO mice developed albuminuria (Figure 3.2). At 8, 12, 16, and 20 weeks after STZ treatment, miR-21 KO and HET mice had significantly higher ACR than the STZ-treated WT littermates, with highest levels in miR-21 KO mice.

STZ-treated miR-21 KO mice had increased mesangial expansion and extracellular matrix deposition

To determine the extent of glomerular damage of STZ-treated miR-21 WT, HET and KO mice, we quantified the area of mesangial expansion by Periodic acid-Schiff (PAS) staining at 20 weeks after STZ treatment. STZ-treated miR-21 KO mice showed increased PAS-positive material deposited in glomeruli compared to STZ-treated miR-21 WT mice (Figure 3.3A). Using quantitative image analysis, the calculated mesangial index (%) was significantly higher in STZ-treated miR-21 KO mice than in STZ-treated WT and HET littermates (Figure 3.3B).

Loss of miR-21 promotes PMC proliferation

To examine the function of miR-21 specifically in mesangial cells, we isolated PMC from miR-21 WT and KO mice. In scratch-wound assay, PMC from miR-21 KO mice showed more rapid wound closure than WT PMCs. This could be due to either increased migration speed or proliferation rate (Figure 3.4). In a colorimetric assay of cell proliferation (MTT assay), we found that PMC from miR-21 KO mice had a higher number of cells than PMC from miR-21 WT mice after 24 hours (Figure 3.5). Based on these findings as well as the findings from other previous studies that miR-21 regulates cell cycle[7,8], we studied the cell cycle distribution of PMC from

miR-21 WT and KO mice at 20 hours after 10% fetal bovine serum stimulation. The cell cycle study indicated that PMC from miR-21 KO mice had a higher percentage of cells accumulating in synthesis phase (S phase) compared to PMC from miR-21 WT mice (Figure 3.6). These results suggest that miR-21 contributes to growth arrest in PMC and loss of miR-21 promotes mesangial cell proliferation.

Loss of miR-21 increases the expression of Cdk6 and Cdc25a

Cdk6 is a member of cyclin-dependent protein kinase family, which facilitates cell cycle progression[9]. Cdc25a is a member of phosphatase family that is required for cell cycle progression[10]. Both of them have been proposed as the sequence-dependent target of miR-21 in cancer cells[8,11]. For that reason, we have performed qrt-PCR to examine the expression of Cdk6 and Cdc25a in STZ-treated miR-21 WT and KO mice. Our result showed that the mRNA expression of Cdk6 and Cdc25a was increased in the glomeruli of STZ-treated miR-21 KO mice compared to STZ-treated miR-21 WT mice (Figure 3.7). Therefore, we proposed that loss of miR-21 aggravates the glomerular injury in diabetic mice by upregulating Cdk6 and Cdc25a in mesangial cells to promote cell proliferation.

Discussion

In this chapter, we investigated whether miR-21 has a protective role in DN by examining kidney function and histology in diabetic miR-21 null mice. We used STZ-induced hyperglycemic mice a model for type I diabetes, to examine the role of miR-21 in DN. Our results revealed that loss of miR-21 induces more severe proteinuria and mesangial expansion in diabetic mice. This evidence supports the previous finding that loss of miR-21 exasperates glomerular damage. Additionally, we noticed that loss of miR-21 promotes mesangial cell proliferation by regulating cell cycle progression.

STZ-induced diabetes is an established mouse model for examining the pathogenesis of human DN, especially in the DBA/2J mouse strain[4]. In STZ-treated DBA/2J mice, hyperglycemia starts to manifest within 2 weeks of STZ treatment and serum glucose levels rise to 500 to 600 mg/dl after 20 weeks STZ treatment[4,12]. ACR in non-treated DBA/2J mice is around 20 to 30 μg/mg and albuminuria develops within 5 weeks of STZ treatment[4]. Consistent with previously published findings[3,4,12], the STZ-treated miR-21 WT and KO mice had typical hyperglycemia manifestation (Figure 3.1) and ACR levels gradually increased after 4 weeks of STZ treatment. Treated miR-21 WT mice had typical albuminuria level (400 to 500 mg/dl) compared to the treated DBA/2J mice in other people's experience[4] and the treated miR-21 KO mice had almost 3 to 4 times more albuminuria compared to their

control WT littermates.

In terms of kidney histopathological change, at as early as 5 weeks after STZ treatment, glomerular hypertrophy is the typical feature in STZ-treated DBA mice[12]. When disease progresses, mesangial expansion becomes the major pathological feature similar to what we have found in treated-miR-21 WT and KO mice at 20 weeks after STZ treatment. Furthermore, mesangial sclerosis developed in treated miR-21 KO mice (Figure 3.3). Other features of DN including arteriolar hyalinosis or nodular glomerulosclerosis seldom develop in STZ-treated DBA/2J mice[12] and there is no current diabetic murine model that recapitulates all of the clinical features of human DN[3]. In addition, despite being more susceptible to DN, STZ-treated DBA/2J mice only develop mesangial expansion and sclerosis, which represent the early stage of DG. Therefore, STZ-treated miR-21 KO mouse is a suitable model to test the protective role of miR-21 in glomerulopathy.

miR-21 is of special interest because in murine models of renal interstitial fibrosis[13] and lung disease[14], miR-21 promotes fibrosis through multiple mechanisms including regulation of TGFβ signaling. On the other hand, in both $TGF\beta_1$ transgenic and diabetic mice, miR-21 protects against glomerulopathy. This diverse function of miR-21 may depend on different organ systems and injuries. It is also likely to be secondary to the differential expression of target genes in different cells.

For example, tumor suppressor PTEN was shown to be target gene of miR-21 in mesangial cells[15] and cancer cells[16]. However, in our culture system, while overexpressing miR-21 in 293T human embryonic kidney cells**,** we did not observe repression of miR-21 on PTEN (Figure 3.8A). We also did not detect the difference in the protein expression of PTEN in miR-21 WT, HET, and KO DBA/2J mice (Figure 3.8B).

The cell cycle, consisting of $G_{0,}$ G_1, S, G_2, and M phases, represents a series of events leading cells from replication to cell division. The check-point of each phase transition is tightly regulated by cyclin and cyclin-dependent kinases (CDK)[17,18]. Dysregulation of these proteins can promote cancer formation[19] as well as contribute to the pathogenesis of DG[17]. *In vitro*, TGFβ has been shown to induce CDK inhibitors, block cell cycle progression, and result in PMC hypertrophy[20-22]. In our PMC culture system, we noticed that loss of miR-21 promoted PMC proliferation. Consistent with our findings, Wang et al. also found that miR-21 targets Cdc25a and inhibits G1 to S transition in colon cancer cells[8]. In addition, miR-21 is reported to upregulate CDK inhibitor, P21, by targeting its transcriptional inhibitor, Nf1b (Nuclear factor 1 B-type)[23]. Our results using a cell proliferation assay and assessing the cell cycle support that loss of miR-21 upregulates cell cycle-related proteins to prompt cell cycle progression.

Cdk6 is a member of the cyclin-dependent protein kinase family. This kinase first appears in mid-G1 phase, together with Cdk4, is important for cell cycle G1 phase progression and G1 to S transition[9]. Cdc25a is a member of phosphatase family that dephosphorylates and activates CDK–cyclin complexes, such as CDK2–cyclin E at the G1–S transition and CDK1–cyclin B at the entry into mitosis[10]. Interestingly, Cdk6 and Cdc25a mRNA has been shown to be a sequence-dependent target of miR-21 in cancer cells[8,11]. Our *in vivo* results also showed that Cdk6 and Cdc25a mRNA level were increased in glomeruli of STZ-treated KO mice. This supports the hypothesis that loss of miR-21 promotes mesangial cell proliferation from upregulating Cdk6 and Cdc25a.

Despite previous findings that TGFβ or hyperglycemia induces CDK inhibitors to cause cell cycle arrest and mesangial cell hypertrophy[24,25], a biphasic growth response of mesangial cells to TGFβ has been described[17]. It is possible that before the hypertrophic stage, an increase of Cdk6 or Cdc25a caused by loss of miR-21 facilitates an initial proliferation stage of mesangial cells leading to mesangial expansion. In support of this, Zhang et al. have shown that overexpression of miR-21 inhibits mesangial cell proliferation in diabetic db/db mice[26].

In summary, the findings in our diabetic mouse model provide additional evidence that miR-21 has a protective role in TGFβ-related glomerulopathy including DG.

miR-21 targets different regulatory mechanisms in different glomerular cells, which reiterates the cell-specific and multi-facet nature of miRNA. Our study suggests an unconventional and unrecognized role of miR-21 in different compartments of kidney.

Methods and Materials

Mouse model. miR-21-KO C57BL/6J mice were generated from disruption of the miR-21 sequence as described[27]. miR-21 WT and KO DBA/2J mice were obtained by backcrossing the C57BL/6J mice colony onto the DBA background strain for 6 or more generations. STZ, dissolved in sodium citrate buffer, was IP injected into 10 weeks old miR-21 WT and KO DBA/2J mice in a dose of 50mg/kg as previously described[28]. These procedures were in accordance with the policies of the University of Michigan Institutional Animal Care and Use Committee.

Blood glucose measurement. Adequate amount of blood was obtained from tail vein of mice. Blood glucose was measured by using Accu-Chek Comfort Curve Diabetic Test Strips before STZ treatment and at 2 weeks, 6 weeks, 12 weeks, and 20 weeks after STZ treatment.

Urine albumin and creatinine measurement. Spot mouse urine was collected non-invasively from mice 1-2 days before STZ treatment and at 4 weeks, 8 weeks, 12 weeks, 16 weeks and 20 weeks after STZ treatment. Urine albumin was measured by Albuwell M kit (Exocell Inc) and urine creatinine was measured by the Creatinine Companion Kit (Exocell Inc).

Tissue staining and analysis. Mouse kidneys were harvested, fixed in 4% paraformaldehyde overnight, and paraffin-embedded. The kidney sections were cut in 3μm thickness, deparaffinized with xylene, and dehydrated in water through graded ethanol. For PAS staining, the kidney section was incubated in 0.5% periodic acid solution for 10 minutes, Schiff reagent for 15 minutes, and then was counterstained with Weigert's hematoxylin for 30 seconds. After the staining, the kidney sections were rehydrated in water through graded alcohol, cleaned, and mounted with Permount.

Mesangial Index. In order to establish what percent of glomerular area is occupied by mesangial matrix, we took a sufficient number of images at 40x magnification to ensure a minimum of 25 glomeruli per animal were represented. The mesangial index quantification was described as before[29]. In brief, ImageJ was used to set a minimum HSI (hue, saturation, intensity) threshold according to PAS-positive material which if exceeded would count as mesangial matrix. The software was further used to calculate the total area and percent area exceeding threshold of each mesangial tuft.

Cell culture. Primary mouse mesangial cells were isolated from glomeruli of 6 to 8 weeks old miR-21 WT and KO mice as described before[30,31]. In brief, mouse kidneys were harvested. Cortex was removed from medulla, cut into 1mm cube, and past through a series of cell strainers from 200μm, 100μm to 70μm. At last, glomeruli were collected on the 70μm cell strainer and digested in collagenase A solution (1mg/ml) for 30 minutes. The digested glomeruli were then cultured in collagen type I-coated 6cm dish for 3 to 5 days. Once the mesangial cell clusters were formed, they were subcultured and kept propagating. The experiments were performed in PMC between 5 to 15 passages. The cells were cultured in RPMI 1640 medium supplemented with 20% fetal bovine serum (FBS), 1% penicillin/streptomycin, and 1% insulin-transferrin-selenium (Invitrogen) and were incubated in 37°C, 5% CO_2 incubator.

Proliferation assay. PMC were trypsinized and cell number was counted using trypan blue exclusion method including trypan blue solution 0.4% (invitrogen) and haemocytometer per manufacturer's protocol. The miR-21 WT and KO PMC were grown in a 96 well plate at the same cell number for 5 repeats. After 24 hours of cell growth in 10% FBS, cell proliferation was examined by MTT (Tetrazolium dye) cell proliferation assay kit per manufacturer's protocol (Cayman Chemical Company).

Cell cycle distribution measurement. PMC were serum-starved (0.2%) for 24 hours and shifted to 10% FBS with or without TGFβ treatment (10ng/ml). After another 20 hours, the cells were harvested and fixed in 70% ethanol. Cell cycle distribution was determined by staining the cells with propidium iodide and examining the staining intensity in flow cytometry as described[32].

Statistical analysis

Proteinuria, mesangial index and picro-sirius staining intensity were compared between miR-21 WT and KO mice using t-test. The cell proliferation and cell cycle distribution were also compared using t-test.

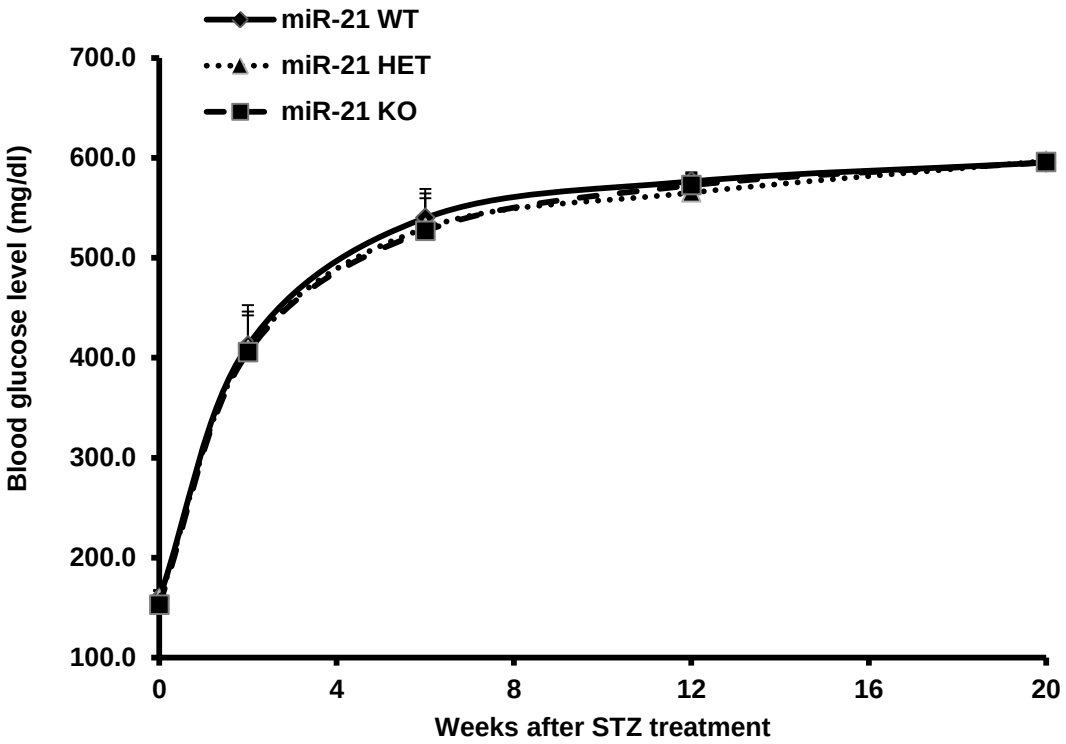

Figure 3.1. Examination of blood sugar in STZ-treated miR-21 WT, HET and KO mice at 0, 2, 6, 12, 20 weeks after STZ treatment. There is no blood glucose level difference among different genotypes (N=7 for each genotype).

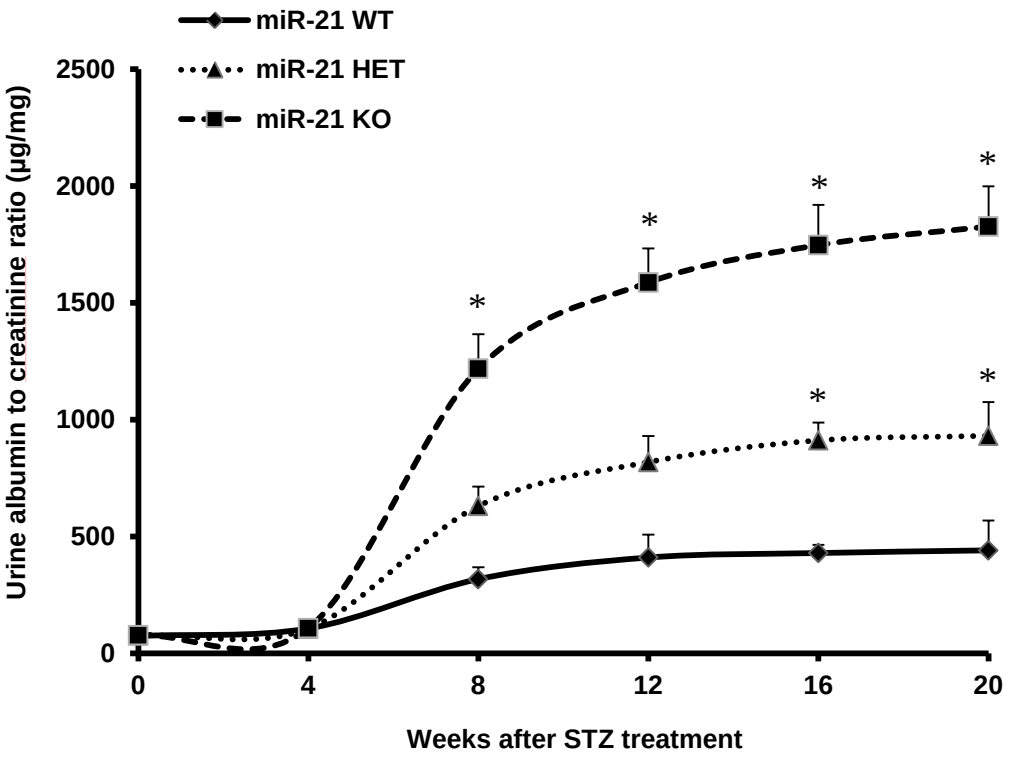

Figure 3.2. Examination of proteinuria in STZ-treated miR-21 WT, HET and KO mice at 0, 4, 8, 12, 16, 20 weeks after STZ treatment. (N=5 to 8 in each genotype; $^{*}P < 0.05$ compared to miR-21 WT mice)

A.

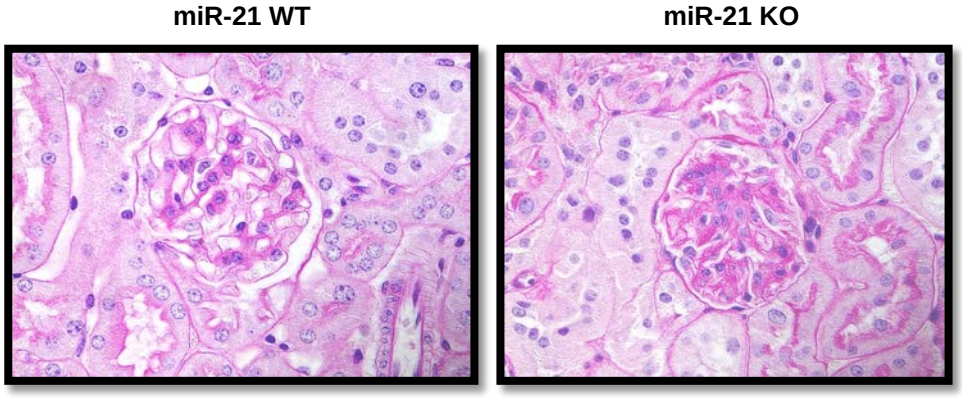

B.

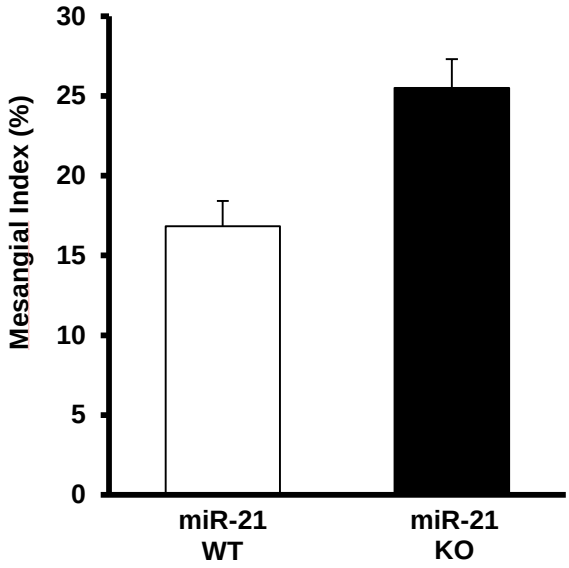

Figure 3.3. Examination of kidney histology by PAS staining in STZ-treated miR-21 WT, HET and KO mice. (A) PAS staining showed increased deposition of PAS in glomeruli of STZ-treated miR-21 KO compared to treated miR-21 WT mice. (B) Histogram and statistical analysis of mesangial index (%) calculating from PAS staining showed significantly higher mesangial expansion in glomeruli of STZ-treated miR-21 KO (N=5) versus treated miR-21 HET or WT mice (N=5 for both HET and WT group; $^{*}P < 0.05$, $^{\#}P < 0.01$).

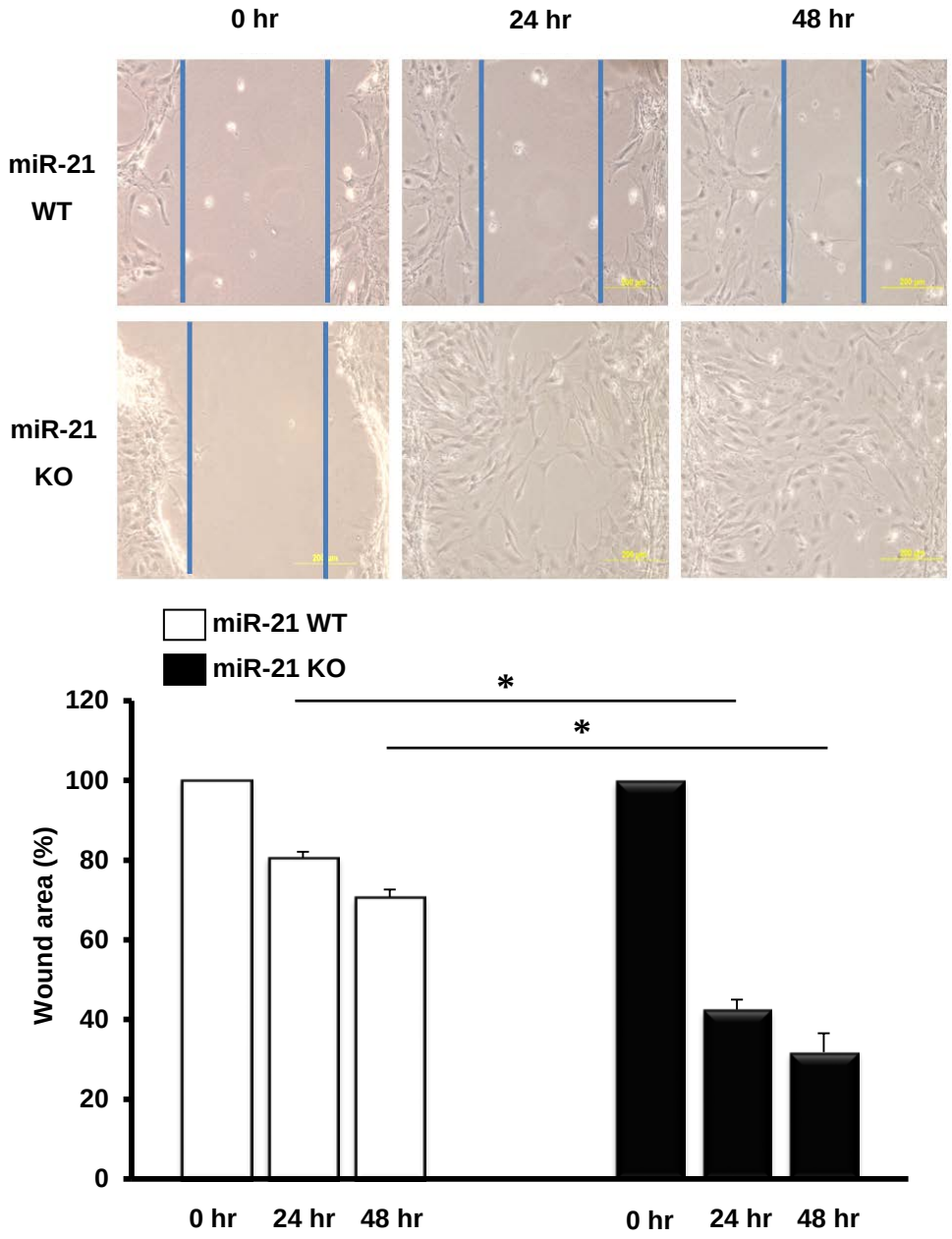

Figure 3.4. Examination of cell migration in miR-21 WT and KO PMC. The scratch-wound assay showed that miR-21KO PMC had significantly higher ability to migrate and close the wound (*P<0.01, N=3).

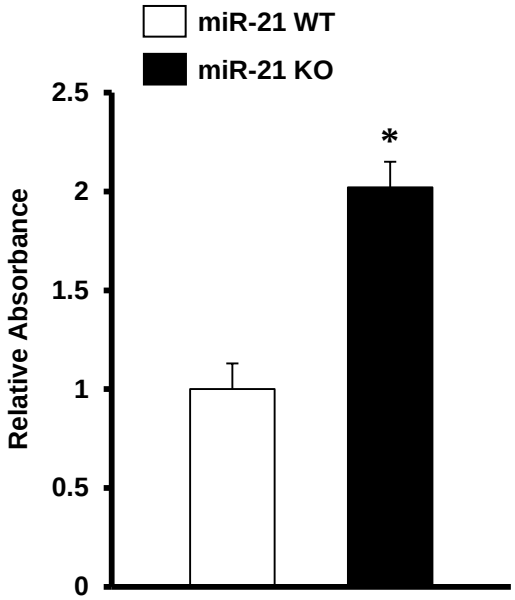

Figure 3.5. Examination of cell proliferation/viability in miR-21 WT and KO PMC. The MTT cell proliferation assay indicated that miR-21 KO PMC had significant higher MTT absorbance or more cells than miR-21 WT PMC after 24 hours of cell growth (*P<0.01, N=3).

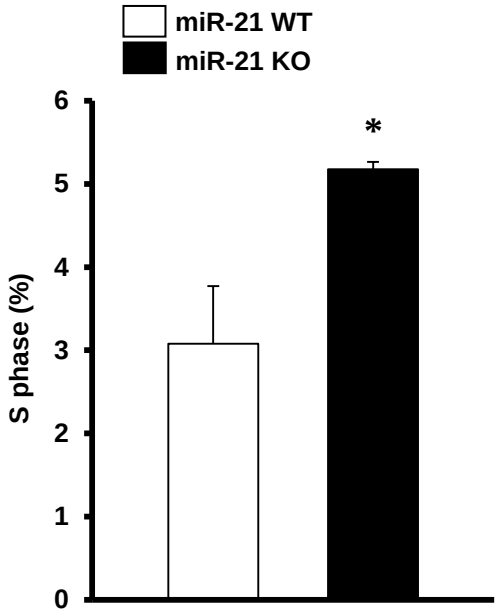

Figure 3.6. Examination of cell cycle distribution in miR-21 WT and KO PMC at 20 hours after 10% FBS supplement. In flow cytometry, the propidium iodide staining showed that miR-21 KO PMC had significantly more cells in S phase than miR-21 WT PMC (*$P < 0.05$).

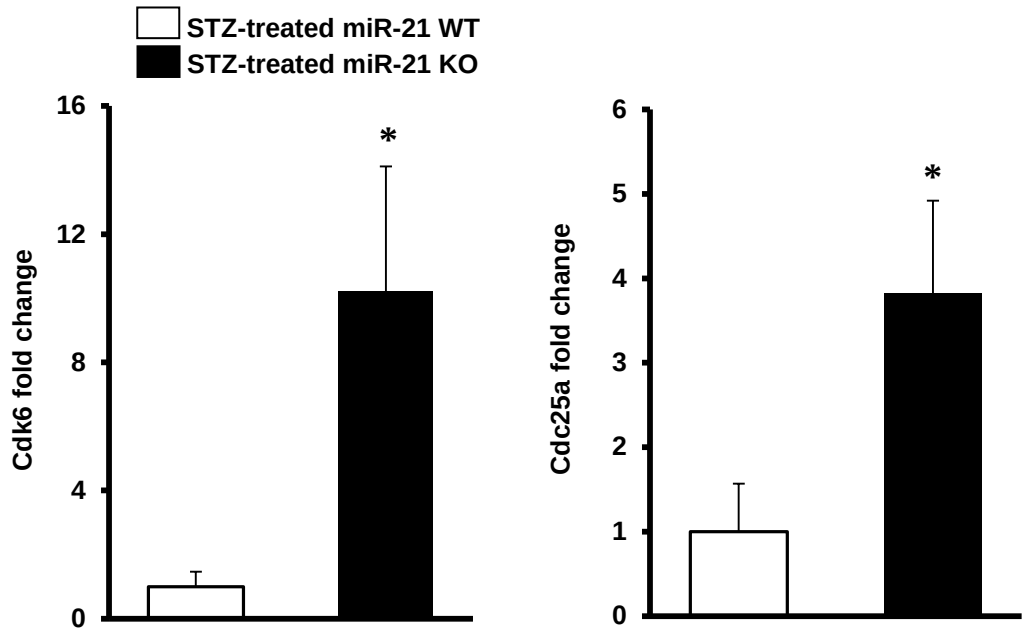

Figure 3.7. Examination of potential regulatory genes of miR-21 in in glomeruli of STZ-treated miR-21 WT and KO mice. The qrt-PCR result showed that there was an increased expression of Cdk6 and Cdc25a in glomeruli of STZ-treated miR-21 KO mice versus STZ-treated miR-21 WT mice (*$P < 0.05$).

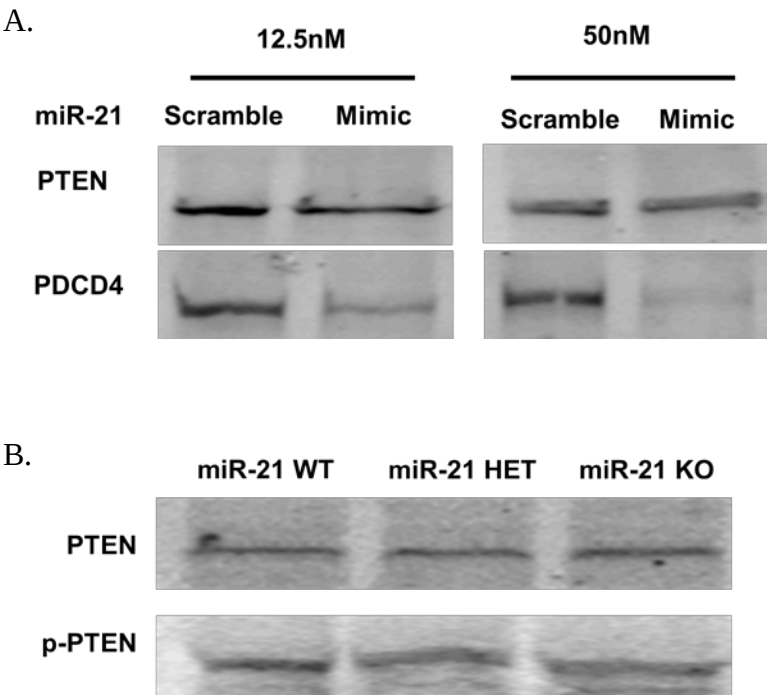

Figure 3.8. Examination of the protein level of PTEN in miR-21 mimic-transfected human embryonic kidney (HEK) cells and DBA/2J mice. (A) The western blot showed that the protein level of PDCD4 was decreased by miR-21 overexpression in HEK cells. However, there was no difference in the protein level of PTEN between miR-21mimic- and scramble-transfected HEK cells. (B) The western blot showed that there was no difference in the protein level of PTEN and phosphorylated-PTEN in the cortex of miR-21 WT, HET, and KO DBA/2J mice.

References

1. Mauer, M., Mogensen, C.E. & Friedman, E.A. Diseases of the Kidney. in *Diabetic nephropathy* (eds. Schrier, R.W. & Gottschalk, C.W.) p.2019-2061 (Little,Brown and Company, New York, 1997).
2. US Renal Data System. USRDS 2011 Annual Data Report: Atlas of Chronic Kidney Disease and Eng Stage Renal Disease in the United States. (National Institutes of Health, National Institute of Diabetes and Digestive and Kidney Diseases, Bethesda, MD, 2011).
3. Brosius, F.C., 3rd, *et al.* Mouse models of diabetic nephropathy. *J Am Soc Nephrol* **20**, 2503-2512 (2009).
4. Qi, Z., *et al.* Characterization of susceptibility of inbred mouse strains to diabetic nephropathy. *Diabetes* **54**, 2628-2637 (2005).
5. Thum, T., *et al.* MicroRNA-21 contributes to myocardial disease by stimulating MAP kinase signalling in fibroblasts. *Nature* **456**, 980-984 (2008).
6. Denby, L., *et al.* miR-21 and miR-214 are consistently modulated during renal injury in rodent models. *Am J Pathol* **179**, 661-672 (2011).
7. Zhong, Z., Dong, Z., Yang, L. & Gong, Z. miR-21 induces cell cycle at S phase and modulates cell proliferation by down-regulating hMSH2 in lung cancer. *Journal of cancer research and clinical oncology* **138**, 1781-1788 (2012).
8. Wang, P., *et al.* microRNA-21 negatively regulates Cdc25A and cell cycle progression in colon cancer cells. *Cancer Res* **69**, 8157-8165 (2009).
9. Ekholm, S.V. & Reed, S.I. Regulation of G(1) cyclin-dependent kinases in the mammalian cell cycle. *Current opinion in cell biology* **12**, 676-684 (2000).
10. Boutros, R., Lobjois, V. & Ducommun, B. CDC25 phosphatases in cancer cells: key players? Good targets? *Nature reviews. Cancer* **7**, 495-507 (2007).
11. Frankel, L.B., *et al.* Programmed cell death 4 (PDCD4) is an important functional target of the microRNA miR-21 in breast cancer cells. *J Biol Chem* **283**, 1026-1033 (2008).
12. Breyer, M.D., *et al.* Mouse models of diabetic nephropathy. *J Am Soc Nephrol* **16**, 27-45 (2005).
13. Chau, B.N., *et al.* MicroRNA-21 promotes fibrosis of the kidney by silencing metabolic pathways. *Sci Transl Med* **4**, 121ra118 (2012).
14. Liu, G., *et al.* miR-21 mediates fibrogenic activation of pulmonary fibroblasts and lung fibrosis. *J Exp Med* **207**, 1589-1597 (2010).

15. Dey, N., *et al.* MicroRNA-21 orchestrates high glucose-induced signals to TOR complex 1, resulting in renal cell pathology in diabetes. *J Biol Chem* **286**, 25586-25603 (2011).
16. Meng, F., *et al.* MicroRNA-21 regulates expression of the PTEN tumor suppressor gene in human hepatocellular cancer. *Gastroenterology* **133**, 647-658 (2007).
17. Wolf, G. Cell cycle regulation in diabetic nephropathy. *Kidney Int Suppl* **77**, S59-66 (2000).
18. Marshall, C.B. & Shankland, S.J. Cell cycle regulatory proteins in podocyte health and disease. *Nephron Exp Nephrol* **106**, e51-59 (2007).
19. Stewart, Z.A., Westfall, M.D. & Pietenpol, J.A. Cell-cycle dysregulation and anticancer therapy. *Trends in pharmacological sciences* **24**, 139-145 (2003).
20. Schoecklmann, H.O., Rupprecht, H.D., Zauner, I. & Sterzel, R.B. TGF-beta1-induced cell cycle arrest in renal mesangial cells involves inhibition of cyclin E-cdk 2 activation and retinoblastoma protein phosphorylation. *Kidney Int* **51**, 1228-1236 (1997).
21. Liu, B. & Preisig, P. TGF-beta1-mediated hypertrophy involves inhibiting pRB phosphorylation by blocking activation of cyclin E kinase. *The American journal of physiology* **277**, F186-194 (1999).
22. Choi, M.E., Kim, E.G., Huang, Q. & Ballermann, B.J. Rat mesangial cell hypertrophy in response to transforming growth factor-beta 1. *Kidney Int* **44**, 948-958 (1993).
23. Dellago, H., *et al.* High levels of oncomiR-21 contribute to the senescence-induced growth arrest in normal human cells and its knock-down increases the replicative lifespan. *Aging cell* (2013).
24. Awazu, M., Omori, S., Ishikura, K., Hida, M. & Fujita, H. The lack of cyclin kinase inhibitor p27(Kip1) ameliorates progression of diabetic nephropathy. *J Am Soc Nephrol* **14**, 699-708 (2003).
25. Wolf, G., *et al.* Glomerular expression of p27Kip1 in diabetic db/db mouse: role of hyperglycemia. *Kidney Int* **53**, 869-879 (1998).
26. Zhang, Z., *et al.* MicroRNA-21 protects from mesangial cell proliferation induced by diabetic nephropathy in db/db mice. *FEBS Lett* **583**, 2009-2014 (2009).
27. Lu, T.X., *et al.* MicroRNA-21 limits in vivo immune response-mediated activation of the IL-12/IFN-gamma pathway, Th1 polarization, and the severity of delayed-type hypersensitivity. *J Immunol* **187**, 3362-3373 (2011).
28. Tesch, G.H. & Allen, T.J. Rodent models of streptozotocin-induced diabetic nephropathy. *Nephrology* **12**, 261-266 (2007).

29. Zhang, H., *et al.* Podocyte-specific overexpression of GLUT1 surprisingly reduces mesangial matrix expansion in diabetic nephropathy in mice. *Am J Physiol Renal Physiol* **299**, F91-98 (2010).
30. Cortes-Hernandez, J., *et al.* Murine glomerular mesangial cell uptake of apoptotic cells is inefficient and involves serum-mediated but complement-independent mechanisms. *Clinical and experimental immunology* **130**, 459-466 (2002).
31. Mene, P. & Stoppacciaro, A. Isolation and propagation of glomerular mesangial cells. *Methods Mol Biol* **466**, 3-17 (2009).
32. Pozarowski, P. & Darzynkiewicz, Z. Analysis of cell cycle by flow cytometry. *Methods Mol Biol* **281**, 301-311 (2004).

Chapter IV

Linking disease-associated miRNA and disease-associated mRNA identifies miRNA-mRNA interaction

Abstract

miRNAs regulate gene expression on a post-transcriptional level by binding to the primary transcript of target genes, thereby repressing translation into protein and facilitating degradation. Because experimental identification of target genes remains challenging, different computational algorithms have been developed to predict miRNA-mRNA interactions. Unfortunately, overlap between different algorithms and prediction accuracy for specific cell types and disease contexts are poor. Therefore, we developed a new algorithm to identify miRNA-mRNA interaction based on associations of expression with disease clinical manifestation.

To test this algorithm, we used miRNA and mRNA expression data obtained from the same micro-dissected glomeruli of kidney biopsies of American Indian patients with DN (testing and validating cohorts, total n=48). The miRNA and mRNA expression levels were correlated independently with patients' urine albumin to

creatinine ratio (ACR). ACR-associated miRNAs and mRNAs were integrated with two computational prediction algorithms and experimental results from Photoactivatable-Ribonucleoside-Enhanced Crosslinking and Immunoprecipitation (PAR-CLIP) RNA sequencing. We determined that among 10 miRNAs, which were highly correlated with ACR ($P < 0.0001$, $R > 0.6$), 6 showed high expression in renal glomeruli and are broadly conserved. 245 transcripts of protein-coding genes were correlated with ACR ($P < 0.0001$, $R > 0.4$ or < -0.4). Among them, 25 transcripts had been found to be candidate targets for at least one of the ACR-associated 6 miRNAs by two prediction algorithms and PAR-CLIP RNA sequencing. We further determined that overexpression of miR-200a repressed RALGPS2, SUPT6H and EXOC7 mRNA levels and that the 3'UTR of EXOC7 is a sequence-dependent target of miR-200a.

We propose that integrating phenotype-associated miRNA and mRNA expression with experimental and computational target identification methods facilitates miRNA-mRNA interactions discovery.

Introduction

Mature miRNAs, with RNA-induced silencing complex (RISC), bind to complementary sequences of mRNA 3'UTR to repress the mRNA expression at a post-transcriptional level[1,2]. The exact repression mechanism, though explored, is still unclear but it is involved in mRNA deadenylation, decapping and translational ribosomal inhibition[3,4]. Lately, miRNAs have also been shown to bind to mRNA 5'UTR and coding region to repress the mRNA expression[5-8]. miRNA are critical in maintaining normal cell physiology and regulating disease pathogenesis[9,10]. The expression of miR-17-92 cluster targets hundreds of genes and is strongly associated with oncogenic activity[11]. On the other hand, depletion of miR-17-92 in mice is postnatal lethal and leads to cardiac and lung defects[12]. Therefore, a significant number of studies have investigated the interaction and targeting between miRNAs and mRNAs. To date, several algorithms are available to predict the targeting between miRNAs and mRNAs, such as TargetScan[13-15], which is based on the matched seed sequences and conservative binding sites. MiRNAanda [16,17], which applies dynamic programming alignment and thermodynamic calculation for complimentary binding between miRNAs and mRNAs, is another commonly used application. However, the false prediction rate for those prediction algorithms remains high[18] and the number of experimentally-verified targets is still low. For example, human miR-21 has only 42

validated target genes according to miRNAecord[19], a resource of experimentally-verified miRNA-target interaction, but it has 164 predicted targets in Targetscan [13-15].

For that reason, many studies developed new approaches to explore miRNA-mRNA interaction more than just sequence binding prediction. That includes MAGIA[20], which integrates miRNA-mRNA correlation from the expression data with pre-existing prediction algorithms. The other tools apply new regression models[21,22] or Bayesian inference[23] to facilitate target genes searching. Nevertheless, it is still unclear whether these approaches improve the preciseness to identify target genes or determine the regulatory role of miRNA-mRNA interaction in disease progression. Therefore, we developed an alternative approach to investigate miRNA-mRNA interaction based on their associations with disease clinical manifestation.

We previously had identified miRNAs that exhibit high correlation with ACR, a disease relevant outcome. We noticed that current knowledge about potential functions of these miRNAs remains very limited and the number of potential target genes predicted by computational algorithms is very large. To facilitate identification of mechanisms regulated by ACR-associated miRNAs, we developed an in-silico approach to link disease-associated miRNAs and disease-associated genes together, based on the correlation with disease clinical manifestation, to uncover

disease-relevant target genes. With this approach, we identify miRNAs target genes as well as the regulatory role of miRNA-mRNA interaction in disease progression.

Result

miRNAs correlate with proteinuria in human diabetic nephropathy

To identify miRNAs relevant for glomerular injury, we profiled the miRNA expression from renal glomeruli of kidney biopsies of 48 American Indian DN patients. To identify miRNAs with potential mechanistic relevance, we associated glomerular miRNA expression levels with clinical relevant manifestations, such as urine ACR or GFR in our cohorts. The participants exhibited a broad range of proteinuria (quantified as ACR in μg/mg), while the mean GFR (iothalamate clearance) was above 90 ml/min/1.73m^2 (Table 4.1). Highly significant and positive correlations with ACR were detected for 49 miRNAs out of 377 ($P < 0.0001$, $R > 0.4$). Interestingly, none of the tested miRNAs exhibited significant negative correlation with ACR. Moreover, we did not notice significant correlation between miRNAs and GFR (P-value > 0.05 for all miRNAs). We listed the top 10 miRNAs, which had the most positive correlation with ACR (Table 4.2). Because highly abundant miRNAs are in general thought to be more likely to mediate significant target gene repression, we ranked the miRNAs by their relative expression level in renal glomeruli and identified the broadly-conserved miRNAs[24,25]. We chose 6 miRNAs, miR-21, miR-135a, miR-200a, miR-218, miR-429, and miR-142-3p that are both highly-expressed in renal glomeruli and broadly-conserved cross species to identify

miRNA-mediated mechanisms of DN.

Most miRNA-correlated genes are not predicted targets of miRNAs

To identify candidate miRNA-mRNA interaction, the mRNA from the same renal glomeruli of kidney biopsies of the same American Indian cohorts was profiled. The correlation analysis was performed between the 6 miRNAs and genes on the array. Table 4.3 listed the top 10 genes that had the most negative correlation (R ranges from -0.48 to -0.67) with each 6 miRNAs. Figure 4.1 illustrated the correlated connection between miRNAs and genes. Among 44 top 10 miRNA-correlated genes, only ANTXR2 and IFNAR1 (4.5%) are predicted as sequence-dependent targets of miRNA218 and miRNA200a based on targetscan[13-15], respectively. If we expand the number up to the top 50 most miRNA-correlated genes, 7 out of 194 correlated genes are targetscan predicted targets (3.6%), and among the top 100 most miRNA-correlated genes, 19 out of 349 correlated genes are targetscan predicted targets of the corresponding miRNA (5.4%).

ACR-correlated genes are ACR-correlated miRNAs' predicted targets

To test our hypothesis that miRNA expression is driven by disease status to negatively feedback the change of disease-associated genes. We correlated mRNA expression

with disease clinical manifestation, ACR. The result showed that 245 mRNAs significantly correlated with ACR ($R > 0.4$ or $R < -0.4$, $P < 0.0001$). Among those 245 genes, 39 genes (16%) are the TargetScan-predicted targets for the previous chosen 6 miRNAs (Table 4.4). We additionally examined whether there were RNA read clusters in those 39 genes 3'UTR by PAR-CLIP RNA sequencing in human embryonic kidney (HEK) cells[26]. We also applied the second prediction algorithm, miRNAanda[16,17], to further verify the possible miRNAs' targets. We found that 25 out of the 39 genes had RNA read clusters in 3'UTR and at the same are predicted as the corresponding miRNA's targets in miRNAanda. Figures 4.2 illustrated the target predictions between the chosen 6 ACR-correlated miRNAs and ACR-correlated genes that both have RNA read clusters in 3'UTR and are predicted targets of the corresponding miRNA's by two prediction algorithms, TargetScan and miRNAanda. We regarded those 25 genes as the most likely targets of the corresponding miRNAs and the interaction with miRNAs might play a role in disease progression.

To further understand the relationship between those 25 genes and their predicted miRNAs, we examined their associations from the miRNA and mRNA expression data by Pearson correlation (Table 4.5). The result showed that the correlation between the most likely targets and their predicted miRNAs was moderate (R ranges from -0.17 to -0.45 and 0.05 to 0.37) and less than 50% of the correlation was

significant ($P < 0.05$). Moreover, the 25 genes did not rank high according to the most negative or positive correlation.

miR-200a has repression effect on SUPT6H and EXOC7

miR-200a is known to regulate epithelial-mesenchymal transition (EMT)[27] and is implicative to protect against DN[28]. To verify the potential targets that were identified by linking ACR-correlated miRNAs and genes, we proceeded to demonstrate the targeting between miR-200a and its potential targets. Among miR-200a potential targets, we chose the top 3 most positively-correlated genes, RALGPS2, LYPD6, AGPS, and top 3 most negatively-correlated genes, NFASC, SUPT6H, EXOC7, to perform the experimental validation.

To identify a suitable cell system to test candidate miR-200a target genes, we first examined the endogenous miR-200a level in different cells. Our qrt-PCR result showed that HEK cells had very low endogenous miR-200a compared to podocyte and renal proximal tubular cell lines (Figure 4.3). ZEB2 is a known target of miR-200a[27]. Consequently, we measured ZEB2, RALGPS2, LYPD6, AGPS, SUPT6H, EXOC7, and NFASC mRNA level by transfecting miR-200a mimic into HEK cells. The qrt-PCR result revealed that the miR-200a mimic-transfected HEK cells had significantly lower ZEB2, RALGPS2, SUPT6H and EXOC7 level compared to the

miR-200a scramble transfection ($P < 0.01$; Figure 4.4A: fold change for ZEB2, SUPT6H, EXOC7 were 0.23, 0.74 and 0.75, respectively. Figure 4.4B: fold change for RALGPS2 was 0.59).

EXOC7 is a target gene of miR-200a

To confirm direct targeting of EXOC7 by miR-200a, we co-transfected HEK cells with EXOC7 3'UTR luciferase construct and miR-200a mimic oligonucleotides. The results demonstrated decreased luciferase activity upon transfection of miR-200a mimic (Figure 4.5; $P < 0.01$), confirming direct targeting of the 3'UTR of EXOC7 by miR-200a, which has not been reported previously.

Discussion

In this study, we identified miRNAs and mRNAs in renal glomeruli that exhibit significant correlation with ACR in patients with DN. We further discovered that many ACR-correlated genes are predicted targets of ACR-correlated miRNAs by two different prediction algorithms and PAR-CLIP RNA sequencing. We verified that EXOC7 are the sequence-dependent target of miR-200a, and RALGPS2 and SUPT6H are regulated by miR-200a. This approach, linking miRNAs and genes by their associations with disease status, provide an alternative way to identify miRNA target genes.

Among the top 10 miRNAs that had the most positive correlation with ACR, 6 were highly-expressed in renal glomeruli and broadly conserved. Some of the significant miRNAs were widely studied in cancer biology. For instance, miR-135a promotes growth and migration of cancer cells[29,30], while miR-218 limits the invasiveness of cancer cells[31], and miR-142-3p regulates myeloid differentiation and leukemia development[32]. Nevertheless, there are miRNAs related to kidney diseases, such as miR-21, which plays a role in renal fibrosis[33,34]. Furthermore, our previous study showed that miR-21 protects against TGFβ-related renal glomerulopathy. In addition, miR-200a and miR-429, which all belong to the miR-200 family, have been shown to regulate EMT and prevent renal fibrosis[27,28].

To identify the target genes of ACR-correlated miRNAs, we correlated the miRNA and mRNA expression from the same samples. Interestingly, we did not find many predicted targets from the negative correlation of mRNAs with miRNAs (Table 4.3). We further correlated genes with ACR, and unexpectedly found that many ACR-correlated genes (both positive and negative correlation) are the predicted targets of the ACR-correlated miRNAs (Table 4.4). However, we also noticed that the correlations between the ACR-correlated miRNAs and their target-predicted ACR-correlated genes are less significant (Table 4.5). As studies have observed that miRNAs can form negative feedback loop in the signaling pathway[35,36], miRNAs might go up with disease progression as an attempt to limit the disease damage. Under this concept, for the miRNA-targeted genes that increase with disease progression (positive correlation with ACR), miRNAs will also increase as an attempt to repress the upregulation. For that reason, we observed many ACR positively-correlated genes are predicted targets of miRNAs (Table 4.4). However, due to the negative feedback cannot completely reverse the original change, we did not detect significant negative correlation between miRNAs and their targets from miRNAs and mRNA expression data (Table 4.5).

We additionally noticed that many ACR negatively-correlated genes are also predicted targets of miRNAs (Table 4.4). Based on this observation, we proposed another

mechanism that genes decrease as a consequence of progression of disease. This concept suggests that miRNAs mediate additional gene repression. This positive enforcement regulation loop was also observed in previous studies[36]. Due to the negatively-correlated genes are directly driven by the disease itself and miRNAs targeting only contributes to additional repression, we did not detect very significant negative correlation between the ACR-correlated miRNAs and their predicted targets, which are negatively correlated with ACR. Importantly, we did not detect miRNAs that were negatively correlated with ACR. This is consistent with our hypotheses that miRNAs increase with disease progression to limit disease-upregulated genes or miRNAs increase with disease progression to further repress the disease-downregualted genes.

Since miR-200a is highly correlated with ACR and together with miR-429, which also belongs to miR-200 sequence family, suppresses EMT to protect against renal fibrosis[27,28], we chose miR-200a to verify the finding from linking the ACR-correlated miRNAs and ACR-correlated genes. Among 245 genes, which are associated with ACR, 10 of them are the targetscan-predicted targets of miR-200a (Table 4.4). The basic functions of those genes were studied. NFASC (neurofascin) is a cell adhesion molecule, which links extracellular matrix to the intracellular cytoskeleton, and plays a role in neuron growth during development[37]. EXOC7 (exocyst complex component

7) is the component of exocytosis complex and it is involved in the docking of exocytic vesicles with fusion sites on the plasma membrane[38]. EXOC7 is required for targeting glucose transporter 4 (Glut4) to the plasma membrane in response to insulin[39]. RALGPS2 (Guanine nucleotide exchange factor for the small GTPase RALA) plays a role in cytoskeleton organization[40]. In addition, SUPT6H (suppressor of Ty 6 homolog), ZNF629 and ZNF793 (zinc finger protein) regulates gene translation[41,42]. Although these genes have not been broadly studied in DN, the new miRNA-mRNA interactions we are proposing here bring a new prospect to DN disease mechanism. Exocytosis forms the basis of the delivery of secretory proteins and intracellular signaling, such as insulin secretion as well as the cellular response to inuslin[43]. Reduced insulin exocytosis in human pancreatic β cells is related type 2 diabetes[44] and diabetes also affects the ability of exocytosis in other cells[45]. Furthermore, Exocytosis is involved in aquaporin 2 water channel activity in renal collecting tubule[46] and has a role in renal ischemia-reperfusion injury[47]. Our result, which showed EXOC7 being the target of miR-200a, provides additional evidence that miR-200a and exocytosis might play an important role in DN, and it urges additional studies to explore these intriguing findings.

Despite our result that miR-200a regulates SUPT6H and EXOC7, compared to the well-known target of miR-200a, ZEB2[27], the repression effect of miR-200a on

EXOC7 and SUPT6H seems marginal (fold change ≈ 0.7; Figure 4.4A). Nevertheless, miRNAs can have tuning interactions with genes to marginally repress the protein to the target level[1]. For example, miR-375 targets myotrophin to lower its level to an optimal level but still remains functional for insulin secretion[48]. miR-8 in Drosophila reduces atrophin to a level to prevent neurodegeneration without compromising viability[49].

Our concepts that miRNAs increase with disease progression to limit gene upregulation or to further repress gene downregulation can effectively narrow down the potential miRNA targets among hundreds of candidates. Nevertheless, our method to link disease-associated miRNA and disease-associated mRNA needs to be accompanied by prediction algorithms or other supporting experiments, such as PAR-CLIP RNA sequencing. Therefore, to effectively identify miRNA's sequence-dependent targets, we proposed creating a ranking system by using disease associations with miRNAs and mRNA plus prediction algorithms and the interaction with AGO proteins.

In summary, we have shown linking disease-associated miRNAs and disease-associated mRNA by target prediction is an alternative way to identify miRNA-mRNA interaction. The findings that miR-200a targets EXOC7 and other genes open up potential disease mechanisms to be explored in the future.

Methods and Materials

Study Subjects. The kidney biopsy samples had been collected from enrolled participants in a randomized, placebo-controlled, clinical trial (ClinicalTrials.gov No. NCT00340678) as the previous chapter described[50]. Urinary albumin and creatinine as well as iothalamate concentrations for GFR determination were measured as described[51] and values of the examination closest to the kidney biopsy were used in the present analyses. This study was approved by the Review Board of the National Institute of Diabetes and Digestive and Kidney Diseases. Each participant gave informed consent.

miRNA expression analysis. miRNA profiling was obtained using TaqMan miRNA assays (Applied Biosystems) as described[52]. In brief, small RNA fraction (<200 nt) was isolated from micro-dissected glomeruli using RNeasy® and MinElute® Cleanup kits (Qiagen) and reverse transcribed using TaqMan Megaplex RT primers (Applied Biosystems). Human glomerular small RNA was amplified by Megaplex PreAmp primers (Applied Biosystems). TaqMan array human and rodent miRNA 'A' cards (Applied Biosystems) were used to obtain miRNA profiles according to the manufacturer's protocol. miRNA expression values, threshold cycle (CT), were normalized by U6 small nuclear RNA (snRNA), and RNU44 and RNU48 small

nucleolar RNA (snoRNA). Delta cycle time (ΔCT) was calculated by subtracting miRNAs' CT from geometric mean of snRNA's and snoRNA's CT. Expression level in arbitrary units were calculated from 2 to the power of delta cycle time ($2^{\Delta\Delta CT}$).

mRNA microarray and analysis. Total RNA was isolated from micro-dissected glomeruli of kidney biopsy according to a protocol, which was described before[53]. The total RNA was reverse-transcribed and linearly amplified to be applied to Affymetrix HG-U133A microarray. The fragmentation, hybridization, staining and imaging were performed by the Affymetrix Expression Analysis Technical Manual. The microarray analysis was described before and Robust Multichip Average (RMA) was used to normalize the data[54].

Batch correction. Our study cohort consisted of one testing cohort (N=22) and one validating cohort (N=26). Subjects of both cohorts tested in this study were pulled from the same pool of participants of the American Indian study. In order to increase analysis power, we combined miRNA or mRNA expression data from two cohorts to increase sample size (total subjects = 48). We applied ComBat[55], a method of combining batches of gene expression microarray data, to adjust the batch effects.

Correlation analysis. Pearson correlation was performed in the correlation analysis. miRNA ΔCT was correlated with mRNA hybridization log2 transformed intensity, mRNA hybridization log2 transformed intensity was correlated with patient's urine albumin-creatinine ratio (ACR), and arbitrary fold change of miRNAs, which was calculated from 2 to the power of ΔCT, was correlated with patient's ACR.

Photoactivatable Ribonucleoside Enhanced Crosslinking and Immunoprecipitation (PAR-CLIP). Argonaute proteins (AGO) 1-4, which are the component of RISC and bind to both miRNAs and mRNA, were immunoprecipitated to examine the binding RNA fragments. The PAR-CLIP method was used and described as previous[26]. In brief, HEK cells stably expressing FLAG/HA-tagged AGO1-4 were grown overnight in the medium supplemented with 100 μM 4-thiouridine (4-SU), which is photoactivatable nucleosides. The living cells were irradiated with 365 nm UV light to introduce crosslinking between the AGO1-4 and RNA. Then, the AGO 1-4 were immunoprecipitated and the binding RNA with the AGO1-4 was recovered to cDNA library to be Solexa deep sequenced.

miRNA transfection. miR-200a mimic oligonucleotides (Thermo Scientific Dhamacon miRNAIDIAN microRNA Mimics) were applied with Lipofectamine®

RNAiMAX Reagent (Invitrogen) to transfect HEK cells. The cell transfection was processed per manufacturer's protocol.

Quantitative real-time PCR. Qrt-PCR for measuring mRNA levels were conducted using TaqMan validated primers and probe sets (Applied Biosystem), according to manufacturer's protocols, on an ABI 7900HT real-time PCR system.

Luciferase reporter assays. The full length EXOC7 3'UTR was constructed with firefly luciferase (abm, BC, Canada). The 3'UTR vector, Renilla luciferase plasmid, and miR-200a mimic oligonucleotides were co-transfected into HEK cells using lipofectamine LTX and plus reagents (Invitrogen). Luciferase activity was measured 48 hours after transfection in luciferase assay plate reader.

Statistical analysis. The correlation analysis and significance was determined by Pearson correlation and R script was used. T-test was used to compare mRNA level and luciferase activity between miR-200a mimic and scramble transfection.

Table 4.1. Characteristics of American Indian cohort

	American Indian
No. of subject	48
Age: Mean (SD)	44.4 (10.2)
Gender: % of female	81%
GFR: Mean (SD)	149.2 (50.6)
ACR: Mean (SD)	358.7 (1151.8)

Table 4.2. The top 10 ACR-correlated miRNAs

miRNA	*Correlation*	*P value*	*Relative expression**	*Broadly conserved miRNA*
miR-642	0.75	<0.0001	medium	no
miR-21	**0.71**	**<0.0001**	**high**	**yes**
miR-135a	**0.69**	**<0.0001**	**medium**	**yes**
miR-32	0.69	<0.0001	low	no
miR-142-5p	0.69	<0.0001	low	no
miR-660	0.67	<0.0001	medium	no
miR-200a	**0.67**	**<0.0001**	**medium**	**yes**
miR-218	**0.66**	**<0.0001**	**medium**	**yes**
miR-429	**0.62**	**<0.0001**	**medium**	**yes**
miR-142-3p	**0.62**	**<0.0001**	**high**	**yes**

*Expression level was defined as high if cycle time value in real-time PCR <25, as medium if cycle time value in real-time PCR ranges from 25-30, as low if cycle time value in real-time PCR >30

Bold font indicates miRNAs that are both highly-expressed and broadly-conserved

Table 4.3. Correlation between genes and ACR-correlated miRNAs*

miRNA	*Correlated gene*	*Correlation*	*miRNA*	*Correlated gene*	*Correlation*	*miRNA*	*Correlated gene*	*Correlation*
miR-21	PDIA5	-0.58	miR-135a	IFNAR1	-0.60	miR-200a	ANTXR2	-0.67
miR-21	FAM53B	-0.51	miR-135a	ANTXR2	-0.60	miR-200a	HYAL2	-0.65
miR-21	ROBO4	-0.50	miR-135a	GNA12	-0.59	miR-200a	LMO2	-0.64
miR-21	ASCC2	-0.50	miR-135a	PTPRG	-0.59	miR-200a	AMMECR1L	-0.64
miR-21	STARD8	-0.50	miR-135a	GCC1	-0.58	miR-200a	ETS2	-0.64
miR-21	RNF151	-0.50	miR-135a	TICAM2	-0.56	miR-200a	SEC14l1	-0.63
miR-21	HTRA3	-0.50	miR-135a	MAP7D1	-0.55	miR-200a	**IFNAR1†**	-0.63
miR-21	UBE2J2	-0.49	miR-135a	SFRS16	-0.54	miR-200a	S1PR1	-0.62
miR-21	S1PR1	-0.49	miR-135a	PDIA5	-0.53	miR-200a	ARRB1	-0.62
miR-21	ID1	-0.49	miR-135a	GOLGA3	-0.53	miR-200a	GFOD1	-0.62
miR-218	BAZ2A	-0.61	miR-429	SNX11	-0.56	miR-142-3p	PDIA5	-0.60
miR-218	PLXND1	-0.61	miR-429	GNA12	-0.55	miR-142-3p	RNF151	-0.55
miR-218	**ANTXR2†**	-0.61	miR-429	ANTXR1	-0.55	miR-142-3p	SNX11	-0.53
miR-218	TNFRSF1A	-0.60	miR-429	TBCD	-0.55	miR-142-3p	ROBO4	-0.53
miR-218	MINK1	-0.59	miR-429	SH3BP5	-0.54	miR-142-3p	NUFIP1	-0.50
miR-218	TICAM2	-0.59	miR-429	ANTXR2	-0.54	miR-142-3p	CARHSP1	-0.50
miR-218	OSBPL5	-0.58	miR-429	NUDT11	-0.54	miR-142-3p	STARD8	-0.50
miR-218	SETD8	-0.57	miR-429	CHFR	-0.54	miR-142-3p	ID1	-0.49
miR-218	MAP7D1	-0.57	miR-429	EDG1	-0.54	miR-142-3p	HTRA3	-0.48
miR-218	TOX2	-0.57	miR-429	CYP26B1	-0.53	miR-142-3p	EML1	-0.48

The P value for correlation is all < 0.0001

*Table only lists the top 10 genes that have the most negative correlation with miRNAs

†Targetscan predicted target for the corresponding miRNA

Table 4.4. Target prediction between ACR-correlated genes and ACR-correlated miRNAs

Gene	*Correlation with ACR*	*PAR-CLIP 3'UTR cluster*	*ACR-correlated miRNA targeting the gene**	*miRanda-predicted targeting between gene and miRNA*
EHD1	-0.5	yes	miR-21	yes
RALGPS2	0.41	yes	miR-21, miR-200a, miR-429	yes
VPS37C	-0.47	yes	miR-135a	yes
SUPT6H	-0.47	yes	miR-135a, miR-200a	yes
UBOX5	-0.45	yes	miR-135a	yes
NAIF1	-0.44	yes	miR-135a	yes
RARA	-0.43	yes	miR-135a, miR-218	yes
ENTPD1	0.41	yes	miR-135a, miR-429	no
STRBP	0.45	yes	miR-135a	no
KCNN3	0.45	yes	miR-135a, miR-218	no
AGPS	0.47	yes	miR-135a, miR-200a	yes
NFASC	-0.59	yes	miR-200a, miR-429	no
EXOC7	-0.53	yes	miR-200a	yes
ZNF793	-0.45	yes	miR-200a	yes
ARHGEF18	-0.42	yes	miR-200a	yes
RBM33	-0.41	yes	miR-200a	yes
ZNF629	-0.41	yes	miR-200a	no
LYPD6	0.43	yes	miR-200a	yes
RIMS3	-0.53	yes	miR-218, miR-429	no
ZNFX1	-0.46	yes	miR-218	no
FLNC	-0.44	no	miR-218	yes
ARL3	-0.44	yes	miR-218, miR-429	yes
SH3TC2	-0.42	no	miR-218	no
OLA1	-0.42	yes	miR-218	yes
N4BP1	-0.42	yes	miR-218	no
DPP6	-0.41	no	miR-218	yes
ABCC4	0.41	yes	miR-218	yes
SLC12A2	0.43	yes	miR-218	yes
SYPL1	0.43	yes	miR-218, miR-142-3p	yes
L3MBTL4	0.44	yes	miR-218	yes
FAM5C	0.44	yes	miR-218	yes
EGLN3	0.45	yes	miR-218	yes
SYDE1	-0.51	no	miR-429	yes
PI4KB	-0.44	yes	miR-429	yes
FYN	-0.44	yes	miR-429	yes
FXR2	-0.43	yes	miR-429	yes
ZFYVE1	-0.42	yes	miR-429, miR-142-3p	no
SP8	-0.46	yes	miR-142-3p	yes
SH2B1	-0.43	no	miR-142-3p	yes

* The target prediction is based on targetscan prediction algorithm. The P value for correlation between gene and ACR is all < 0.0001. Bold font indicates genes that have RNA cluster in 3'UTR in PAR-CLIP data and are predicted targets of the corresponding miRNAs in targetscan and miRanda

Table 4.5. Correlation between ACR-correlated miRNAs and their target-predicted ACR-correlated genes

ACR-correlated miRNA	*Predicted ACR-correlated gene*	*Correlation*	*P value*	*Correlation ranking**
miR-21	**EHD1**	-0.31	0.03	584
miR-21	**RALGPS2**	0.34	0.02	208
miR-135a	**VPS37C**	-0.17	0.27	4249
miR-135a	**SUPT6H**	-0.21	0.17	3097
miR-135a	**UBOX5**	-0.23	0.12	2494
miR-135a	**NAIF1**	-0.45	0.002	93
miR-135a	**RARA**	-0.32	0.03	972
miR-135a	**AGPS**	0.19	0.2	2221
miR-200a	**EXOC7**	-0.30	0.04	2172
miR-200a	**SUPT6H**	-0.33	0.02	1646
miR-200a	**ZNF793**	-0.23	0.13	3920
miR-200a	**ARHGEF18**	-0.23	0.12	3803
miR-200a	**RBM33**	-0.35	0.02	1400
miR-200a	**AGPS**	0.22	0.14	2042
miR-200a	**LYPD6**	0.12	0.44	3627
miR-218	**ARL3**	-0.20	0.18	3276
miR-218	**RARA**	-0.30	0.04	1415
miR-218	**OLA1**	-0.29	0.05	1612
miR-218	**ABCC4**	0.31	0.04	934
miR-218	**SLC12A2**	0.06	0.68	5420
miR-218	**SYPL1**	0.26	0.09	1510
miR-218	**L3MBTL4**	0.37	0.01	433
miR-218	**FAM5C**	0.21	0.17	2251
miR-218	**EGLN3**	0.33	0.03	725
miR-429	**PI4KB**	-0.33	0.02	773
miR-429	**FYN**	-0.30	0.04	1154
miR-429	**ARL3**	-0.25	0.09	2109
miR-429	**FXR2**	-0.29	0.05	1349
miR-142-3p	**SP8**	-0.27	0.07	910
miR-142-3p	**SYPL1**	0.05	0.72	4877

*The gene was ranked by the most negative or positive correlation with the corresponding miRNA
Bold font indicates genes that have RNA cluster in 3'UTR in PAR-CLIP data and are predicted targets of the corresponding miRNA in targetscan and miRanda

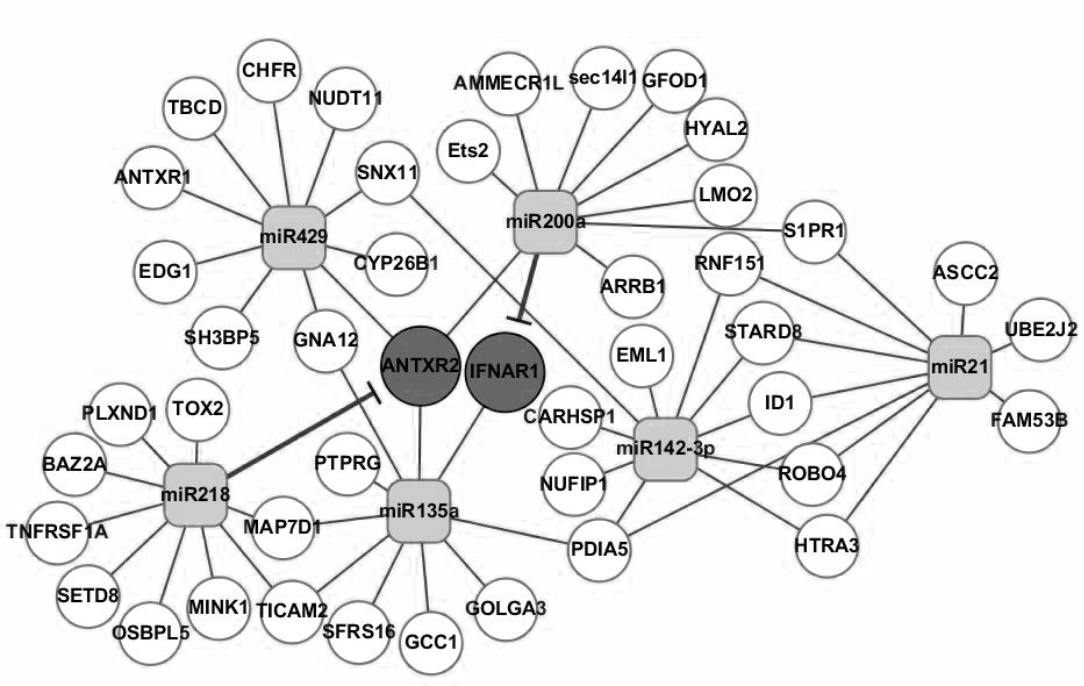

Figure 4.1. Cytoscape illustration of correlation between ACR-correlated miRNAs and genes in the same American Indian cohort. The 6 chosen ACR-correlated miRNAs are in gray round rectangle node. Top 10 genes that have the most negative correlation with each ACR-correlated miRNAs are in white and black circle node and have black straight edge connecting to the negatively-correlated miRNAs. Among them (N=44), only two are targetscan-predicted targets of miR-200a and miR-218 (black circle node and T arrow edge).

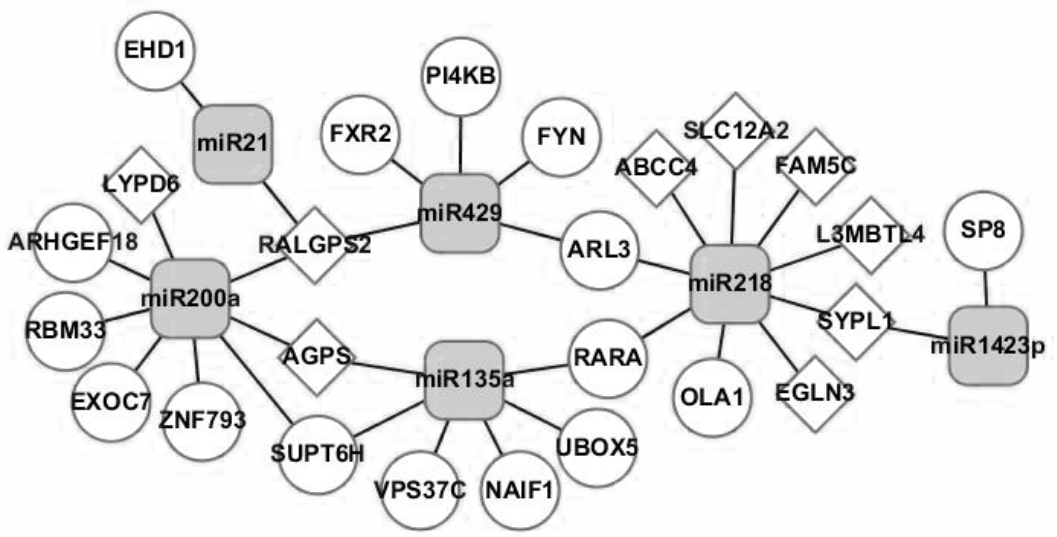

Figure 4.2. Cytoscape illustration of the target prediction between ACR-correlated miRNAs and ACR-correlated genes. ACR-correlated genes (white circle: negative correlation ith ACR; white diamond: positive correlation with ACR) are predicted targets of their connected ACR-correlated miRNAs (gray round rectangle) in targetscan. The targetscan-predicted targets also have RNA cluster in 3'UTR in PAP-clip data and are predicted as the corresponding miRNA targets in the second prediction algorithm, miRanda.

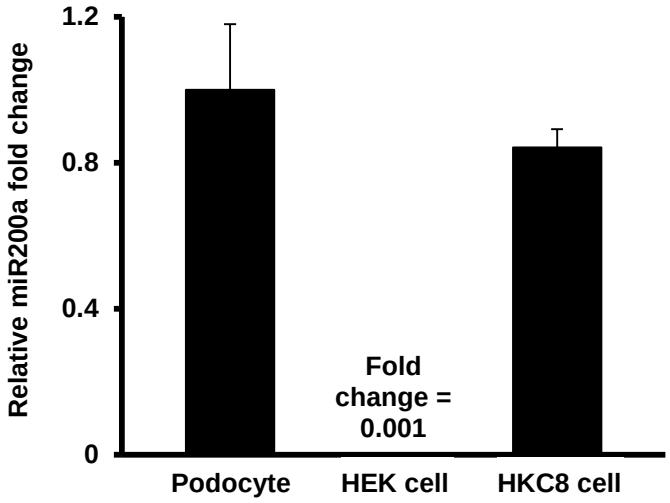

Figure 4.3. Examination of miR-200a level in different cell lines. Quantitative real time-PCR showed relatively low endogenous miR-200a level in human embryonic kidney (HEK) cells compared to human podocyte cell lines and human renal proximal tubular cell lines (HKC8).

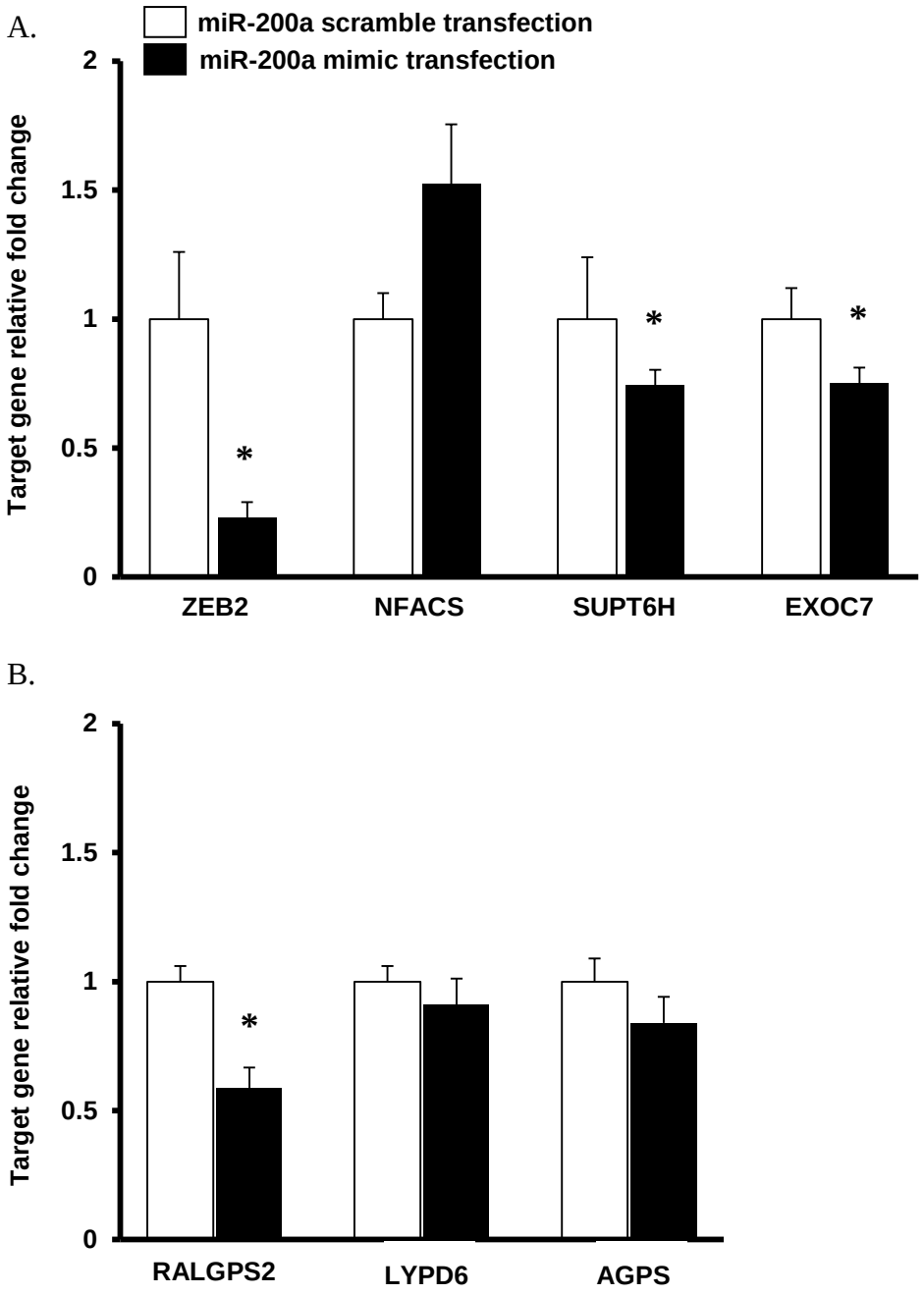

Figure 4.4. Examination of the predicted target between miR-200a and selected ACR-correlated genes. (A) Quantitative real time-PCR showed that miR-200a mimic transfection significantly suppressed ZEB2, SUPT6H and, EXOC7 mRNA levels in human embryonic kidney (HEK) cells (*P < 0.01, fold change for ZEB2, SUPT6H, EXOC7 were 0.23, 0.74 and 0.75, N=5). There is no repression effect of miR-200a mimic on NFACS. (B) Quantitative real time-PCR showed that miR-200a mimic transfection significantly suppressed RALGPS2 mRNA levels in human embryonic kidney (HEK) cells (*P < 0.01, fold change for RALGPS2 was 0.59, N=3). There is no repression effect of miR-200a mimic on LYPD6 and AGPS.

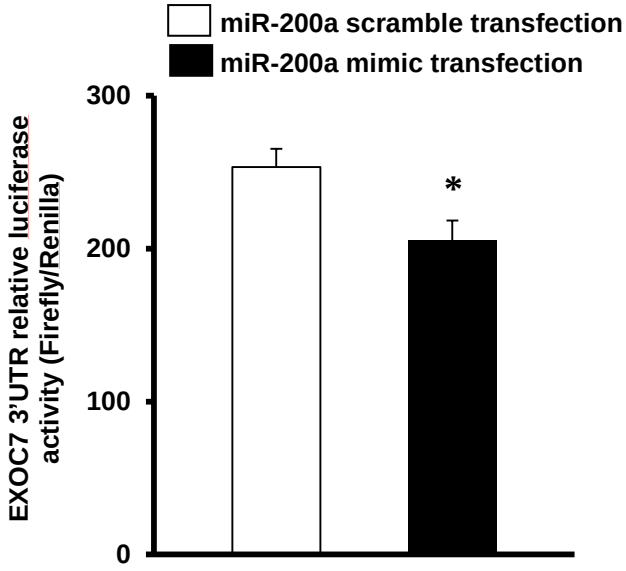

Figure 4.5. Examination of direct target between EXOC7 and miR-200a. Luciferase assay of HEK cells co-transfected with EXOC7 3'UTR luciferase construct and miR-200a mimic oligonucleotides showed that there was a decreased EXOC7 3'UTR luciferase construct activity in miR-200a overexpression (*P < 0.01, N=3).

Reference

1. Bartel, D.P. MicroRNAs: target recognition and regulatory functions. *Cell* **136**, 215-233 (2009).
2. Kusenda, B., Mraz, M., Mayer, J. & Pospisilova, S. MicroRNA biogenesis, functionality and cancer relevance. *Biomed Pap Med Fac Univ Palacky Olomouc Czech Repub* **150**, 205-215 (2006).
3. Filipowicz, W., Bhattacharyya, S.N. & Sonenberg, N. Mechanisms of post-transcriptional regulation by microRNAs: are the answers in sight? *Nature reviews. Genetics* **9**, 102-114 (2008).
4. Shukla, G.C., Singh, J. & Barik, S. MicroRNAs: Processing, Maturation, Target Recognition and Regulatory Functions. *Molecular and cellular pharmacology* **3**, 83-92 (2011).
5. Lytle, J.R., Yario, T.A. & Steitz, J.A. Target mRNAs are repressed as efficiently by microRNA-binding sites in the 5' UTR as in the 3' UTR. *Proc Natl Acad Sci U S A* **104**, 9667-9672 (2007).
6. Ajay, S.S., Athey, B.D. & Lee, I. Unified translation repression mechanism for microRNAs and upstream AUGs. *BMC genomics* **11**, 155 (2010).
7. Tay, Y., Zhang, J., Thomson, A.M., Lim, B. & Rigoutsos, I. MicroRNAs to Nanog, Oct4 and Sox2 coding regions modulate embryonic stem cell differentiation. *Nature* **455**, 1124-1128 (2008).
8. Orom, U.A., Nielsen, F.C. & Lund, A.H. MicroRNA-10a binds the 5'UTR of ribosomal protein mRNAs and enhances their translation. *Mol Cell* **30**, 460-471 (2008).
9. Wolf, G., Chen, S. & Ziyadeh, F.N. From the periphery of the glomerular capillary wall toward the center of disease: podocyte injury comes of age in diabetic nephropathy. *Diabetes* **54**, 1626-1634 (2005).
10. Thum, T., *et al.* MicroRNAs in the human heart: a clue to fetal gene reprogramming in heart failure. *Circulation* **116**, 258-267 (2007).
11. Olive, V., Jiang, I. & He, L. mir-17-92, a cluster of miRNAs in the midst of the cancer network. *Int J Biochem Cell Biol* **42**, 1348-1354 (2010).
12. Park, C.Y., Choi, Y.S. & McManus, M.T. Analysis of microRNA knockouts in mice. *Human molecular genetics* **19**, R169-175 (2010).
13. Lewis, B.P., Burge, C.B. & Bartel, D.P. Conserved seed pairing, often flanked by adenosines, indicates that thousands of human genes are microRNA targets. *Cell* **120**, 15-20 (2005).
14. Grimson, A., *et al.* MicroRNA targeting specificity in mammals: determinants beyond seed pairing. *Mol Cell* **27**, 91-105 (2007).

15. Friedman, R.C., Farh, K.K., Burge, C.B. & Bartel, D.P. Most mammalian mRNAs are conserved targets of microRNAs. *Genome Res* **19**, 92-105 (2009).
16. Enright, A.J., *et al.* MicroRNA targets in Drosophila. *Genome Biol* **5**, R1 (2003).
17. Betel, D., Wilson, M., Gabow, A., Marks, D.S. & Sander, C. The microRNA.org resource: targets and expression. *Nucleic Acids Res* **36**, D149-153 (2008).
18. Yue, D., Liu, H. & Huang, Y. Survey of Computational Algorithms for MicroRNA Target Prediction. *Curr Genomics* **10**, 478-492 (2009).
19. Xiao, F., *et al.* miRecords: an integrated resource for microRNA-target interactions. *Nucleic Acids Res* **37**, D105-110 (2009).
20. Sales, G., *et al.* MAGIA, a web-based tool for miRNA and Genes Integrated Analysis. *Nucleic Acids Res* **38**, W352-359 (2010).
21. Li, X., Gill, R., Cooper, N.G., Yoo, J.K. & Datta, S. Modeling microRNA-mRNA interactions using PLS regression in human colon cancer. *BMC Med Genomics* **4**, 44 (2011).
22. Muniategui, A., *et al.* Quantification of miRNA-mRNA interactions. *PLoS One* **7**, e30766 (2012).
23. Huang, J.C., Morris, Q.D. & Frey, B.J. Bayesian inference of MicroRNA targets from sequence and expression data. *J Comput Biol* **14**, 550-563 (2007).
24. Kozomara A, G.-J.S. miRBase: integrating microRNA annotation and deep-sequencing data. NAR 2011 2039(Database Issue):D2152-D2157.
25. Ambros, V., *et al.* A uniform system for microRNA annotation. *RNA* **9**, 277-279 (2003).
26. Hafner, M., *et al.* Transcriptome-wide identification of RNA-binding protein and microRNA target sites by PAR-CLIP. *Cell* **141**, 129-141 (2010).
27. Gregory, P.A., *et al.* The miR-200 family and miR-205 regulate epithelial to mesenchymal transition by targeting ZEB1 and SIP1. *Nat Cell Biol* **10**, 593-601 (2008).
28. Wang, B., *et al.* miR-200a Prevents renal fibrogenesis through repression of TGF-beta2 expression. *Diabetes* **60**, 280-287 (2011).
29. Zhou, W., *et al.* MiR-135a promotes growth and invasion of colorectal cancer via metastasis suppressor 1 in vitro. *Acta Biochim Biophys Sin (Shanghai)* **44**, 838-846 (2012).
30. Chen, Y., *et al.* miRNA-135a promotes breast cancer cell migration and invasion by targeting HOXA10. *BMC Cancer* **12**, 111 (2012).
31. Liu, Y., *et al.* MiR-218 reverses high invasiveness of glioblastoma cells by targeting the oncogenic transcription factor LEF1. *Oncol Rep* **28**, 1013-1021

(2012).
32. Wang, X.S., *et al.* MicroRNA-29a and microRNA-142-3p are regulators of myeloid differentiation and acute myeloid leukemia. *Blood* **119**, 4992-5004 (2012).
33. Zhong, X., Chung, A.C., Chen, H.Y., Meng, X.M. & Lan, H.Y. Smad3-mediated upregulation of miR-21 promotes renal fibrosis. *J Am Soc Nephrol* **22**, 1668-1681 (2011).
34. Chau, B.N., *et al.* MicroRNA-21 promotes fibrosis of the kidney by silencing metabolic pathways. *Sci Transl Med* **4**, 121ra118 (2012).
35. Petrocca, F., *et al.* E2F1-regulated microRNAs impair TGFbeta-dependent cell-cycle arrest and apoptosis in gastric cancer. *Cancer Cell* **13**, 272-286 (2008).
36. Mendell, J.T. & Olson, E.N. MicroRNAs in stress signaling and human disease. *Cell* **148**, 1172-1187 (2012).
37. Kriebel, M., Wuchter, J., Trinks, S. & Volkmer, H. Neurofascin: a switch between neuronal plasticity and stability. *Int J Biochem Cell Biol* **44**, 694-697 (2012).
38. Kee, Y., *et al.* Subunit structure of the mammalian exocyst complex. *Proc Natl Acad Sci U S A* **94**, 14438-14443 (1997).
39. Inoue, M., Chang, L., Hwang, J., Chiang, S.H. & Saltiel, A.R. The exocyst complex is required for targeting of Glut4 to the plasma membrane by insulin. *Nature* **422**, 629-633 (2003).
40. Ceriani, M., *et al.* Functional analysis of RalGPS2, a murine guanine nucleotide exchange factor for RalA GTPase. *Experimental cell research* **313**, 2293-2307 (2007).
41. Endoh, M., *et al.* Human Spt6 stimulates transcription elongation by RNA polymerase II in vitro. *Mol Cell Biol* **24**, 3324-3336 (2004).
42. Hall, T.M. Multiple modes of RNA recognition by zinc finger proteins. *Curr Opin Struct Biol* **15**, 367-373 (2005).
43. Gerber, S.H. & Sudhof, T.C. Molecular determinants of regulated exocytosis. *Diabetes* **51 Suppl 1**, S3-11 (2002).
44. Rosengren, A.H., *et al.* Reduced insulin exocytosis in human pancreatic beta-cells with gene variants linked to type 2 diabetes. *Diabetes* **61**, 1726-1733 (2012).
45. Gaspar, J.M., *et al.* Diabetes differentially affects the content of exocytotic proteins in hippocampal and retinal nerve terminals. *Neuroscience* **169**, 1589-1600 (2010).
46. Procino, G., *et al.* AQP2 exocytosis in the renal collecting duct -- involvement

of SNARE isoforms and the regulatory role of Munc18b. *J Cell Sci* **121**, 2097-2106 (2008).

47. Yasuda, K., *et al.* Functional consequences of inhibiting exocytosis of Weibel-Palade bodies in acute renal ischemia. *Am J Physiol Renal Physiol* **302**, F713-721 (2012).
48. Poy, M.N., *et al.* A pancreatic islet-specific microRNA regulates insulin secretion. *Nature* **432**, 226-230 (2004).
49. Karres, J.S., Hilgers, V., Carrera, I., Treisman, J. & Cohen, S.M. The conserved microRNA miR-8 tunes atrophin levels to prevent neurodegeneration in Drosophila. *Cell* **131**, 136-145 (2007).
50. Weil, E.J., *et al.* Podocyte detachment in type 2 diabetic nephropathy. *Am J Nephrol* **33 Suppl 1**, 21-24 (2011).
51. Weil EJ, *et al.* Effect of losartan on prevention and progression of early diabetic nephropathy in American Indians with type 2 diabetes. *Diabetes* **in press**(2013).
52. Bitzer, M., Ju, W., Jing, X. & Zavadil, J. Quantitative analysis of miRNA expression in epithelial cells and tissues. *Methods Mol Biol* **820**, 55-70 (2012).
53. Hodgin, J.B., *et al.* Identification of Cross-Species Shared Transcriptional Networks of Diabetic Nephropathy in Human and Mouse Glomeruli. *Diabetes* (2012).
54. Cohen, C.D., *et al.* Improved elucidation of biological processes linked to diabetic nephropathy by single probe-based microarray data analysis. *PLoS One* **3**, e2937 (2008).
55. Johnson, W.E., Li, C. & Rabinovic, A. Adjusting batch effects in microarray expression data using empirical Bayes methods. *Biostatistics* **8**, 118-127 (2007).

Chapter V

Conclusions and future directions

Conclusions

CKD is an important public health issue consuming a significant portion of medical resources and has limited options for effective treatment. To prevent development and progression of CKD, new targets for intervention need to be identified and it requires better understanding of the underlying mechanisms. DN accounts for more than 40% of new cases of ESRD in the United States[1]. Despite significant improvement made for understanding the mechanism for DN, current interventions have limited success.

TGFβ is a cytokine that mediates the progression of DN and other types of kidney disease. Because TGFβ is a multi-functional cytokine that also exhibits protective effects after renal injury including limiting the inflammatory response[2], inhibition of TGFβ itself harbors significant complications. Thus, it is critical to identify new therapeutic targets other than TGFβ.

Recent data suggest a mechanistic involvement of miRNAs in the progression of DN as well as other kidney diseases[3-6]. To identify candidate miRNAs that may mediate glomerular injury in human DN, we quantitatively determined miRNA expression in the glomeruli of patients with DN and examined the association of miRNAs with relevant clinical outcomes. Our analysis uncovered that the expression of miR-21 in glomeruli was highly associated with the severity of glomerulopathy. miR-21 is known to regulate TGFβ signaling activity[7,8] and has been shown to promote fibrosis after tubular injuries kidney[3-6]. However, the role of miR-21 in glomerular injury has not been examined and the function of miR-21 has been shown to be cell type-specific[9]. Therefore, we questioned whether miR-21 plays a different role in glomerular injury. We interrogated this question by examining the impact of loss of miR-21 on two mice models of glomerulopathy, TGFβ$_1$ transgenic mice and STZ-induced diabetic mice in which the expression of miR-21 increases early during disease development.

In TGFβ$_1$ transgenic mice, we determined that loss of miR-21 resulted in accelerated glomerular injury and loss of podocytes. We also found that miR-21 inhibits podocyte apoptosis in vivo and in vitro. Furthermore, we showed that miR-21 represses the activity of multiple TGFβ-regulated pro-apoptotic pathways. In

STZ-induced diabetic mice, miR-21 appeared to inhibit cell cycle regulators, Cdk6 and Cdc25a, to inhibit mesangial expansion. These findings suggest that miR-21 mediates cell type-specific functions in the kidney.

Through our investigations, we suggest that miRNAs exhibit specific functions in glomeruli through the repression of disease relevant mRNAs. Computational algorithms for predicting targets of miRNAs were widely used. However, due to the lack of preciseness of the prediction, new methods are still needed to guide mechanistic studies. Therefore, we developed a novel approach integrating disease-associated miRNAs and mRNAs with target predictions. We determined that miR-200a, which has been implicated as a regulator of DN, represses the expression of EXOC7, RALGPS2, and SUPT6H. These newly identified target genes of miR-200a may constitute novel regulators of DN.

This work has identified a novel role of miR-21 in glomerular injury and developed a new approach, which is based on the association of miRNAs and mRNAs with specific disease phenotypes, to identify candidate miRNA targets. These findings provide new directions for future research projects. Here, we elaborated on the conclusion from this body of work and discussed the perspectives of the possible

future projects aiming at determining the cell-type specific role of miR-21 and the regulatory role of other miRNAs in DN.

miRNAs and human DN

Significant differences in gene expression have been observed between patients with DN and murine models of DN[10]. Therefore, we determined the expression of miRNA in patients with DN. Interestingly, we found that the expression of several miRNAs, such as miR-21 and miR-200a, was positively correlated with the levels of proteinuria of patients with DN. Although these associations do not reveal the function of miRNAs in human DN, examining associations between miRNAs and clinical manifestations can suggest candidate mechanisms. In addition, these data enable us to generate new hypotheses on specific miRNAs and potentially build models of mechanistic interactions.

miR-21 and TGFβ-related glomerulopathy

We discovered that miR-21 is protective in glomerulopathy. In $TGF\beta_1$ transgenic mice, miR-21 inhibits TGFβ-induced podocyte apoptosis and protects against glomerulosclerosis. miR-21 targets many tumor suppressor genes and has anti-apoptotic effect in cancer cells[11,12]. The innovation of the current finding lies on

the ability of miR-21 to inhibit podocyte apoptosis and the protective effect of miR-21 in glomerular injury.

miR-21 elevates with renal damage in mice with different injury models and in patients with transplant nephropathy[6,13,14]. The increase of miR-21 promotes interstitial fibrosis after renal ischemia reperfusion and unilateral ureteral obstruction in mice[6,13]. However, the fibrogenic role of miR-21 remains controversial because results across different studies have not always been consistent[15-17]. For example, the inhibition of miR-21 in the heart disease induced by pressure overload attenuates interstitial fibrosis in mice, while the miR-21 null mice do not have the improved phenotype in the same disease model.

In TGFβ_1 transgenic mice, a model of progressive glomerulopathy, miR-21 increased with the severity of the renal damage. Podocyte apoptosis induces glomerulopathy in TGFβ_1 transgenic mice and miR-21 inhibits apoptosis of cancer cells. For that reason, we hypothesized that miR-21 can inhibit podocyte apoptosis to ameliorate glomerulopathy.

Our experiments in mice confirmed the hypothesis that miR-21 is protective in

glomerulopathy, as TGFβ_1 transgenic/miR-21 null mice displayed increased proteinuria, glomerulosclerosis, and ECM deposition in the glomeruli. The determination of podocyte number and the examination of podocyte apoptosis in TGFβ_1 transgenic/miR-21 null mice confirmed that miR-21 protects against glomerulopathy through the inhibition of podocyte apoptosis. The anti-apoptotic effect of miR-21 was also shown in the cultured mouse podocytes. miR-21 inhibition in mouse podocytes promoted cell apoptosis while miR-21 overexpression attenuated TGFβ-induced podocyte apoptosis.

miR-21 targets multiple pro-apoptotic pathways, including Tgfbr2, Tgfbi, Smad7 and Tp53. miR-21 also targets ECM-related factors, such as Timp3 and Col4a1. This is supported by our findings that the expression of those genes was increased in the glomeruli of TGFβ_1 transgenic/miR-21 null mice. In addition, inhibition of miR-21 in mouse podocytes increased the level of phosphorylation of Smad3, consistent with activation of TGFβ/Smad signaling. The inhibition of miR-21 in mouse podocytes also increased the protein level of PDCD4, a pro-apoptotic factor and a well-known target of miR-21.

The luciferase assay confirmed that Smad7 is the sequence-dependent target of

miR-21. Other genes including Tgfbr2, Timp3, and Col4a1 have been reported as the direct target of miR-21[18-20]. Taken together, miR-21 targets multiple genes regulated by TGFβ, possibly as a feedback mechanism to limit TGFβ-induced podocyte apoptosis and ECM deposition in glomerulopathy.

miR-21 and diabetic glomerulopathy

The concept that miR-21 inhibits the devlopment of glomerulopathy is also supported by the fact that loss of miR-21 increased proteinuria and podocyte loss in STZ-treated miR-21 KO mice versus WT mice (Figure 5.1). In addition, we have detected increased mesangial expansion in STZ-treated miR-21 KO mice, which can be secondary to increased proliferation or activation of mesangial cells.

To understand the mechanism of increased mesangial expansion in diabetic miR-21 KO mice, we isolated primary mesangial cells (PMC) from miR-21 WT and KO mice. The scratch-wound assay, the MTT cell proliferation assay, and the examination of cell cycle distribution all indicated that loss of miR-21 promotes cell growth of PMC. Together with previous studies, our results strongly suggest that miR-21 regulates cell cycle in mesangial cells[21,22]. The further examination did reveal that the expression of Cdk6 and Cdc25a, which facilitates cell cycle

progression[23,24], was increased in the glomeruli of STZ-treated miR-21 KO mice versus STZ-treated miR-21 WT mice. We further hypothesize that miR-21 limits mesangial cell proliferation by targeting Cdk6 and Cdc25a.

The hypothesis requires further experimental validation. However, it can be speculated that the dominant effect of miR-21 in mesangial cells is to inhibit cell growth, whereas in podocytes is to inhibit apoptosis. This may also explain the discrepancy in the results that miR-21 is deleterious in tubulointerstitial injury yet miR-21 is protective in glomerular injury. These findings do not support that overexpression of miR-21 will ameliorate DN or other kidney diseases, unless cell-type specific increase of miR-21 can be achieved, but rather provide evidence that miR-21 and other miRNAs are multi-faceted. This adds complexity in future clinical application of miRNAs as targets to treat kidney diseases.

Disease-associated miRNAs and disease-associated miRNAs

In chapter 4, we investigated the associations of the expression of miRNA and mRNA with clinical manifestations of DN. We discovered that the expression of miRNAs and mRNAs in the glomeruli of patients with DN was correlated with urine albumin-to-creatinine ratio (ACR) of patients. Using results from PAR-CLIP

experiments and prediction algorithms based on sequence complementarity, we were able to identify a candidate target interaction between ACR-correlated miRNAs and ACR-correlated mRNAs. Accordingly, we found EXOC7 is the sequence-dependent target of miR-200a and RALGPS2 and SUPT6H are repressed by miR-200a in renal cells.

Several different prediction algorithms to search for miRNA targets are available. However, experimental validation of those prediction algorithms is limited. Studies have proposed that differentially-expressed mRNAs are targets of inversely differentially-expressed miRNA in disease condition versus control[25,26]. Here, we presented a novel method revealing disease-associated mRNAs are targets of disease-associated miRNAs. Our rationale is that miRNAs, which are part of the disease mechanism, increase with disease progression in order to limit the upregulation of mRNAs associated with disease progression. This attempt of miRNAs aims at limiting the change of mRNAs, which are driven by the disease, thus no good inverse correlation was observed between the expression of miRNAs and the expression of their target mRNAs from the same study subjects.

Our analysis showed that miR-200a was positively correlated with ACR. One gene,

RALGPS2, which was also positively correlated with ACR, was repressed by miR-200a in human embryonic kidney (HEK) cells. This finding supports the hypothesis that miRNAs increase with the disease progression in order to limit the upregulation of mRNAs associated with the disease progression. Interestingly, our experiments also revealed two genes, EXOC7 and SUPT6H, which were negatively correlated with ACR, were also repressed by miR-200a in HEK cells. According to this finding, we assume that miRNAs, increase with the disease progression, serve another purpose to aid the downregulation of mRNAs associated with the disease progression.

Therefore, this approach represents an alternative method to facilitate the identification of miRNA targets. Our computational work also uncovered several ACR-correlated miRNAs. Additional research into the role of those miRNAs in DN is still needed. Although our research did not directly reveal the role of miR-200a and its targets in the progression of DN, it opens up possible new regulatory mechanisms of miR-200a in DN. Such a result strongly supports the future investigation into the association of miRNAs and clinical manifestations of specific diseases.

Future Directions

Cell-specific role of miR-21

In the body of our work, we discovered that miR-21 inhibits podocyte apoptosis and limits mesangial expansion in glomerulopathy. This protective role of miR-21 is contrary to the finding that miR-21 promotes fibrogenesis in tubulointerstitial injury. This controversy adds to the complexity of therapeutic application aimed at using miR-21 inhibitor as a therapeutic drug in human kidney diseases. Additional research into the cell type-specific role and the mechanisms leading to this cell type-specific action of miR-21 is urgently needed.

Although our initial result is intriguing, further studies need to be conducted to accurately define the cell type-specific role of miR-21. One standard approach to address this question is to challenge podocyte-specific or tubular cell-specific conditional miR-21 knockout (KO) mice with specific renal injury and examine the renal phenotype. The Podocin-Cre and Cdh16-Cre mice are mice expressing Cre recombinase specific to podocytes and renal tubule cells, respectively[27,28]. By crossing Podocin-Cre or Cdh16-Cre mice with miR-21 flox/flox mice[29], we can evaluate the impact of loss of miR-21 on podocytes or tubule cells in specific renal injuries and explore the cell type-specific regulatory mechanisms of miR-21. If

miR-21 has a bi-faceted role of inhibiting podocyte apoptosis in renal glomeruli and promoting fibrotic change of tubular cells in tubulointerstitium[6], we can interrogate the question whether the protective effect of miR-21 outweighs the deleterious effect of miR-21 in specific renal injuries. To answer this question, we now need to generate double podocyte-specific and tubular cell-specific conditional miR-21 KO mice. Challenging the double cell-specific miR-21 KO mice with glomerular and tubulointerstitial injury, we can more accurately evaluate the therapeutic effect of the inhibition of miR-21. Unfortunately, at present, mice expressing Cre recombinase specific to mesangial cells are not available.

miR-21 as a biomarker in human kidney disease

Our experiment showed that miR-21 increases with renal damage. This finding is consistent across different studies with different renal injuries and even in humans with different kidney diseases[6,13,14]. If the levels of miR-21 reflect the severity of renal damage, one can speculate that miR-21 serves as a biomarker of kidney damage and its higher level predicts the decline of renal function. This capacity of miR-21 would be independent of its function, but rather reflect its regulation by disease-promoting mechanisms, including TGFβ, TNF-alpha, and interleukins[29].

For long, the level of albuminuria has been used as the primary predictive marker for the progression of DN. However, recent studies have revealed the uncoupling between the progression of albuminuria and the declining of renal function[30-32]. The predictive accuracy of albuminuria by itself is still unsatisfactory. Despite many new biomarkers described, proper validation for the predictive ability of those new biomarkers is lacking[33]. To date, research into additional biomarkers is still needed.

Urine collection is easily accessible and non-invasive. The analyses of urinary components other than albumin and the expression of genes, which are derived from urinary cells, have been described to monitor disease activity[33-35]. Lately, miRNAs have also been identified in urine supernatant containing microvesicles, which are the membrane-enclosed structure released by renal cells[36,37]. Because of these exciting results, we have established the method to measure the expression of miRNAs in urine supernatant. Using this assay, we are able to quantify the levels of miR-21 in the urine. The hypothesis is that miR-21, increased with renal damage, will be released by renal cells to urine supernatant either by microvesicles or in a circulating form. Future experiments will correlate the levels of urinary miR-21 with the expression of renal miR-21. If the levels of urinary miR-21 reflect the levels of miR-21 in the kidney, the next logical step is to correlate the levels of urinary

miR-21 with the severity of renal damage, such as kidney morphometry. Ultimately, we will examine the predictive ability of the levels of urinary miR-21 in the decline of renal function and in the development of end stage renal disease.

Identify regulatory mechanism of miR-21 in diabetic mice

Our findings suggest that miR-21 limits mesangial cell proliferation by targeting Cdk6 and Cdc25a,. To stringently test this hypothesis, confirmation of the protein level of Cdk6 and Cdc25a in renal glomeruli using immunohistochemical staining or western blot is required. In addition, in vitro experiments need to be conducted to support the findings in mice. We will examine the proliferation, cell cycle distribution, and the expression of Cdk6 and Cdc25a in PMC expressing antisense miR-21 oligonucleotides to test whether miR-21 targets Cdk6 and Cdc25a to inhibit mesangial cell growth.

miR-200a and diabetic glomerulopathy

In chapter 4, we have shown that miR-200a correlates with ACR of patients. We also developed a new computational method to identify potential targets of miRNAs. By this method, we discovered that miR-200a targets EXOC7 and miR-200a regulates RALGPS2 and SUPT6H in HEK cells.

At present, the role of miR-200a in diabetic glomerulopathy is still unclear. Kato et al. proposed that miR-200a, upregulated by TGFβ, targets Zeb1/Zeb2 to promote the expression of collagen1a2 in mesangial cells[38]. However, other studies showed that the downregulation of miR-200a by TGFβ increases the expression of Zeb1/Zeb2 to induce epithelial-to-mesenchymal transition (EMT) in cancer cells[39,40]. To address this issue, we need to first determine the level of the expression of miR-200a in the glomeruli of diabetic mice. To further determine the role of miR-200a in diabetic glomerulopathy, we will generate the miR-200a null diabetic mice or inject the diabetic mice with antisense miR-200a oligonucleotides. If there is a regulation or a role of miR-200a in diabetic glomerulopathy, the expression of Exoc7, Ralgps2, and Supt6h will also be determined in the glomeruli of the mice. From these data, additional hypotheses regarding the interrelation of miR-200a and its targets in diabetic glomerulopathy can be generated.

Identity disease-associated miRNAs

Our analyses identified several miRNAs exhibit significant correlation with ACR. The functions of some of those miRNAs have been explored in cancer model systems, including miR-135a promoting growth and migration of cancer cells[41,42],

miR-218 limiting the invasiveness of cancer cells[43], and miR-142-3p regulating differentiation of myeloid cells[44]. For each miRNA, new hypotheses can be generated and validated in animal models of DN.

The data of kidney morphometry of the kidney biopsies of patients with DN, which were used for profiling the expression of miRNAs and mRNAs, are available. Examining associations of miRNAs and mRNAs with kidney morphometry can identify miRNAs and mRNAs correlating with specific parameters. Using the newly-proposed method in chapter 4 for discovering targets of miRNAs, we are able to generate additional hypotheses about the modulations among miRNAs, mRNAs, and DN. Besides validating the hypotheses experimentally in tissue culture as well as in mouse models, we will further use Ingenuity Pathway Analysis[45] to construct dynamic pathway networks among kidney morphometry-associated miRNAs and mRNAs. This approach will generate a broader view of how miRNAs modulate DN and possible other diseases through an intertwining regulatory complex.

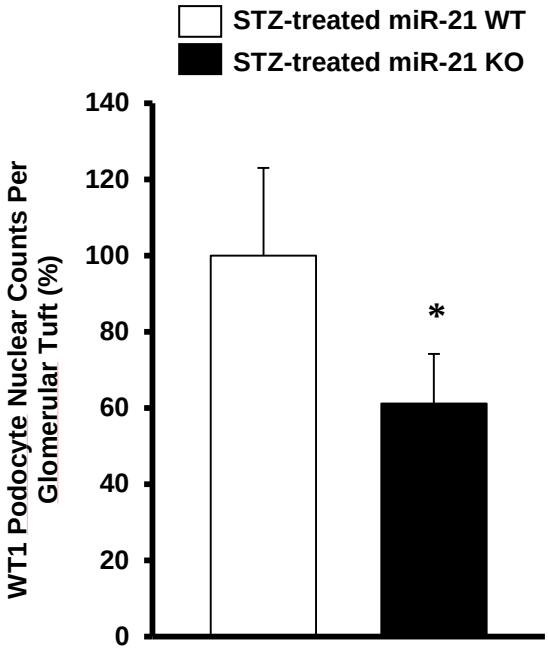

Figure 5.1. Examination of podocyte number in glomeruli of STZ-treated miR-21 WT and KO mice. At 20 weeks after STZ treatment, podocyte number significantly decreased in STZ-treated miR-21-KO mice versus WT mice (N=5) (*P < 0.05; Podocyte counts were normalized by WT mice and presented as percentage)

References

1. Molitch, M.E., *et al.* Nephropathy in diabetes. *Diabetes care* **27 Suppl 1**, S79-83 (2004).
2. Yang, L. TGFbeta, a potent regulator of tumor microenvironment and host immune response, implication for therapy. *Curr Mol Med* **10**, 374-380 (2010).
3. Kato, M., *et al.* MicroRNA-192 in diabetic kidney glomeruli and its function in TGF-beta-induced collagen expression via inhibition of E-box repressors. *Proc Natl Acad Sci U S A* **104**, 3432-3437 (2007).
4. Krupa, A., *et al.* Loss of MicroRNA-192 promotes fibrogenesis in diabetic nephropathy. *J Am Soc Nephrol* **21**, 438-447 (2010).
5. Godwin, J.G., *et al.* Identification of a microRNA signature of renal ischemia reperfusion injury. *Proc Natl Acad Sci U S A* **107**, 14339-14344 (2010).
6. Zhong, X., Chung, A.C., Chen, H.Y., Meng, X.M. & Lan, H.Y. Smad3-mediated upregulation of miR-21 promotes renal fibrosis. *J Am Soc Nephrol* **22**, 1668-1681 (2011).
7. Davis, B.N., Hilyard, A.C., Lagna, G. & Hata, A. SMAD proteins control DROSHA-mediated microRNA maturation. *Nature* **454**, 56-61 (2008).
8. Davis, B.N., Hilyard, A.C., Nguyen, P.H., Lagna, G. & Hata, A. Smad proteins bind a conserved RNA sequence to promote microRNA maturation by Drosha. *Mol Cell* **39**, 373-384 (2010).
9. Krichevsky, A.M. & Gabriely, G. miR-21: a small multi-faceted RNA. *Journal of cellular and molecular medicine* **13**, 39-53 (2009).
10. Hodgin, J.B., *et al.* Identification of Cross-Species Shared Transcriptional Networks of Diabetic Nephropathy in Human and Mouse Glomeruli. *Diabetes* (2012).
11. Chan, J.A., Krichevsky, A.M. & Kosik, K.S. MicroRNA-21 is an antiapoptotic factor in human glioblastoma cells. *Cancer Res* **65**, 6029-6033 (2005).
12. Meng, F., *et al.* MicroRNA-21 regulates expression of the PTEN tumor suppressor gene in human hepatocellular cancer. *Gastroenterology* **133**, 647-658 (2007).
13. Chau, B.N., *et al.* MicroRNA-21 promotes fibrosis of the kidney by silencing metabolic pathways. *Sci Transl Med* **4**, 121ra118 (2012).
14. Zhong, X., *et al.* miR-21 is a key therapeutic target for renal injury in a mouse model of type 2 diabetes. *Diabetologia* **56**, 663-674 (2013).
15. Eddy, A.A. The TGF-beta route to renal fibrosis is not linear: the miR-21

viaduct. *J Am Soc Nephrol* **22**, 1573-1575 (2011).
16. Thum, T., *et al.* MicroRNA-21 contributes to myocardial disease by stimulating MAP kinase signalling in fibroblasts. *Nature* **456**, 980-984 (2008).
17. Patrick, D.M., *et al.* Stress-dependent cardiac remodeling occurs in the absence of microRNA-21 in mice. *J Clin Invest* **120**, 3912-3916 (2010).
18. Yu, Y., *et al.* MicroRNA-21 induces stemness by downregulating transforming growth factor beta receptor 2 (TGFbetaR2) in colon cancer cells. *Carcinogenesis* **33**, 68-76 (2012).
19. Gabriely, G., *et al.* MicroRNA 21 promotes glioma invasion by targeting matrix metalloproteinase regulators. *Molecular and Cellular Biology* **28**, 5369-5380 (2008).
20. Mase, Y., *et al.* MiR-21 is Enriched in the RNA-Induced Silencing Complex and Targets COL4A1 in Human Granulosa Cell Lines. *Reprod Sci* **19**, 1030-1040 (2012).
21. Zhong, Z., Dong, Z., Yang, L. & Gong, Z. miR-21 induces cell cycle at S phase and modulates cell proliferation by down-regulating hMSH2 in lung cancer. *Journal of cancer research and clinical oncology* **138**, 1781-1788 (2012).
22. Wang, P., *et al.* microRNA-21 negatively regulates Cdc25A and cell cycle progression in colon cancer cells. *Cancer Res* **69**, 8157-8165 (2009).
23. Boutros, R., Lobjois, V. & Ducommun, B. CDC25 phosphatases in cancer cells: key players? Good targets? *Nature reviews. Cancer* **7**, 495-507 (2007).
24. Ekholm, S.V. & Reed, S.I. Regulation of G(1) cyclin-dependent kinases in the mammalian cell cycle. *Current opinion in cell biology* **12**, 676-684 (2000).
25. Mayor-Lynn, K., Toloubeydokhti, T., Cruz, A.C. & Chegini, N. Expression profile of microRNAs and mRNAs in human placentas from pregnancies complicated by preeclampsia and preterm labor. *Reprod Sci* **18**, 46-56 (2011).
26. Nam, S., *et al.* MicroRNA and mRNA integrated analysis (MMIA): a web tool for examining biological functions of microRNA expression. *Nucleic Acids Res* **37**, W356-362 (2009).
27. Moeller, M.J., Sanden, S.K., Soofi, A., Wiggins, R.C. & Holzman, L.B. Podocyte-specific expression of cre recombinase in transgenic mice. *Genesis* **35**, 39-42 (2003).
28. Shao, X., Somlo, S. & Igarashi, P. Epithelial-specific Cre/lox recombination in the developing kidney and genitourinary tract. *J Am Soc Nephrol* **13**,

1837-1846 (2002).
29. Lu, T.X., *et al.* MicroRNA-21 limits in vivo immune response-mediated activation of the IL-12/IFN-gamma pathway, Th1 polarization, and the severity of delayed-type hypersensitivity. *J Immunol* **187**, 3362-3373 (2011).
30. Perkins, B.A., *et al.* Microalbuminuria and the risk for early progressive renal function decline in type 1 diabetes. *J Am Soc Nephrol* **18**, 1353-1361 (2007).
31. Tsalamandris, C., *et al.* Progressive decline in renal function in diabetic patients with and without albuminuria. *Diabetes* **43**, 649-655 (1994).
32. Perkins, B.A., Ficociello, L.H., Roshan, B., Warram, J.H. & Krolewski, A.S. In patients with type 1 diabetes and new-onset microalbuminuria the development of advanced chronic kidney disease may not require progression to proteinuria. *Kidney Int* **77**, 57-64 (2010).
33. Jim, B., Santos, J., Spath, F. & Cijiang He, J. Biomarkers of diabetic nephropathy, the present and the future. *Current diabetes reviews* **8**, 317-328 (2012).
34. Thongboonkerd, V. Practical points in urinary proteomics. *Journal of proteome research* **6**, 3881-3890 (2007).
35. Thongboonkerd, V. Urinary proteomics: towards biomarker discovery, diagnostics and prognostics. *Molecular bioSystems* **4**, 810-815 (2008).
36. Wang, G. & Szeto, C.C. Methods of microRNA quantification in urinary sediment. *Methods Mol Biol* **1024**, 211-220 (2013).
37. Wang, G., *et al.* Expression of microRNAs in the urine of patients with bladder cancer. *Clinical genitourinary cancer* **10**, 106-113 (2012).
38. Kato, M., Arce, L. & Natarajan, R. MicroRNAs and their role in progressive kidney diseases. *Clinical journal of the American Society of Nephrology : CJASN* **4**, 1255-1266 (2009).
39. Gregory, P.A., *et al.* The miR-200 family and miR-205 regulate epithelial to mesenchymal transition by targeting ZEB1 and SIP1. *Nat Cell Biol* **10**, 593-601 (2008).
40. Burk, U., *et al.* A reciprocal repression between ZEB1 and members of the miR-200 family promotes EMT and invasion in cancer cells. *EMBO reports* **9**, 582-589 (2008).
41. Zhou, W., *et al.* MiR-135a promotes growth and invasion of colorectal cancer via metastasis suppressor 1 in vitro. *Acta Biochim Biophys Sin (Shanghai)* **44**, 838-846 (2012).
42. Chen, Y., *et al.* miRNA-135a promotes breast cancer cell migration and invasion by targeting HOXA10. *BMC Cancer* **12**, 111 (2012).

43. Liu, Y., *et al.* MiR-218 reverses high invasiveness of glioblastoma cells by targeting the oncogenic transcription factor LEF1. *Oncol Rep* **28**, 1013-1021 (2012).
44. Wang, X.S., *et al.* MicroRNA-29a and microRNA-142-3p are regulators of myeloid differentiation and acute myeloid leukemia. *Blood* **119**, 4992-5004 (2012).
45. The <networks, functional analyses, etc.> were generated through the use of Ingenuity Pathways Analysis (Ingenuity® Systems, www.ingenuity.com).".